NBER WORKING PAPER SERIES

THE MACROECONOMIC IMPACT OF CLIMATE CHANGE: GLOBAL VS. LOCAL TEMPERATURE

Adrien Bilal
Diego R. Känzig

Working Paper 32450
http://www.nber.org/papers/w32450

NATIONAL BUREAU OF ECONOMIC RESEARCH
1050 Massachusetts Avenue
Cambridge, MA 02138
May 2024, January 2026

We thank Marios Angeletos, Marshall Burke, Gabriel Chodorow-Reich, Simon Dietz, Stephane Hallegatte, Jim Hamilton, Xavier Jaravel, Ben Jones, Eben Lazarus, Pooya Molavi, Ishan Nath, Ben Olken, Esteban Rossi-Hansberg, Toan Phan, Jón Steinsson, Jeffrey Shrader, Jim Stock, Chris Wolf, and numerous participants at conferences and seminars for helpful comments and suggestions. We thank Krzysztof Lisiecki, Lilian Hartmann, Ramya Raghavan, and Cathy Wang for outstanding research assistance. Adrien Bilal gratefully acknowledges support from the Chae Family Economics Research Fund at Harvard University. The views expressed herein are those of the authors and do not necessarily reflect the views of the National Bureau of Economic Research.

The Macroeconomic Impact of Climate Change: Global vs. Local Temperature
Adrien Bilal and Diego R. Känzig
NBER Working Paper No. 32450
May 2024, revised January 2026
JEL No. E01, E23, F18, O44, Q54, Q56

ABSTRACT

This paper estimates that the macroeconomic damages from climate change are an order of magnitude larger than previously thought. Exploiting natural global temperature variability, we find that 1°C warming reduces world GDP by over 20% in the long run. Global temperature correlates strongly with extreme climatic events, unlike country-level temperature used in previous work, explaining our larger estimate. We use this evidence to estimate damage functions in a neoclassical growth model. Business-as-usual warming implies a present welfare loss of more than 30%, and a Social Cost of Carbon in excess of $1,200 per ton. These impacts suggest that unilateral decarbonization policy is cost-effective for large countries such as the United States.

Adrien Bilal
Stanford University
Department of Economics
and NBER
adrienbilal@stanford.edu

Diego R. Känzig
Northwestern University
Department of Economics
and NBER
dkaenzig@northwestern.edu

1 Introduction

Climate change is frequently described as one of the defining economic challenges of our time. This view, however, stands in sharp contrast to empirical estimates of its impact on economic activity: they imply that a permanent 1°C rise in temperature reduces world output by 1-3%. Under conventional discounting and background economic growth, these effects seem modest. Why, then, does climate change loom so large in economic debate? Do existing estimates not account for the full impact of climate change, or are its true economic consequences indeed limited?

In this paper, we show that the macroeconomic impacts of climate change are an order of magnitude larger than previously documented. We rely on time-series local projections to estimate the impact of global temperature on Gross Domestic Product (GDP). This approach exploits natural variability in global mean temperature—the source of variation closest to climate change—which we show to be a stronger predictor of damaging extreme climatic events than country-level temperature. Our estimates imply that a permanent 1°C rise in global temperature lowers world GDP by over 20%. We then use our reduced-form results to estimate structural damage functions in a neoclassical growth model. Climate change of 2°C by 2100 leads to a present-value welfare loss of more than 30% and a Social Cost of Carbon (SCC) in excess of $1,200 per ton of carbon dioxide.

In the first part of the paper, we develop our time-series approach. We assemble two climate-economy datasets whose strengths complement each other. The first dataset builds on the Barro-Ursúa measures of economic activity, complemented with global mean temperature information from the National Oceanic and Atmospheric Administration (NOAA). This dataset spans 43 countries over 160 years, from 1860 to 2019. We refer to it as the 'BU' sample.

The second dataset draws on the Penn World Tables, providing economic data on GDP, consumption, investment, and productivity. It spans a broader set of 173 countries, though over a shorter period, from 1960 to 2019. To measure climate conditions, we construct global and country-level temperatures from high-resolution gridded land and ocean surface air data from Berkeley Earth. We further incorporate reanalysis-based indicators of extreme weather—capturing heat, drought, wind speed, and precipitation at a

granular level—from the Inter-Sectoral Impact Model Intercomparison Project (ISIMIP). We refer to this dataset as the 'PWT' sample.

Identifying the impact of temperature on GDP per capita is complicated by their jointly trending behavior. We thus construct global and local (country-level) *temperature shocks*: innovations to the temperature process that are orthogonal to their long-run trends and persist for two years using the approach in Hamilton (2018). Our choice of period is motivated by the geoscience literature. Natural climate variability is driven by multiple phenomena. External causes such as solar cycles and volcanic eruptions lead to medium- and short-run fluctuations in the Earth's mean temperature. Internal climate variability—interactions within the climatic system itself—lead to irregular fluctuations in temperature and weather extremes. For instance, the El Niño cycle varies unpredictably between 2 to 7 years.

We map out the dynamic causal effects of our global temperature shocks on world GDP per capita using local projections. In the broader PWT sample, a global temperature shock scaled to 1°C leads to a gradual decline in world GDP per capita that peaks at 14% after 6 years with a 95% confidence interval of (6%, 22%), and is statistically significant at the 5% level in years 2 to 8. In the longer BU sample, the same temperature shock leads to a peak effect at 18% after 5 years with a 95% confidence interval of (6%, 30%), and is statistically significant at the 5% level in years 0 to 6. In both cases, impacts do not fully mean-revert even after 10 years. Our results remain unchanged for alternative detrending approaches, such as one-step ahead forecast errors, a one-sided Hodrick-Prescott filter, or taking simple first differences.

Importantly, the temperature *shocks* have a partially persistent effect on the *level* of temperature, that remains near 0.5°C for multiple years after the shock. As in an instrumental variable approach, the fundamental determinant of output is the temperature level, while the temperature shock simply extracts quasi-experimental variation. Hence, the 14-18% impacts 6 years out reflect the accumulated effects of persistently elevated global temperature itself, but are less than the implied effect of a permanent 1°C increase in the level of temperature.

We convert these estimates identified from partially transitory global temperature shocks to the effect of a permanent increase in global temperature by taking the ratio

of the cumulative impulse responses of GDP per capita and global temperature. Our reduced-form estimates imply that a permanent 1°C rise in global temperature leads to a 22-34% reduction in world GDP per capita in the PWT and BU samples, respectively.

Although climate change occurs in a sequence of small increments, this conversion relies on the same conditions that underpin existing estimates of temperature impacts: the relationship between temperature and GDP holds beyond the range of temperature shocks observed in sample, and it holds for expected permanent temperature changes in addition to medium-run unexpected temperature changes. We partly address these limitations with our structural model which accounts for long-run expectations and adaptation through capital adjustment.

The causal interpretation of our headline results is subject to three identification concerns. We address each of them in a series of robustness exercises. First, we account for omitted variable bias: global temperature shocks may coincide with the global economic and financial cycle. We control for rich measures of world economic performance: indicators for global economic recessions, global macro-financial variables (past world and country real GDP, commodity prices and interest rates), and regional economic trends. Our results remain unaffected by the specific set of controls and are not driven by any particularly influential years, indicating that temperature shocks are largely unrelated to economic shocks.

Second, we account for reverse causality: as output declines after a temperature shock, energy consumption and greenhouse gas emissions fall, lowering temperatures and increasing output going forward. Qualitatively, reverse causality thus leads us to underestimate the true impact of a global temperature shock. Quantitatively, it is likely negligible because short-run fluctuations in emissions imply small temperature variations. We confirm these arguments by explicitly adjusting for the impact of past greenhouse gas and aerosol emissions with a climate model and find virtually identical results.

Third, we verify that our estimates are stable across time periods and causes of temperature variation. Our main analysis reveals similar estimates in the shorter PWT sample (1960-2019) and in the longer BU sample (1860-2019). We find comparable estimates in shorter time periods (1860-1928, 1940-2019, 1980-2019, 1960-2007) as well as when we exclude El Niño and volcanic eruptions from our identifying variation. Collectively, our

robustness exercises suggest that our specification captures the causal effect of global temperature on economic activity.

Our estimated impact of temperature shocks on world GDP contrasts with existing estimates. Comparable approaches to ours in Nordhaus (1992), Dell et al. (2012), Moore and Diaz (2015), Burke et al. (2015) and Nath et al. (2024) imply that a permanent 1°C rise in temperature reduces GDP by at most 3%. Why do we find effects that are an order of magnitude larger?

We focus on a different source of variation. Changes in *global* mean temperature capture the comprehensive impact of climate change. By contrast, previous work exploits changes in *country-level, local* temperature. When we estimate the impact of *local* temperature on country-level GDP with the same empirical specification, we find similarly modest and imprecise effects to previous studies: 1% per 1°C temperature shock, implying a 3% decline following a permanent 1°C rise in temperature. These effects are not significant at the 5% level. Econometrically, panel analyses using *local* temperature net out common impacts of *global* temperature through time fixed effects. Instead, we focus on these common impacts.

Why, then, does global temperature depress economic activity more than local temperature? We argue that global temperature is fundamentally different from local temperature. The geoscience literature shows that droughts, extreme wind and precipitation are outcomes of the global climate that depend on ocean temperatures and atmospheric humidity throughout the globe, rather than outcomes of local temperature realizations (Seneviratne et al., 2016; Wartenburger et al., 2017; Seneviratne et al., 2021; Domeisen et al., 2023).

In line with this view, we find that ocean temperature, rather than land temperature, is responsible for the majority of the effects of global temperature on economic activity. In addition, global temperature shocks predict a pronounced and persistent rise in the frequency of four extreme climatic events that cause economic damage: extreme temperature, droughts, extreme wind, and extreme precipitation. By contrast, local temperature shocks only predict a weak rise in these extremes.

Quantitatively, including these four extreme events accounts for half of the estimated impact of global temperature. We reach this conclusion by estimating the impact of ex-

treme events on GDP, which we combine with the dynamic correlation between global temperature shocks and extreme events to construct a counterfactual impact of global temperature on GDP. Of course, our aggregation exercise is unlikely to account for the full effect of global temperature on GDP: we would need to specify and measure the universe of channels whereby global temperature affects the economy. Using global temperature directly bypasses this challenge. By contrast, we do not find evidence that economic spillovers through international trade alone can quantitatively account for the gap between local and global temperature impacts.

How and where do the worldwide GDP impacts of global temperature materialize? We document that capital, investment and productivity all decline after a global temperature shock. Warm and low-income countries appear to be more strongly affected than cold and high-income countries, although these comparisons are somewhat noisy. Overall, however, global temperature has more uniformly detrimental effects than local temperature.

In the second part of the paper, we develop a simple neoclassical growth model to translate our medium-run reduced-form estimates into long-run output and welfare effects. Consistent with Nordhaus (1992), we remain purposefully parsimonious and let global temperature affect aggregate productivity.

We estimate productivity shocks that correspond to a global temperature shock by matching the estimated impulse response function of output. This mapping has a closed-form expression that guarantees identification. In doing so, we account for the internal persistence of global mean temperature in response to temperature shocks. We remain conservative and impose persistent level effects rather than growth effects. The estimated damage function implies that a one-time transitory 1°C rise in global mean temperature leads to a 4% peak productivity decline when targeting the PWT estimates. The estimated model also matches the untargeted impulse response of capital to a temperature shock.

Our main counterfactual is a gradual increase in global mean temperature that starts in 2024 and reaches 3°C above preindustrial levels by 2100, so 2°C above 2024 temperatures, with a 2% rate of time preference. Climate change implies a 53% GDP per capita decline by 2100, or 26% per 1°C. The long-run adjustment of capital amplifies the effect of global temperature on GDP by one fifth relative to the reduced-form estimates. This

amplification mechanism is muted in the reduced-form estimates based on smaller and more transitory temperature changes. Capital and consumption drop by 51% and 53% respectively, leading to a 35% welfare loss in permanent consumption equivalent in 2024. Of course, these counterfactuals represent losses relative to a baseline trend in economic activity between 2024 and 2100, not absolute losses relative to 2024. These counterfactuals also reflect estimation uncertainty. For instance, the 95% confidence interval for 2100 output losses ranges from 29% to 77%. Even at the lower end of the confidence interval, our baseline counterfactuals are comparable to the economic losses caused by the 1929 Great Depression, but experienced permanently.

If the economic effects of global temperature are substantial, why were they not noticed after nearly 1°C of global warming since 1960? Because climate change occurs in small increments, its effects are hidden behind background economic variability. We show that since 1960, climate change caused a gradual reduction in the annual world growth rate that reaches one third of baseline by 2019. Because climate change is also permanent, its effects keep accumulating over time. According to our counterfactual, world GDP per capita would be more than 20% higher today had no warming occurred between 1960 and 2019.

We characterize the SCC using the global temperature response to a CO2 pulse from Dietz et al. (2021a) and Folini et al. (2024). We obtain a SCC in excess of $1,200 per ton. This value is six times larger than the high end of existing estimates ($185 per ton, Rennert et al., 2022). The 95% confidence interval for the SCC ranges from $399 per ton to $2,015 per ton. While this range is non-trivial, its lower bound is multiple times larger than conventional SCC values. Our focus on global temperature shocks accounts for this difference. When we re-estimate our model based on the impact of local temperature shocks as in previous research, the welfare cost of our climate change scenario is 5% and the SCC is $149 per ton. Neither of these values is statistically significant at the 5% level.

How sensitive are these results to specification choices? Targeting the empirical estimates in the BU sample implies a 61% GDP per capita loss by 2100 and a SCC in excess of $1,500. Any plausible discount rate and warming scenario results in welfare losses in excess of 15% and a SCC above $370 per ton. Discount rates close to 1% imply a SCC exceeding $2,500 per ton. Scenarios with 2100 warming 5°C above preindustrial levels lead

to welfare losses larger than 50%. Varying the climate sensitivity by a factor two implies a SCC between $600 and $2,400 per ton.

We conclude by delineating the consequences of our results for decarbonization policy, which we explore further in a companion paper (Bilal and Känzig, 2025). Decarbonization interventions cost $80 per ton of CO2 abated on average (Bistline et al., 2023). A conventional SCC value of $149 per ton based on local temperature implies that these policies are cost-effective only if governments internalize benefits to the entire world, as captured by the SCC. However, a government that only internalizes domestic benefits values decarbonization using a Domestic Cost of Carbon (DCC). The DCC is always lower than the SCC because damages to a single country are lower than at a global scale. Under conventional estimates, the DCC of the United States is below policy costs, making unilateral emissions reduction prohibitively expensive. Under our estimates based on global temperature, the DCC of the United States exceeds policy costs. In that case, unilateral decarbonization policy is cost-effective for a large economy such as the United States.

Our paper contributes to an influential literature measuring economic damages from climate change surveyed in Burke et al. (2023) and Moore et al. (2024). The conventional panel approach estimates the effect of small, short-run *local* temperature shocks (Dell et al., 2012; Dell et al., 2014; Burke et al., 2015; Moore and Diaz, 2015; Newell et al., 2021; Kahn et al., 2021; Barrage and Nordhaus, 2024). Across all these studies, estimates consistently imply that a permanent 1°C rise in temperature leads to a 1-3% reduction in GDP. Our paper takes a fundamentally different approach: we directly exploit time-series variation in a more comprehensive metric of climate change—global mean temperature.

Local temperature estimates can lead to larger long-run economic effects if one assumes growth effects—that short-run economic effects persist forever (Dell et al., 2012; Moore and Diaz, 2015; Burke et al., 2015). Our treatment of persistence builds on Nath et al. (2024) who show how to distinguish empirically between the polar assumptions of growth effects and level effects for local temperature. Our local temperature estimates are quantitatively consistent with theirs—a 2-3% GDP loss per permanent 1°C increase—which we use as our benchmark.

Few studies have explored time-series variation in temperature (Bansal and Ochoa, 2011; Berg et al., 2024; Neal et al., 2025). They emphasize either contemporaneous ef-

fects, GDP dispersion, or spillover effects. All of them focus on average land temperature rather than global temperature inclusive of oceans. By contrast, we show that global ocean temperature—rather than land temperature—is the main driver of aggregate impacts, that their delayed peak outweighs contemporaneous effects, and that extreme events rather than spillovers help bridge the gap between global and local temperature impacts.

As such, our paper relates to the literature studying the economic impact of natural disasters such as storms, heatwaves or El Niño (Barro, 2006; Barro, 2009; Deschênes and Greenstone, 2011; Hsiang et al., 2011; Deryugina, 2013; Hsiang and Jina, 2014; Tran and Wilson, 2023; Callahan and Mankin, 2023; Dingel et al., 2023). We evaluate the impact of global temperature directly and provide new evidence on the relationship between global temperature and a wide range of extreme climatic events.

This "top-down" approach connects to the literature using integrated assessment models surveyed in Nordhaus (2013). Our counterfactuals suggest that these models often found limited costs of climate change because they were calibrated to local temperature, not due to incomplete economic foundations (Nordhaus, 2013; Stern et al., 2022).

More recently, "bottom-up" models featuring rich regional heterogeneity, migration (Desmet et al., 2021; Cruz and Rossi-Hansberg, 2023) and capital investment (Krusell and Smith, 2022; Bilal and Rossi-Hansberg, 2023) match micro-level estimates and aggregate using the model. Our "top-down" global temperature approach holistically captures damages without having to quantify each channel, but remains necessarily limited in assessing distributional and adaptation effects.

In fact, both our global temperature and the conventional local temperature approaches capture adaptation only imperfectly, as both rely on moderate short-run variation. Although assessing the role of adaptation is beyond the scope of this paper, the stability of our estimates across time periods suggests that it does not play a major role (Burke et al., 2024). Should there be an unprecedented uptake in adaptation in the future, our numbers would still represent an upper bound on damages absent adaptation and society's willingness to pay for it.

The rest of this paper is organized as follows. Section 2 describes the data and estimates the macroeconomic effects of global temperature shocks in the time series. Section 3

confirms the impact of global temperature in the panel of countries and discusses identification concerns. Section 4 compares the effects of global and local temperature. Section 5 introduces our dynamic model and describes our structural estimation approach. Section 6 evaluates the welfare implications of climate change. Section 7 concludes.

2 Global Temperature and Economic Growth

We aim to estimate the effects of climate change on economic activity. Climate change is a transformation in a wide range of weather patterns, ocean currents and atmospheric conditions relative to preindustrial times. The Intergovernmental Panel for Climate Change (IPCC) summarizes this complex phenomenon with a single, scalar measure: global mean temperature. Therefore, we use global mean temperature as our main metric of a changing climate and investigate how it affects the economy.

2.1 Climate-Economy Data

To study the effects of temperature on the economy, we assemble two complementary datasets. We use global aggregates from these datasets in this section, and country-level outcomes in Section 3 below.

Our first dataset is based on the Barro and Ursúa (2008) macroeconomic data, which provides GDP and population figures for 43 countries from 1860 to 2007. We extend this data using the World Bank Development Indicators, yielding coverage from 1860 through 2019. We obtain a consistent, direct measure of global mean temperature over this long time frame from NOAA. In the following, we refer to this dataset as the 'BU' sample.[1]

Our second dataset builds on the Penn World Tables. We obtain information on GDP, population, consumption, investment and productivity for 173 countries from 1960 to 2019. We refer to this dataset as 'PWT' sample. We also rely on the World Bank Development Indicators as an alternative over this time frame.

We complement the PWT dataset with richer climate and weather information given its more recent time coverage. We obtain temperature data from the Berkeley Earth Sur-

[1]We thank Robert Barro for kindly sharing the GDP and population data underlying their GDP per capita indices.

face Temperature Database. It provides temperature anomaly data at a spatial resolution of $1^\circ \times 1^\circ$ of latitude and longitude. Based on this gridded data, we construct population- and area-weighted temperature measures at the country level. We also construct area-weighted measures of global temperature, which includes land and ocean surface air temperature. Reassuringly, our measure correlates virtually perfectly with the direct measure from NOAA.

In addition, we incorporate indicators of extreme weather events—covering heat, drought, wind, and precipitation—from ISIMIP's observed climate dataset. This source provides global, daily reanalysis data on temperature, wind speed, and precipitation from 1901 to 2019 at a $0.5^\circ \times 0.5^\circ$ resolution, with higher quality measurements in the second half of the 20^{th} century. We construct exposure indices by recording, for each country and year, the fraction of days in which observed weather exceeds (or falls below) fixed percentiles of the 1950-1980 daily weather distribution. We further detail data sources and construction in Appendix A.

Together, the BU and PWT datasets allow us to leverage the strengths of each in our analysis. The BU dataset provides a long time frame of 160 years, while the PWT dataset offers broader country coverage in a more recent period when climatic information is more accurately measured.

2.2 Global Temperature Shocks

Figure 1 displays the evolution of global average temperature and world real GDP per capita since 1860 in our dataset. In the early stages of the industrial period, global mean temperature remains relatively stable near 14°C. However, from the 1920s onward, global average temperature begins to steadily rise. At the same time, we observe relatively stable economic growth over the entire sample, both in the PWT and BU samples.

The trending behavior of the two series in Figure 1 complicates the identification of the economic effects of temperature increases. A simple regression of global GDP per capita on temperature will yield a spurious correlation between the two variables (Granger and Newbold, 1974). In our case, reverse causality is an additional challenge. Economic growth is associated with higher greenhouse gas emissions which eventually translate into higher temperature over long horizons. Therefore, we do not focus on the level of

Figure 1: Global Average Temperature and Output Since 1860

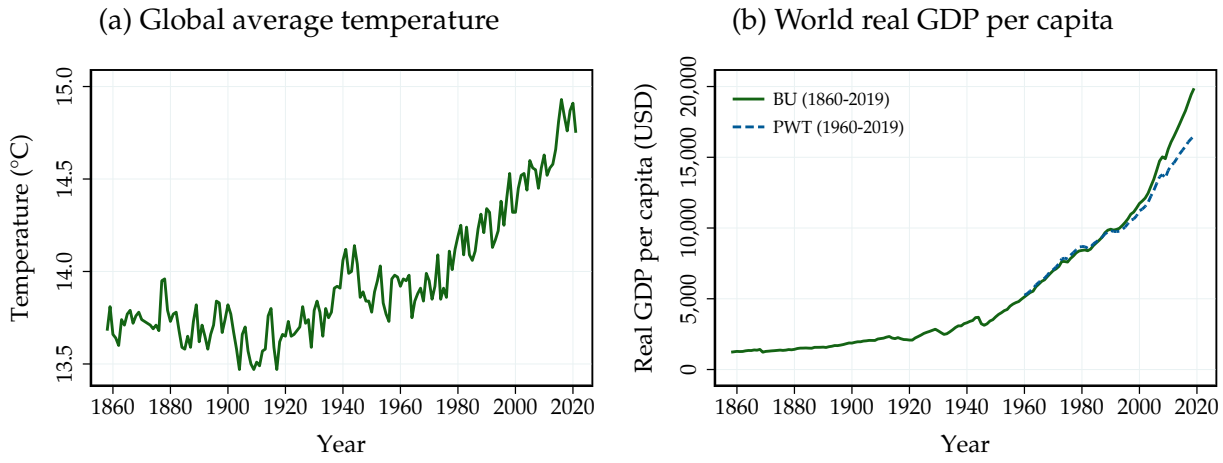

Panel (a): evolution of global average temperature from NOAA since 1860. Panel (b): evolution of world real GDP per capita (in 2017 USD) computed based on PWT (1960-2019, dashed blue) and BU (1860-2019, green) data.

temperature as the treatment in our projections, but instead focus on so-called *temperature shocks*. We define such shocks as possibly persistent deviations from the long-run trend in global mean temperature.

What drives these variations in temperature around the trend? The geoscience literature indicates two types of causes. First, external causes such as solar cycles and volcanic eruptions lead to short-run fluctuations in the Earth's mean temperature. Solar cycles have a typical period of 10 years and can warm the Earth by as much as 0.1°C (National Oceanic and Atmospheric Administration, 2009). Volcanic eruptions have shorter-lived cooling effects of up to 2 years due to sulphuric aerosols that increase albedo (National Oceanic and Atmospheric Administration, 2005). Second, internal climate variability—interactions within the climatic system itself that lead to irregularly recurring events—also affects temperatures. For instance, the El Niño-La Niña cycle varies unpredictably between 2 to 7 years and substantially affects global mean temperatures and weather extremes (Kaufmann et al., 2006; National Oceanic and Atmospheric Administration, 2023).

How to isolate the trend and transient components of temperature? To estimate the effects of temperature on future economic outcomes, it is critical to preserve the causality of the data in a time-series sense: we cannot rely on future values of temperature to identify the trend in the current period. In addition, the physical properties of natural climate variability suggest to allow for somewhat persistent deviations from trend.

Figure 2: Global Temperature Shocks

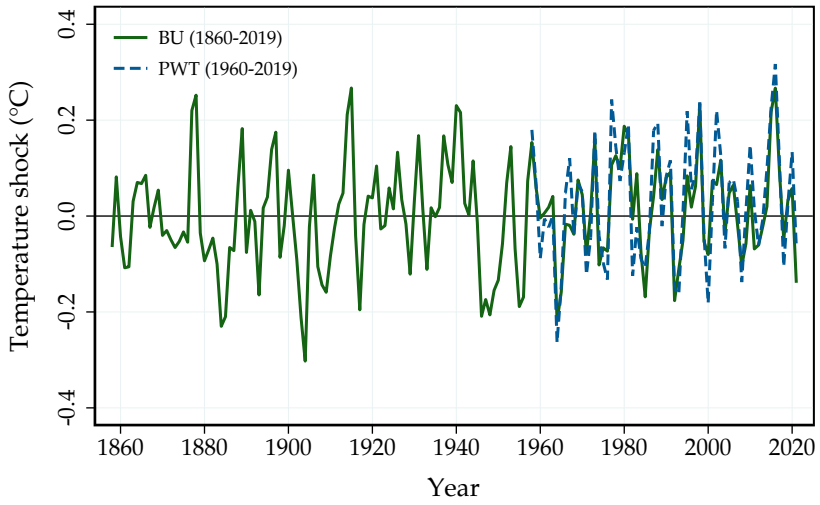

Global temperature shocks, computed using Hamilton (2018) filter. PWT: $h = 2$, $p = 2$, 1960-2019, dashed line. BU: $h = 2$, $p = 6$, 1860-2019, solid line.

An approach that satisfies our needs along both these dimensions is the method proposed by Hamilton (2018) and used in Nath et al. (2024) for local temperature. We regress global mean temperature on its lags as of period $t - h$ and construct the temperature shock as the corresponding innovation:

$$\widehat{T_t^{\text{shock}}} = T_t - (\widehat{\alpha} + \widehat{\beta}_1 T_{t-h} + \ldots + \widehat{\beta}_{p+1} T_{t-h-p}), \tag{1}$$

where $\widehat{\beta}_i$ denotes the coefficient estimates of the regression of temperature on its lag $j = h+i-1$ and $\widehat{\alpha}$ is the estimated intercept. This exercise amounts to isolating shocks that persist typically for h periods. Selecting the horizon h is of course an important choice. Motivated by the fact that the climatic events that we consider can last for up to several years, we select a horizon of $h = 2$. We set the number of lags to $p = 2$ in the PWT sample. In the BU sample, we use $p = 6$ to capture the more pronounced curvature in the temperature series over a longer horizon. As we show in Section 3.2 below, varying these values leaves our results essentially unchanged.

Figure 2 shows the resulting global temperature shocks over our sample of interest. As expected, the temperature shocks fluctuate around zero with an almost equal number of positive and negative shocks. The largest temperature shocks in our sample are

near 0.3°C. Figure B.1 in Appendix B.1 indicates that the series is also weakly autocorrelated, because we allow for relatively persistent deviations from the long-run temperature trend. In our empirical specification, we therefore control for lagged temperature shocks as well. Otherwise, serial correlation may bias the estimated impacts.

2.3 The Effect of Temperature Shocks in the Time Series

The economic effects of temperature shocks may take time to materialize. Therefore, we focus on the dynamic effects of temperature shocks up to 10 years out. We evaluate directly these medium-run effects of temperature without extrapolating short-term temperature impacts.

We estimate the dynamic causal effects to global temperature shocks using local projections as in Jordà (2005). This approach involves estimating the following series of regressions, one for each horizon $h = 0, \ldots, 10$:

$$y_{t+h} - y_{t-1} = \alpha_h + \theta_h T_t^{\text{shock}} + \mathbf{x}_t' \boldsymbol{\beta}_h + \varepsilon_{t+h}, \tag{2}$$

where y_t is the outcome variable of interest, T_t^{shock} is the temperature shock and θ_h is the dynamic causal effect of interest at horizon h. We refer to the latter as the impulse response function. $\mathbf{x}_t$ is a vector of controls and ε_t is a potentially serially correlated error term. Our main outcome variable of interest is (log) world real GDP per capita. Because we use the cumulative growth rate as the dependent variable, we estimate a possibly persistent level effect. The estimation sample is 1960-2019 for the PWT data, and 1860-2019 for the BU data.[2]

We use local projections in our main analysis because they tend to be robust at longer horizons (Montiel Olea et al., 2024). Compared to Vector Autoregressions (VARs) or distributed lag models, local projections directly estimate the effects of interest rather than extrapolating from the first few autocovariances and allow for more flexible controls. Yet, we obtain similar results under alternative estimation models in Appendix B.3.

To account for the serial correlation in GDP growth and temperature shocks, we in-

[2]Leveraging that temperature data is available for a longer period than GDP data, we estimate temperature shocks based on this longer sample (1950-2022 for PWT, and 1850-2022 for BU) to mitigate the influence from observations at the beginning and the end of the sample.

Figure 3: The Effect of Global Temperature Shocks on Temperature and World Output

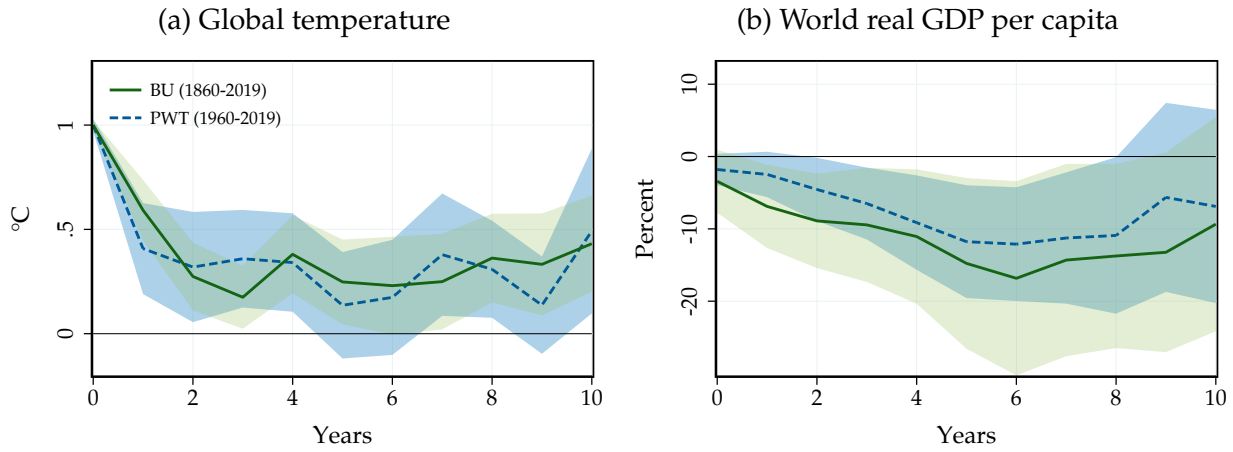

Impulse responses of global mean temperature and world real GDP per capita to a global temperature shock, estimated based on (2). Controls: Lags of dependent variable, temperature shock, world real GDP growth, current and lagged recession dummies, and linear time trend. Lag length differs by sample (2 lags in PWT; 4 lags in BU). Lines: point estimate in PWT (dashed) and BU sample (solid). Shaded areas: 95% confidence bands for PWT (darker) and BU sample (lighter).

clude lags of real GDP growth per capita and of the global temperature shock. To net out the global business cycle more comprehensively, we control for large economic shocks, such as the post-World War recessions, the large oil shocks in the 1970s or the Great Recession, using one common dummy variable for all recessions.[3] For the shorter sample starting in 1960, we include two lags of our controls; for the longer sample, we include four lags. We also include a linear time trend to account more flexibly for trending behavior. Inference uses heteroskedasticity and autocorrelation consistent (HAC) standard errors that account for potential serial correlation in the local projection error terms.[4]

Figure 3 shows the impulse responses of global temperature and world real GDP per capita to a global temperature shock scaled to 1°C. The lines denote point estimates and the shaded areas are 95% confidence bands. By construction, global temperature increases by 1°C on impact in panel (a). The effect of a global temperature shock on global temperature turns out to be highly persistent in the PWT and BU samples: after 10 years global

[3]Our definition of global recession dates follows the World Bank (Kose et al., 2020). Specifically, we focus on the following episodes: 1873-1877, 1893-1897, 1918-1921, 1921-1939, 1945-1947, 1973-1975, 1979-1983, 1990-1992, 2007-2009, and 2011-2012. To allow for potential persistent effects of recessions, we also include lags of the global recession indicator variable.

[4]Our main specification does not account for estimation uncertainty in the global temperature shock. However, we alternatively conduct inference using bootstrapping techniques or jointly estimate the effect of temperature on GDP per capita with longer lag lengths. Both approaches take estimation uncertainty into account and yield very similar inference. See Appendices B.2 and B.3 for more details.

temperature is still elevated by nearly 0.5°C.

The persistent rise in global temperature leads to meaningful economic effects. Panel (b) shows that, on impact, world GDP falls by 2-3% in the PWT and BU datasets, respectively. However, the effect builds up over time. After six years, world GDP per capita falls by 12-16%, with effects that persist up to eight to ten years out. Our estimates are comparable up to statistical precision in the PWT and BU datasets, indicating that focusing on the more recent period with broader country coverage or on a longer time span with fewer, higher-income countries leads to similar results. The effect is statistically significant at the 5% level from years 2 to 8 in both samples. The magnitude of our estimates scaled to a 1°C temperature shock is similar to growth impacts that typically occur after severe financial crises (Cerra and Saxena, 2008; Reinhart and Rogoff, 2009).

The gradual decline in world GDP reflects not only the direct impact of the initial temperature shock, but also the subsequent effects of persistently elevated temperature that accumulate over time. As in an instrumental variable approach, the fundamental determinant of output is the temperature level, while the temperature shock is simply an identification device. Hence, the 12-16% impacts 6 years out exceed the effect of a one-time, fully transitory 1°C increase in temperature, but are less than the effect of a permanent 1°C increase.

To assess the role of persistence, we first construct a counterfactual path of output that would correspond to a fully transitory global temperature change with a linear combination of the output and temperature impulse response functions (Sims, 1986). Figure B.5 in Appendix B.4 shows that the accumulated effects of persistently elevated temperature account for a substantial part of the peak effect: the new peak then just exceeds 5% instead and occurs five years after the shock.

Next, we infer what the impact of a permanent 1°C rise in global temperature would be. We follow standard practice and calculate the ratio of the cumulative impulse response of output per capita to the cumulative impulse response of temperature, which corresponds to a special case of the method in Sims (1986). We find that a permanent 1°C rise in global temperature leads to a 20% long-run reduction in world GDP per capita in the PWT dataset, and 29% in the BU dataset.

Although climate change occurs in a sequence of small increments, scaling our esti-

mates to a 1°C increase relies on two conditions. Importantly, the same conditions also underpin existing estimates based on local temperature variation. The first condition is that the relationship between temperature and GDP per capita holds beyond the range of temperature shocks observed in sample. A 1°C global temperature shock is a large shock that does not occur directly in our historical sample: we observe smaller shocks of 0.1-0.2°C in practice. In effect, we abstract from potential non-linearities.

Among the relatively small shocks we observe, we do not find much evidence for non-linearities. Figure B.6 in Appendix B.5 reports comparable impacts of small, larger, or only positive shocks. In principle, a changing climate might affect economic activity as long it differs from preindustrial conditions irrespectively of the sign of global temperature changes. Our results instead suggest that both the sign and magnitude of global temperature changes are relevant as long as global temperature accurately summarizes climate change: positive shocks lower GDP while negative shocks raise GDP.

These results do not imply that non-linearities do not matter for larger changes that have not yet materialized. However, in the presence of potential future tipping points, one may expect larger effects than predicted by our linear estimates (Dietz et al., 2021b). If costly adaptation to global temperature impacts becomes more prevalent in the future than it has historically, then realized impacts may be lower than our estimates.

The second condition making our scaling consistent is that the estimated relationship between GDP per capita and global temperature holds for expected permanent temperature changes. We assess whether allowing capital investment to respond to expectations of long-run changes affects our counterfactuals with our structural model in Sections 5 and 6.

3 Global Temperature Shocks in the Panel of Countries

So far we have evaluated the impact of global temperature shocks directly on world GDP per capita. We now aim to achieve three distinct goals. Our first goal in this section is to use a country-level econometric specification that is more directly comparable to previous work. Our second goal is to further corroborate our results when controlling for a wider set of variables and varying the time span of our analysis. Our third goal in Section 4

is to contrast the impact of global temperature with existing work that has focused on country-level temperature.

3.1 Global Temperature Shocks in the Panel

To estimate the dynamic causal effects of temperature shocks in the panel, we employ the panel local projections approach in Jordà et al. (2020). In this section, we still estimate the effect of global temperature shocks, now averaged across 173 countries in the PWT dataset, and across 43 countries in the BU dataset. Specifically, we estimate the following series of panel regressions for horizons $h = 0, \dots, 10$:

$$y_{i,t+h} - y_{i,t-1} = \alpha_{i,h} + \theta_h T_t^{\text{shock}} + \mathbf{x}_t' \boldsymbol{\beta}_h + \mathbf{x}_{i,t}' \boldsymbol{\gamma}_h + \varepsilon_{i,t+h}, \tag{3}$$

where $y_{i,t}$ is the outcome variable of interest for country i in year t, T_t^{shock} is the global temperature shock and θ_h is the dynamic causal effect of interest at horizon h. $\mathbf{x}_t$ is a vector of global controls, $\mathbf{x}_{i,t}$ is a vector of country-specific controls and $\varepsilon_{i,t}$ is an error term.

The panel specification (3) is closer to the standard panel estimators used to study the effects of local temperature shocks (e.g. Dell et al., 2012; Burke et al., 2015; Nath et al., 2024). Of course, the identifying variation in global temperature shocks T_t^{shock} remains common across all countries, and thus we cannot include year fixed effects. Therefore, we include global controls as in the aggregate time-series specification (2). For the same reason, the error term is potentially serially and cross-sectionally correlated. Inference thus relies on Driscoll and Kraay (1998) standard errors that are robust to cross-sectional and serial dependence.

To assess whether our results hold across a wide range of specifications, we include a richer set of control variables. Specifically, we now also control for lags of world commodity prices and the U.S. treasury yield.[5] In addition, we flexibly absorb lags of country-level GDP per capita and region-specific linear trends. Our main outcome variable of interest is country-level log real GDP per capita. The PWT sample is an unbalanced panel spanning

[5]For the PWT sample, we use the WTI crude price and the 1-year treasury yield; for the BU sample we use an energy price index including coal and oil and the 10-year treasury yield.

Figure 4: The Effect of Global Temperature Shocks: Panel vs. Time Series

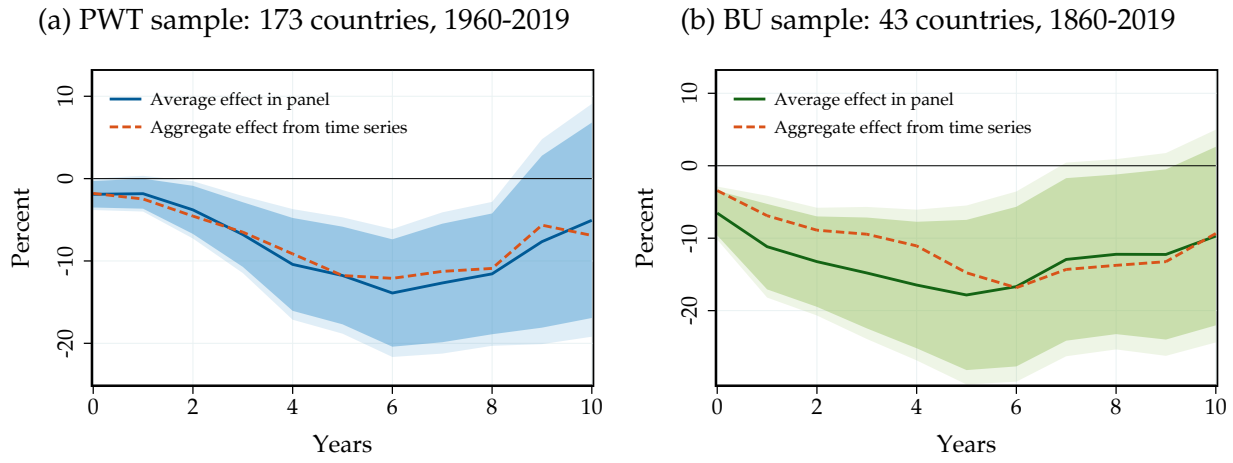

Impulse responses of real GDP per capita to a global temperature shock estimated in the panel using (3). Controls: Lags of dependent variable, temperature shock, world real GDP growth, commodity price inflation, U.S. treasury yield, current and lagged recession dummies, and sub-region specific time trends. Lag length differs by sample (2 lags in PWT; 4 lags in BU). Left: PWT sample (173 countries, 1960-2019). Right: BU sample (43 countries, 1860-2019). Lines: baseline estimates from panel specification (solid) against time-series response from (2) (dashed). Dark and light shaded areas: baseline 90 and 95% confidence bands.

1960-2019 and the BU sample is an unbalanced panel spanning 1860-2019.

Figure 4 displays the impulse responses to a global temperature shock, estimated in the panel of countries. Consistent with our aggregate time-series evidence, global temperature shocks lead to a significant fall in real GDP per capita. In the broader PWT sample, a global temperature shock scaled to 1°C leads to a gradual decline in world GDP that peaks at 14% after 6 years with a 95% confidence interval of (6%, 22%), and is statistically significant at the 5% level in years 2 to 8. In the longer BU sample, the same temperature shock leads to a peak effect at 18% after 5 years with a 95% confidence interval of (6%, 30%), and is statistically significant at the 5% level in years 0 to 6. We then use the same approach as in Section 2.3 to convert our estimates into the effect of a permanent increase in temperature. We obtain that a permanent 1°C rise in global temperature leads to a 22-34% reduction in long-run GDP per capita.

Although our dependent variable is disaggregated at the country level, the time-series nature of our identifying variation in global temperature requires care in interpreting our results. We now demonstrate that our main estimate is robust to accounting for a range of identification concerns.

3.2 Sensitivity to Specification Choices

In this section we explore whether variants of our baseline econometric specification lead to similar or different results.[6]

Omitted variable bias. In small samples, global temperature innovations may happen to be correlated with the global economic cycle over time. For instance, if a severe El Niño event increases global temperature at the same time that a global recession occurs for unrelated reasons, we may mistakenly attribute adverse economic impacts to climatic variations.

To account for this possibility, we already include a rich set controls of the world economic performance in our main specification in equation (3). In Figures 5(a)-(b), we show that our results hold regardless of the particular set of macroeconomic and country-level controls separately for the PWT and BU datasets. We consider multiple specifications based on more parsimonious sets of controls: a specification that does not include oil prices and the treasury yield, a specification that also excludes the global recession dates, and a specification that omits the region-specific trends. We also consider an expanded specification where we control for more lags of all our global controls (4 lags in the PWT sample and 8 lags in the BU sample).

The point estimates are similar across specifications, suggesting that global temperature shocks and economic shocks are largely unrelated in our sample. However, the additional controls help reduce sampling uncertainty and lead to more precise estimates. If anything, omitting to control for worldwide recessions appears to lead to smaller rather than larger effects.

We confirm that spuriously correlated economic shocks are unlikely to drive our results by examining how each year in the sample affects our estimates. For all years t, Figures 5(c)-(d) plot the change in GDP 6 years later at $t + 6$—the peak effect in the PWT sample—against the temperature shocks at time t after residualizing both from our set of controls and averaging across countries. The negative relationship turns out to be a robust one and is not driven by a specific set of outliers. Figure B.8 in Appendix B.7 displays

[6]For completeness, we also reproduce these variants in the time-series specification of Section 2.3 in Figure B.7, Appendix B.6. We find similar results.

Figure 5: Sensitivity of the Effect of Global Temperature Shocks (I)

(a) PWT: Sensitivity with respect to controls

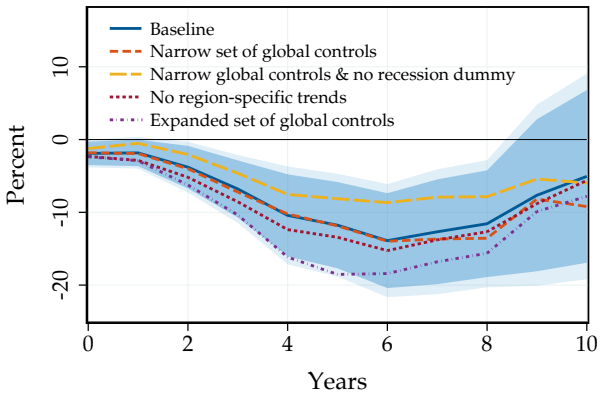

(b) BU: Sensitivity with respect to controls

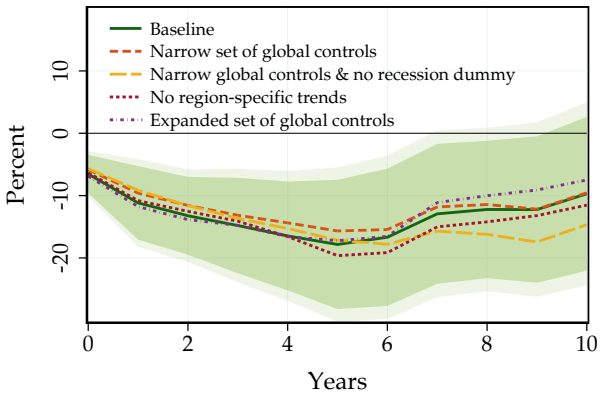

(c) PWT: Scatter plot at $h = 6$

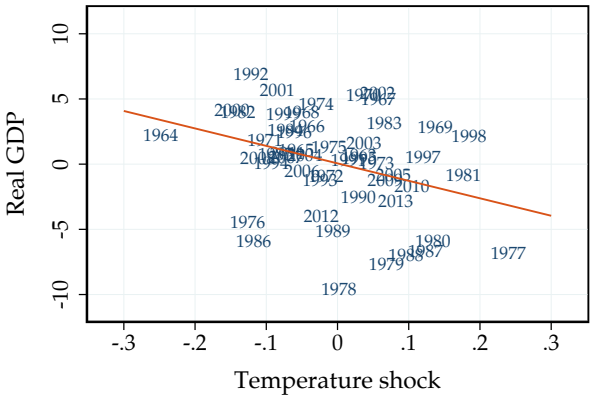

(d) BU: Scatter plot at $h = 6$

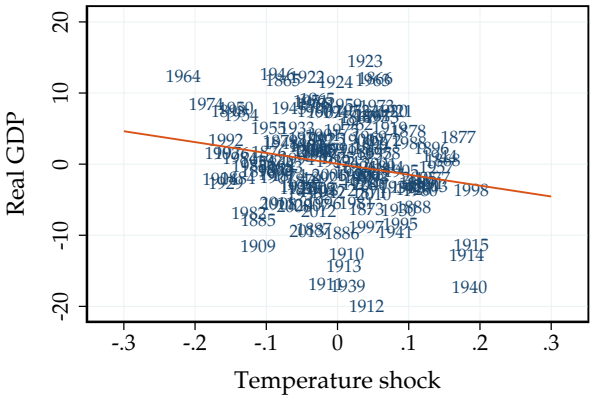

(e) PWT: Construction of temperature shock

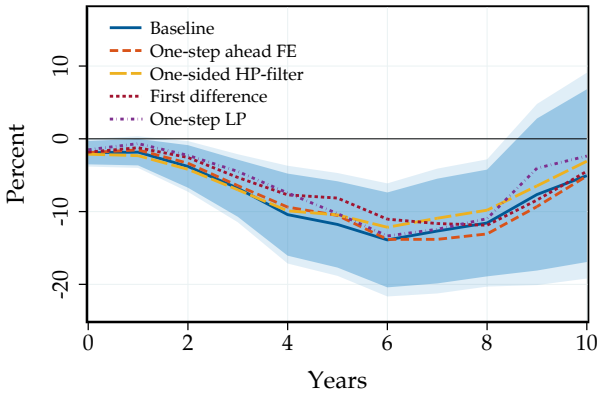

(f) BU: Construction of temperature shock

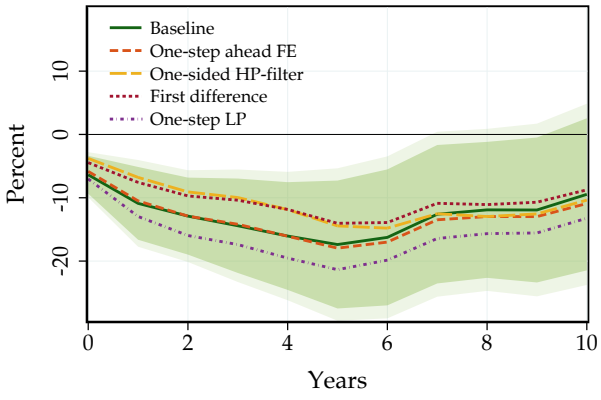

Impulse responses of real GDP per capita to a global temperature shock, estimated from (3). Left column: PWT dataset (173 countries, 1960-2019. Right column: BU dataset (43 countries, 1860-2019). Top row: sensitivity to controls included: Narrow set of global controls includes only world real GDP growth (omitting commodity price inflation and the treasury yield); expanded set includes 4 lags of global controls in PWT and 8 lags in BU. Middle row: scatter plot of temperature shocks against the cumulative change in real GDP per capita 6 years out, both after residualizing our set of controls and averaging across countries. Bottom row: sensitivity to the construction of temperature shock: baseline with $h = 2$; one-step ahead forecast error $h = 1$ (with confidence bands in Figure B.13, Appendix B.9); one-sided HP filter; first difference; one-step LP estimation with global temperature level. Lines: point estimate. Dark and light shaded areas: baseline 90 and 95% confidence bands.

a systematic jackknife exercise in which we censor one year at a time and find that our estimates are not driven by specific years.[7] Overall, these results indicate that our estimates are unlikely to be driven by economic shocks spuriously correlated to temperature shocks.[8]

Definition of temperature shock. We show that our results hold across a variety of definitions of temperature shocks. In our baseline specification, we measure temperature shocks using the Hamilton (2018) filter with a horizon $h = 2$. In Figures 5(e)-(f), we show that constructing temperature shocks as one-step ahead forecast errors $h = 1$ following previous work (see e.g. Bansal and Ochoa, 2011; Nath et al., 2024), using a one-sided HP filter, or based on simple first differences produces similar results.

Figures 5(e)-(f) also show that our results are virtually unchanged when we directly estimate the effects of temperature on world GDP per capita without highlighting the identifying variation through global temperature shocks. In that case, instead of estimating temperature shocks in a first step using a filter, and then projecting world real GDP on temperature shocks in a second step, we directly project world real GDP per capita on temperature levels, including sufficiently many lags of temperature. Both approaches are numerically equivalent when we construct the shocks as one-step ahead forecast errors with the same controls. We provide more details in Appendix B.3.

3.3 Reverse Causality and Sample Stability

In this section we explore whether accounting for reverse causality or changing the underlying time period affects our estimates.

Reverse causality. Changes in economic activity may affect short-run variations in temperature: a decline in economic activity lowers emissions and temperature, hence increas-

[7] The year 1940 appears as a potentially exceptional observation in the BU sample. It corresponds to the post-World War II contraction six years later. Yet, our jackknife exercise in Figure B.8, Appendix B.7, reveals that dropping this observation does not change our estimates materially. Our results in the BU sample are not particularly sensitive to any individual observation due to the larger number of data points. In addition, we show that our estimates remain similar in several subsamples in Section 3.3.

[8] In Appendix C.3, we further establish that unobserved global shocks are not driving our results by exploiting an intermediate level of spatial aggregation of temperature shocks. This specification allows us to control for time fixed effects and reassuringly, the results are broadly comparable.

Figure 6: Sensitivity of the Effect of Global Temperature Shocks (II)

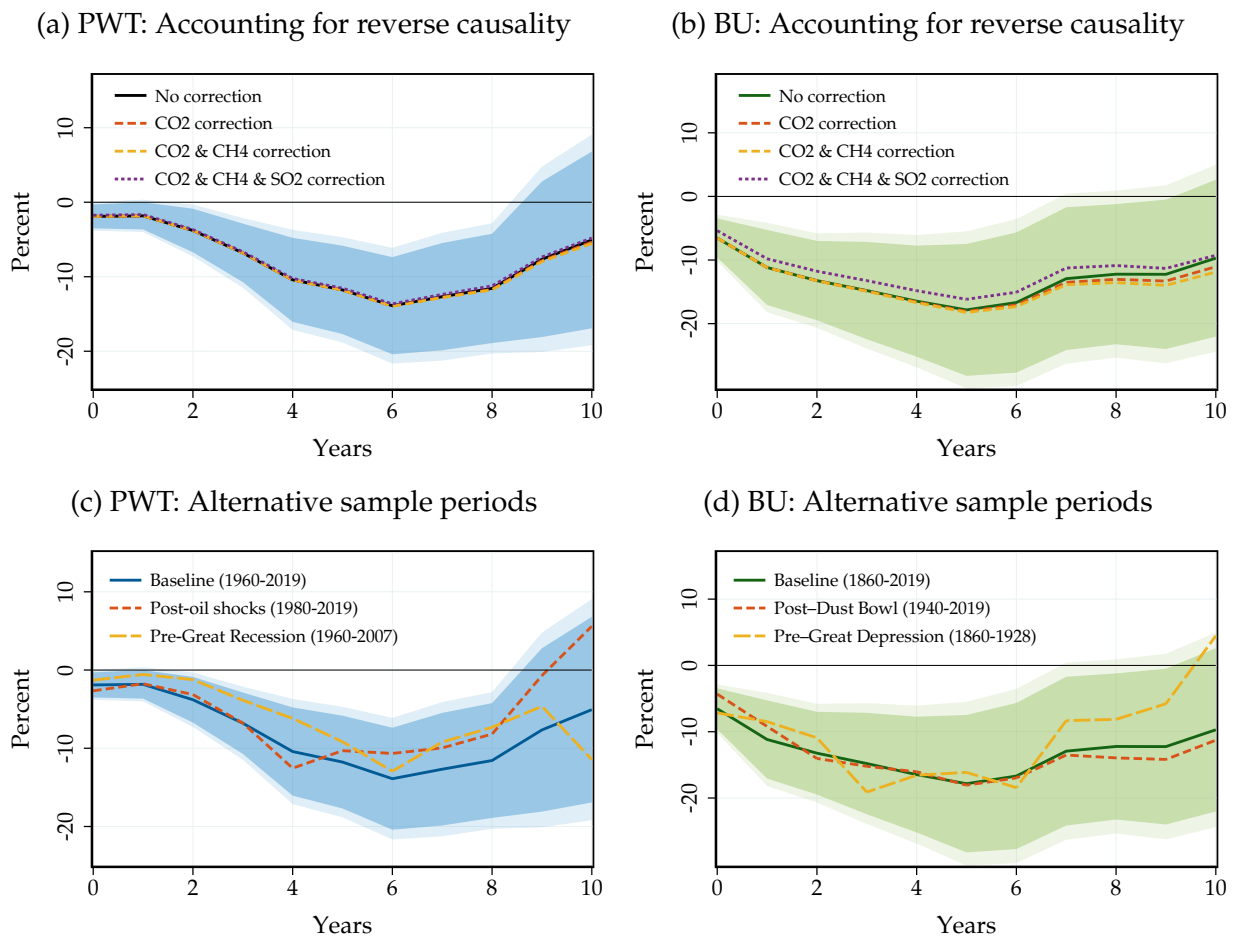

Impulse responses of real GDP per capita to a global temperature shock, estimated from (3). Left column: PWT dataset (173 countries, 1960-2019. Right column: BU dataset (43 countries, 1860-2019). Top row: GDP per capita response after adjusting for reverse causality due to the temperature feedback of carbon dioxide (CO2), methane (CH4), and sulfur dioxide (SO2). Bottom row: results for alternative subsamples; PWT: 1980-2019 and 1960-2007; BU: 1940-2019 and 1860-1928. Lines: point estimate. Dark and light shaded areas: baseline 90 and 95% confidence bands.

ing output going forward, and potentially biasing our estimates.

There are two reasons why reverse causality due to greenhouse gases is unlikely to substantially affect our interpretation. First, this reverse causality concern typically leads us to underestimate the effect of temperature on economic output. As temperature rises and economic activity initially declines, the resulting fall in greenhouse gas emissions implies lower future temperatures and thus higher future output. Thus, true damages would be larger than our estimates.

Second, annual fluctuations in emissions imply negligible temperature variations relative to the typical temperature shocks that we exploit. For instance, typical year-to-

year fluctuations in CO2 emissions are of the order of 2 gigatons. After accounting for oceanic and biosphere absorption, these annual fluctuations translate into 1 gigaton of atmospheric CO2. This magnitude corresponds to 0.1 part per million (ppm) in atmospheric CO2 concentration. Current CO2 atmospheric concentration is just above 400 ppm. Given a climate sensitivity of 1.5, year-to-year fluctuations in emissions thus imply year-to-year fluctuations in temperature of approximately 0.005°C—an order of magnitude below natural climate variability which is of the order of 0.1°C.

Aerosol emissions can also lead to reverse causality, for instance due to sulfur dioxide (SO2). Aerosols have the opposite effect of greenhouse gases and reduce global temperature by reflecting incoming sunlight. Aerosols are shorter-lived than greenhouse gases in the atmosphere, which may amplify or dampen reverse causality concerns relative to greenhouse gases depending on the horizon of interest.

Two exercises confirm that reverse causality is unlikely to affect our results. First, we test whether our temperature shocks are forecastable by past macro-financial variables with a series of Granger-causality tests in Table B.1, Appendix B.1. We find no evidence that global temperature shocks are forecastable, consistently with the substantial lag and small sensitivity between emissions and temperature changes.

Second, we explicitly account for the feedback between output and temperature through emissions. We consider the two most important greenhouse gases: carbon dioxide (CO2) and methane (CH4). We also include the main source of aerosol emissions: sulfur dioxide (SO2). We use standard estimates of the emissions-to-GDP elasticity and leading estimates of the dynamic sensitivity of temperature to an emissions impulse to construct our adjustment. Figures 6(a)-(b) confirm that explicitly adjusting for reverse causality has no meaningful effect on our results. We provide more details in Appendix B.8.

Sample period. Figures 6(c)-(d) evaluate whether our results depend on the sample period. We obtain similar results in the PWT in two subsamples (1960-2007 and 1980-2019). Macroeconomic controls such as global recessions, global oil prices and the U.S. treasury yields are important to ensure subsample stability in the PWT data: the smaller the subsample, the more likely that global temperature shocks happen to be spuriously corre-

lated with unrelated economic shocks. Our results also continue to hold in subsamples of the BU data (1860-1928, 1940-2019) up to statistical precision. Given the continued rise of global temperature over the course of the 20th century, the stability of our estimates across time periods suggests a lack of adaptation to temperature shocks, at least historically.

3.4 Additional Exercises

We conduct an additional set of robustness exercises in Appendix B.9, whose conclusions we summarize below.

External validity. We show that our results do not depend on specific sources of global temperature variation. Figure B.9 re-evaluates our results after netting out temperature variation generated by El Niño by controlling for an Oceanic Niño Index in our main specification. The responses are close to our baseline estimates. Similarly, controlling for volcanic eruptions also yields virtually unchanged results. These exercises indicate that our main results capture a broad effect of global temperature on economic activity that is not specific to particular sources of temperature variation.

Weighting. Figure B.10 shows that our results in the panel are unaffected when weighting observations by country GDP. This consistency is not surprising given that we already show in Figure 4 that our time series and panel results are similar.

Pre-trends. We investigate whether our results may be due to differential pre-trends. Although Table B.1 in Appendix B.1 already suggests that Granger causality is unlikely to be a concern, we do not detect any statistically significant nor economically meaningful pre-trend in the years prior to the shock in Figure B.10.

Data choices. We show that our results are robust with respect a range of alternative data choices. Figures B.11 and B.12 in Appendix B.9 reveal similar results with GDP data from the World Development Indicators, with temperature data from NOAA and NASA, when restricting the analysis to the countries studied in Dell et al. (2012) and Burke et al. (2015), and with different numbers of lags included in our local projections. Overall, our

robustness exercises confirm the persistently negative effect of global temperature shocks on real GDP per capita.

4 Global vs. Local Temperature

4.1 Local Temperature and Economic Activity

How do the effects of global temperature shocks compare to those of local temperature shocks? Conventional estimates that do not assume growth effects imply that a permanent 1°C rise in local temperature reduces GDP by 1-3% (Dell et al., 2012; Burke et al., 2015; Moore and Diaz, 2015; Kahn et al., 2021; Nath et al., 2024). To ensure that our findings are not driven by differences in econometric specifications or data choices, we reproduce the effects of local temperature shocks in our empirical framework. We focus on the shorter PWT dataset, as most studies of local temperature rely on the more recent sample beginning in the 1960s. We measure local temperature shocks using the Hamilton (2018) filter similarly to Nath et al. (2024), as we do in Section 2.2 for global temperature, but now based on population-weighted country-level temperature data.

Local and global temperature shocks turn out to be only weakly correlated. Often, global shocks do not correspond to local shocks and they frequently move in different directions. Figure C.1 in Appendix C.1 shows two illustrative examples of local temperature shocks, for the United States and South Africa.

To estimate the responses to local shocks, we rely on our panel specification (3), with the critical difference that the temperature shock is a *country-specific* temperature shock $T^{\text{shock}}_{i,t}$. In this first specification, we do not include time fixed effects to maximize comparability with (3). However, we also consider two alternative specifications:

$$y_{i,t+h} - y_{i,t-1} = \alpha_{i,h} + \theta^{\text{global}}_h T^{\text{shock}}_t + \theta^{\text{local}}_h T^{\text{shock}}_{i,t} + \mathbf{x}'_t \boldsymbol{\beta}_h + \mathbf{x}'_{i,t} \boldsymbol{\gamma}_h + \varepsilon_{i,t+h} \tag{4a}$$

$$y_{i,t+h} - y_{i,t-1} = \alpha_{i,h} + \delta_{t,h} + \theta_h T^{\text{shock}}_{i,t} + \mathbf{x}'_{i,t} \boldsymbol{\gamma}_h + \varepsilon_{i,t+h} \tag{4b}$$

In specification (4a), we estimate the impacts of global and local temperature shocks jointly. This provides a straightforward way to assess whether the two responses are

Figure 7: The Effect of Global vs. Local Temperature Shocks

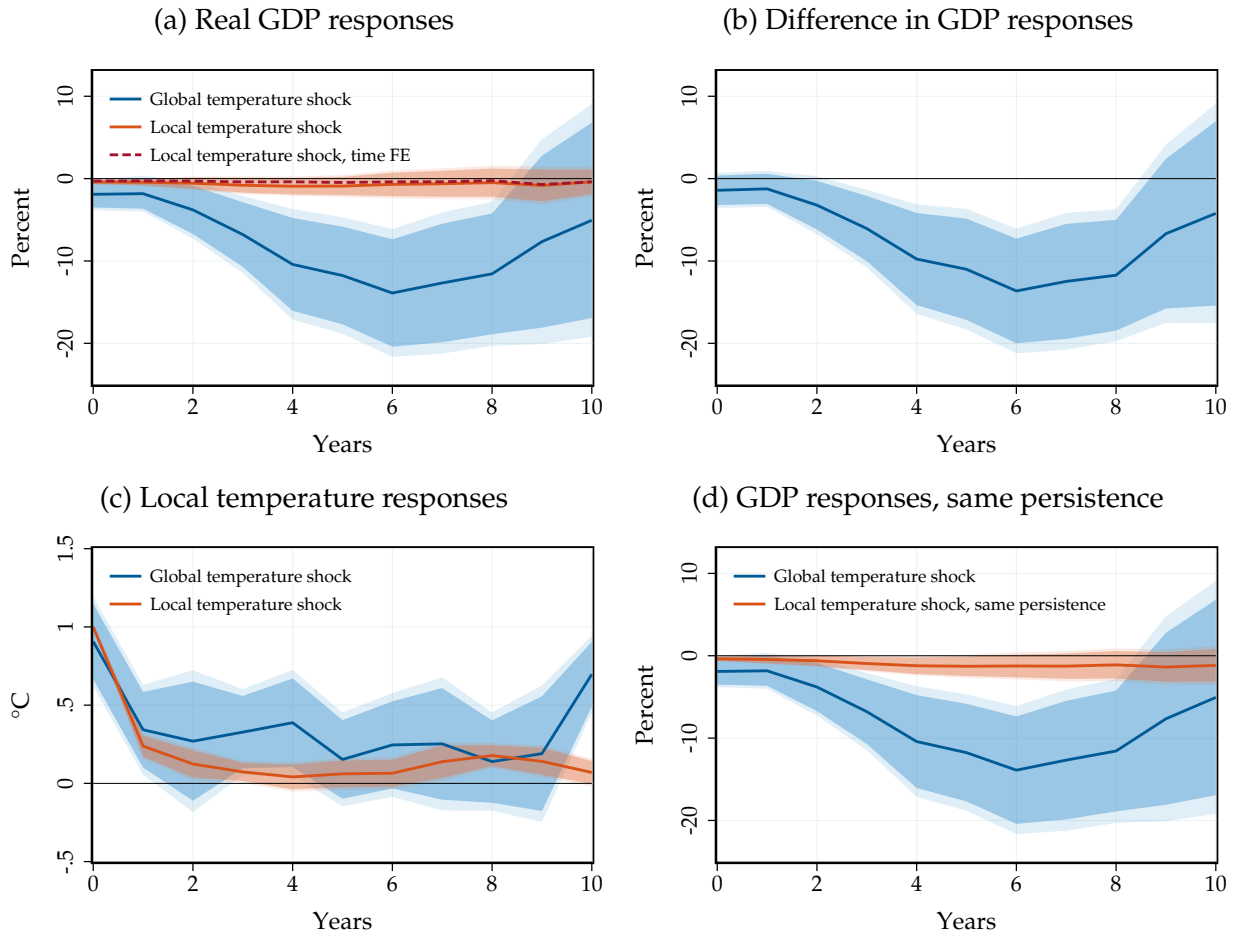

Impulse responses of GDP per capita, estimated in the PWT dataset over the period 1960-2019. Panel (a): solid lines: GDP responses to global and local temperature shocks based on (3); dashed red: GDP response to local temperature shock from model with time fixed effects, (4b). Panel (b): difference between GDP responses to global and local temperature shocks based on joint model (4a). Panel (c): local temperature response to temperature shocks. Panel (d): GDP responses imposing the persistence of the global temperature response on local temperature. Dark and light shaded areas: 90 and 95% confidence bands.

statistically different from each other. Specification (4b) includes time fixed effects, which allows us to flexibly control for any unobserved common shocks. In that case, the time fixed effects absorb the global temperature shocks and any other global controls.

Figure 7(a) shows the estimated impulse responses to a local temperature shock of 1°C, together with the responses to a global temperature shock from Section 3.1. Local temperature shocks lead to a fall in real GDP, even though the response is not statistically significant at the 5% level. On impact, the effect stands at -0.5% and reaches -1% after 4 years. These point estimates and associated uncertainty are similar to previous findings in Dell et al. (2012), Burke et al. (2015), Moore and Diaz (2015), Kahn et al. (2021) and Nath

et al. (2024) when aggregated across all countries and accounting for the empirical degree of persistence, and of course mask a substantial degree of underlying heterogeneity. Controlling for time fixed effects does not make much of a difference. If at all, the inclusion of time fixed effects attenuates the impacts of local temperature somewhat.

The comparison reveals that global temperature shocks have more pronounced impacts on economic activity than local temperature shocks. The estimated effects of global temperature shocks are an order of magnitude larger than those of local temperature shocks, based on the same empirical model and the same sample period. This difference is not only economically but also statistically significant. Panel (b) reveals that the responses of GDP to global and local temperature shocks over our horizon of interest based on (4a) are statistically different at the 5% level in years 3 to 8.[9]

One possible explanation for the differential impact of global and local temperature shocks is statistical: global temperature shocks may lead to a more pronounced increase in local temperature. Figure 7(c) shows the response of local temperature to a local and a global temperature shock, respectively. On impact, both local and global temperature shocks lead to an increase in local temperature near 1°C. Yet, the increase in local temperature is somewhat more persistent after a global temperature shock.[10]

To account for this difference in persistence, we construct a counterfactual local temperature shock, imposing the same internal persistence as for the global shock, using again the method in Sims (1986). Figure 7(d) shows that the difference in persistence cannot account for the differential impact of global and local temperature shocks. Imposing the same persistence increases the impacts of local temperature somewhat, but the cumulative effects of global temperature shocks are still an order of magnitude larger.

Alternatively, we convert our local temperature estimates into the counterfactual impact of a permanent 1°C rise in local temperature. As in Section 2, we calculate the ratio of the cumulative impulse response of output per capita to the cumulative impulse response of local temperature. We find that a permanent 1°C rise in local temperature leads to a 3%

[9]Estimating the effect of both shocks simultaneously does not change the univariate impulse responses materially, reflecting that different variation identifies the impact of global and local temperature shocks. See Appendix C.2 for details.

[10]Our unweighted regression implies that the time 0 impact of global temperature is close to 1°C. When area-weighted, the global temperature time 0 impact is larger than 1°C, as land warms more than oceans on average. See Figure C.7 in Appendix C.6.

reduction in long-run world GDP, almost exactly as in Nath et al. (2024). However, this effect is not statistically distinguishable from zero at the 5% level in our sample.

Our analysis thus indicates that the key difference lies in the nature of the shock itself rather than in the set of global controls, time fixed effects or persistence of temperature to the shock. Climatic variation within country or even smaller geographic units may help alleviate identification concerns, but misses any global effects of climate change—itself a global phenomenon. By contrast, our approach purposefully studies these common effects by focusing on climatic variation at the global level.

4.2 Reconciling the Impacts of Global and Local Temperature

Why, then, does global temperature cause larger economic losses than local temperature? We start with our main hypothesis: global temperature shocks are inherently different from local temperature shocks and capture potentially damaging climatic implications that local temperature does not. Next, we discuss alternative explanations based on economic spillovers.

We first investigate whether global temperature predicts meaningful shifts in climatic phenomena. We ask how temperature shocks correlate with the likelihood of extreme weather events: extreme temperature, drought, extreme precipitation, and extreme wind speed. As detailed in Section 2.1 and Appendix A, we define an exposure index for each of these events as follows. We start by constructing average temperature, precipitation and wind speed for each country and day. Next, we count the fraction of days within each year and country for which this country weather average exceeds or falls below a given threshold. This exposure index can thus be interpreted as a probability. We use the panel local projection specification (3) and denote by θ_h^X the impact of a 1°C temperature shock on the exposure index of event X at horizon h. Figure 8 displays our results.

Local temperature shocks lead to an increase in the share of extreme heat and drought days. However, global temperature shocks lead to a noticeably larger increase in these extremes. Our extreme heat and drought indices have a baseline probability of 0.05 and 0.25 in 1950-1980, respectively. Thus, a 1°C global temperature shock correlates with a five-fold rise in the frequency of extreme heat and a 15% increase of the frequency of droughts—an order of magnitude more than for local temperature shocks. The contrast

Figure 8: Extreme Weather Events and Temperature

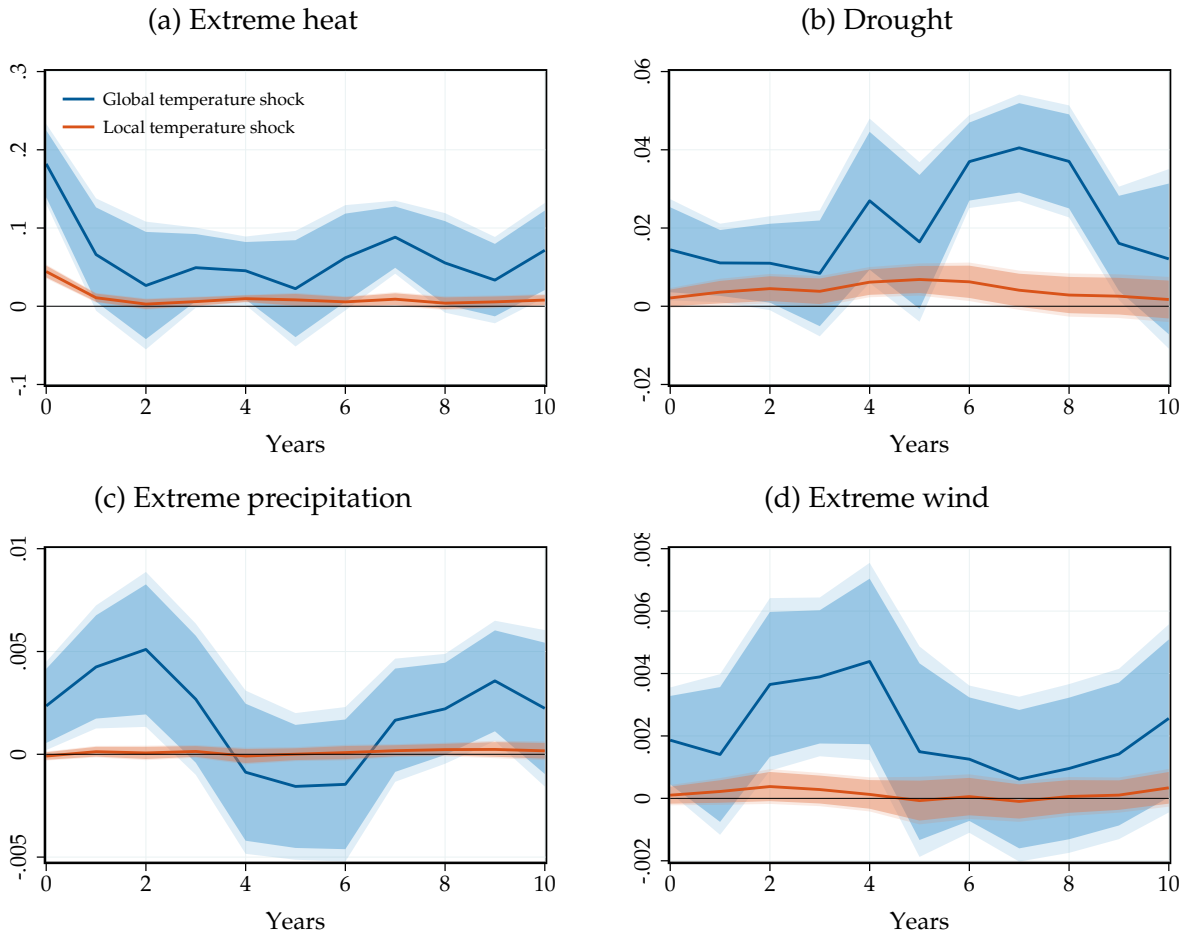

Impulse responses θ_h^X of extreme temperature, drought, extreme precipitation, and extreme wind exposures to global and local temperature shocks, estimated based on (3) with the expanded set of global controls over PWT sample 1960-2019. Extreme weather exposure indices record the share of days in a given year and country where country-level average daily temperature, precipitation, or wind speed are above or below a threshold. We define thresholds using the daily weather distribution in 1950-1980. Temperature: above 95th percentile. Drought: below the 25th percentile. Precipitation: above the 99th percentile. Wind: above the 99th percentile. Though not necessary for our results, we smooth the precipitation and wind measures with a backward-looking (current and previous two years) moving average to remove their inherent noise. Solid lines: point estimate. Dark and light shaded areas: 90 and 95% confidence bands.

is even starker for extreme precipitation and extreme wind speed: global temperature shocks predict a large increase in their frequency, while local temperature shocks have no significant effect. We construct extreme precipitation and wind indices to have a baseline probability of 0.01 in 1950-1980. Thus, a 1°C global temperature shock correlates with an increase in the frequency of extreme precipitation by over 50% and extreme wind by nearly 40%.

These findings are consistent with the geoscience literature: wind speed and precip-

itation are outcomes of the global climate—through oceanic warming and atmospheric humidity—rather than outcomes of local temperature distributions (Seneviratne et al., 2016; Wartenburger et al., 2017; Seneviratne et al., 2021; Domeisen et al., 2023). Given that extreme climatic events are known to cause economic damage (Deschênes and Greenstone, 2011; Hsiang and Jina, 2014; Bilal and Rossi-Hansberg, 2023), the differential correlation of global versus local temperature shocks on extreme climatic events may rationalize the larger economic effects of global temperature shocks.

To gauge the quantitative importance of this channel, we start by estimating the impact of local extreme events in a panel local projection specification, detailed in Appendix C.4. We estimate these impacts jointly to account for the potential correlation between extreme events. We denote by ϕ_h^X the impact of extreme event X's exposure index on GDP at horizon h. Figure C.4 in Appendix C.4 reveals that these events are associated with economic damages. A five-fold rise in extreme heat exposure at the country level lowers GDP by 2% at peak. A 15% rise in drought exposure lowers GDP by 1.5%. A 50% increase in extreme precipitation lowers GDP by 0.5% and a 40% increase in wind exposure lowers output by 0.4%.

Next, we aggregate the local impacts of extreme events. We interact the increase in extreme event exposure following a global temperature shock θ_h^X from Figure 8 with the GDP loss associated with these extreme events from Figure C.4 in Appendix C.4. To do so, we adjust the estimates ϕ_h^X to correspond to a one-time fully transitory rise in exposure using again the method in Sims (1986). This persistence adjustment transforms the initial estimates ϕ_h^X into new estimates ψ_h^X. In practice, this adjustment has minor consequences because extreme events have low unconditional internal persistence. We then aggregate these impacts according to $\Theta_h = \sum_X \sum_{t=0}^{h} \theta_t^X \psi_{h-t}^X$, where the sum over X includes the four extreme events and local temperature. Thus, the aggregate impact Θ_h now factors in the persistent response of extreme events to a global temperature shock $\{\theta_h^X\}_h$.

Figure 9(a) displays our results. The rise in local temperature and extremes leads to a meaningfully larger economic impact than for local temperature alone. The peak effect on GDP is in excess of 6% and the cumulative impact represents over half of the cumulative effect of a global temperature shock. This result indicates that global temperature has a larger impact on economic activity than local temperature largely because the physical

Figure 9: The Role of Ocean Temperature and Extreme Events

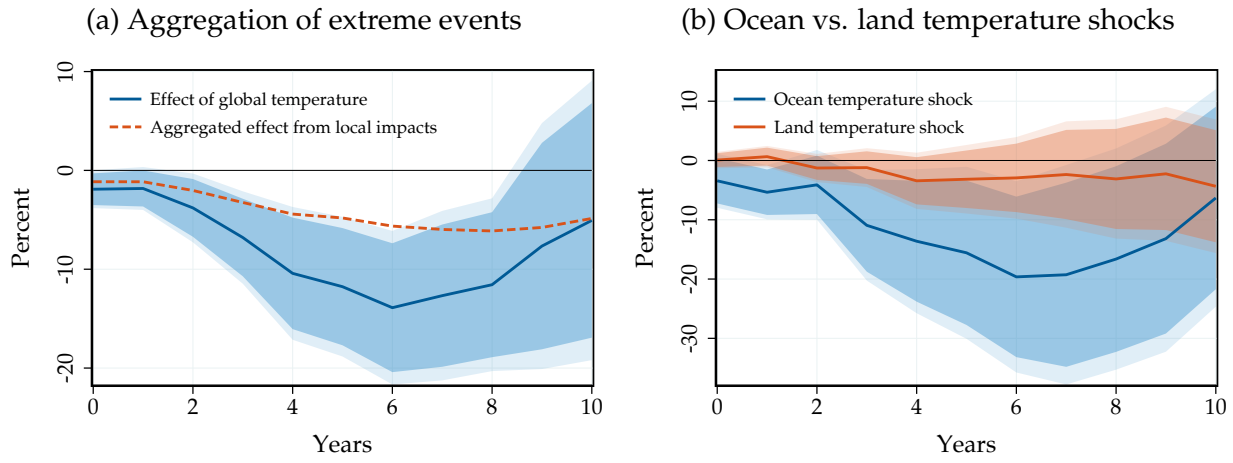

Panel (a): aggregated effect on GDP based on local temperature and extreme events impacts Θ_h (dashed red) together with the impulse responses to a global temperature shock based on our baseline empirical model (3) in PWT sample 1960-2019. Panel (b): impulse responses of GDP to an ocean temperature and a land temperature shock, estimated jointly using (4a). Dark and light shaded areas: 90 and 95% confidence bands.

nature of the shock is different: it captures the broader implications of warming and in particular the rise in damaging extreme events.

We confirm our transmission channel of global temperature shocks through extreme events by considering ocean and land temperature. Since oceanic warming is critical for the formation of some of our extreme events, we expect it to account for a large part of our global temperature impacts. We jointly estimate the impact of ocean and land temperature shocks on GDP in Figure 9(b). The impact of ocean temperature on GDP aligns with the overall effect of global temperature—if anything, it is larger—suggesting that ocean temperatures are key to understand the impact of warming on economic activity. The impact of land temperature is smaller than ocean temperature, though more pronounced than the impact of local temperature, suggesting that spatially correlated changes in local temperature may co-move with more extreme events than idiosyncratic temperature fluctuations. Yet, these comparisons are noisy and should be interpreted with caution.

Our results highlight that it is critical to consider climatic outcomes beyond local temperature in panel approaches, but also illustrate the challenges associated with such "bottom-up" aggregation exercises. Capturing all relevant local impacts individually is challenging: researchers need to know ex-ante which variables to consider, be able to measure them consistently throughout the world, and accurately estimate their degree of

internal persistence. Even then, Figure 9(a) suggests that this "bottom-up" aggregation approach still underestimates the full impact of global temperature even with four measures of extreme events. A key advantage of our time-series approach is that it directly encompasses all relevant local impacts that are predictable by global temperature.

A prominent alternative explanation to rationalize the gap between local and global temperature impacts is that local temperature is the true determinant of damages but compounds through economic spillovers that are however netted out in the panel specification. We empirically test this possibility using bilateral trade data in Appendix C.5. Consistent with our geophysical interpretation, we find that although trade spillovers do appear to matter marginally, they fall short of accounting for a sizable fraction of the gap between local and global temperature estimates.

4.3 Margins of GDP and Regional Impacts

We have documented that global temperature shocks lower world GDP, but how and where does GDP respond most?

We evaluate the effects of global temperature shocks on capital, investment and productivity in our PWT panel in Figure 10. Global temperature shocks lead to a significant fall in investment and in the capital stock. Consistently with Hsiang and Jina (2014), we find that disasters associated with global warming do not stimulate growth. Instead, national income, productive capital and investment all dwindle. Total Factor Productivity (TFP) as estimated in the Penn World Tables and labor productivity fall significantly after global temperature shocks. The effects strengthen from -2% on impact to over -10% after four years.

In addition to unpacking the margins of GDP, we analyze how the impact of global temperature varies across different regions. Are warmer or lower-income countries more affected? Figure 11 displays the impact of global temperature shocks on nine regions of the world. Almost all regions experience GDP losses. We estimate the strongest negative effects—close to -20% at peak—in hot regions such as Southeast Asia and Sub-Saharan Africa. Contrary to local temperature, global temperature leads to adverse economic effects even in higher-income, colder regions. The peak effect in North America and in Europe is near -10%, albeit not very precisely estimated.

Figure 10: Transmission of Global Temperature Shocks

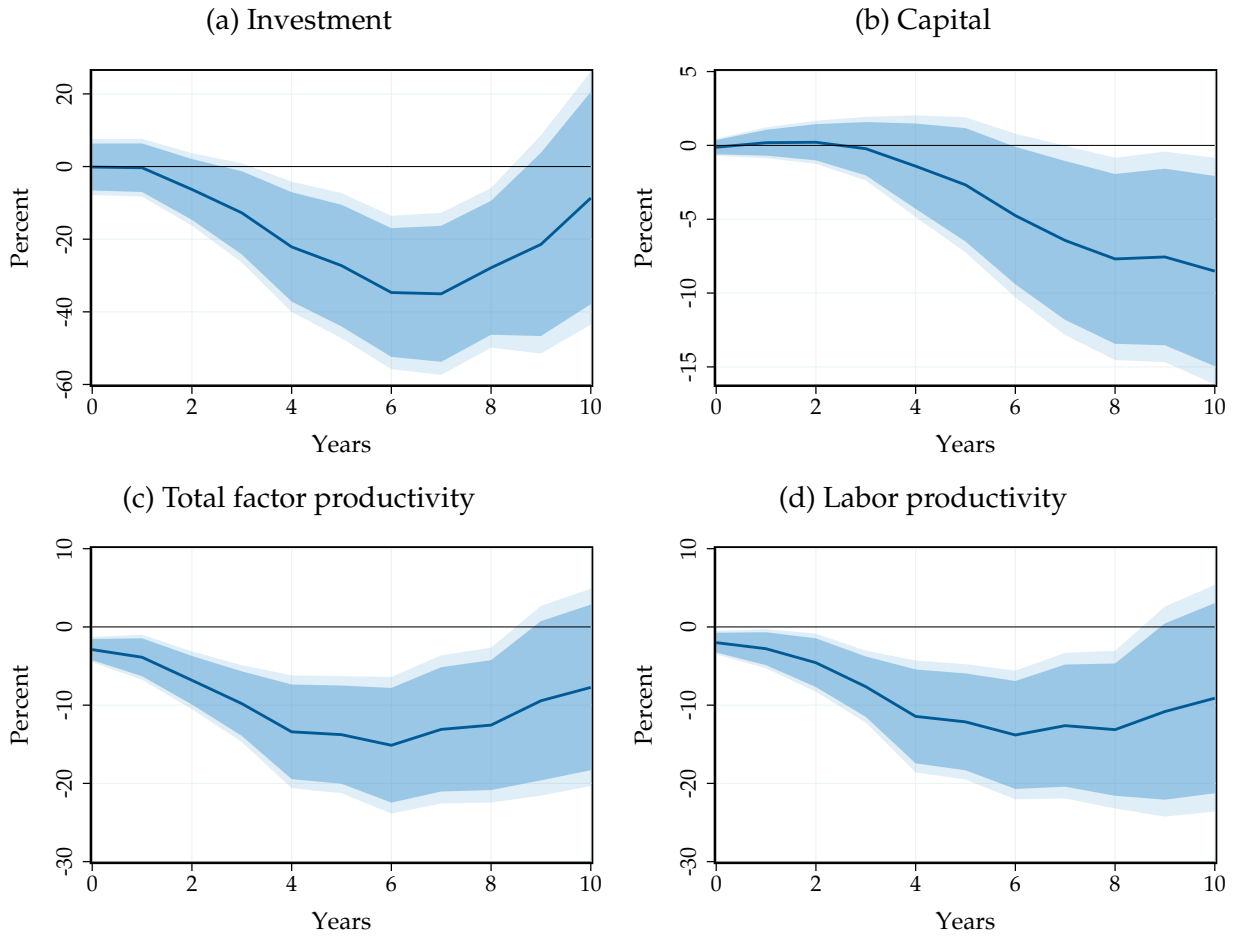

Impulse responses of investment per capita, the capital stock per capita, total factor productivity and labor productivity to a global temperature shock, estimated based on (3) over PWT sample 1960-2019. Labor productivity: output over employment. Total factor productivity: Penn World Tables. Solid line: point estimate. Dark and light shaded areas: 90 and 95% confidence bands.

We corroborate that our estimates are not driven by particularly affected regions by re-estimating our world specification from Section 3 after excluding Sub-Saharan Africa from the sample. Figure B.12 in Appendix B.9 reveals that the average world impacts remain largely unchanged.

We evaluate whether the impact of global temperature shocks systematically varies by country baseline temperature and income level in Figure C.9, Appendix C.7. Although somewhat imprecisely estimated, we find suggestive evidence that warm and low-income countries display stronger adverse effects of global temperature shocks, while cold and high-income countries are less sensitive to global temperature shocks. This result is qualitatively consistent with previous evidence on local temperature (Dell

Figure 11: Regional Impacts of Global Temperature Shocks

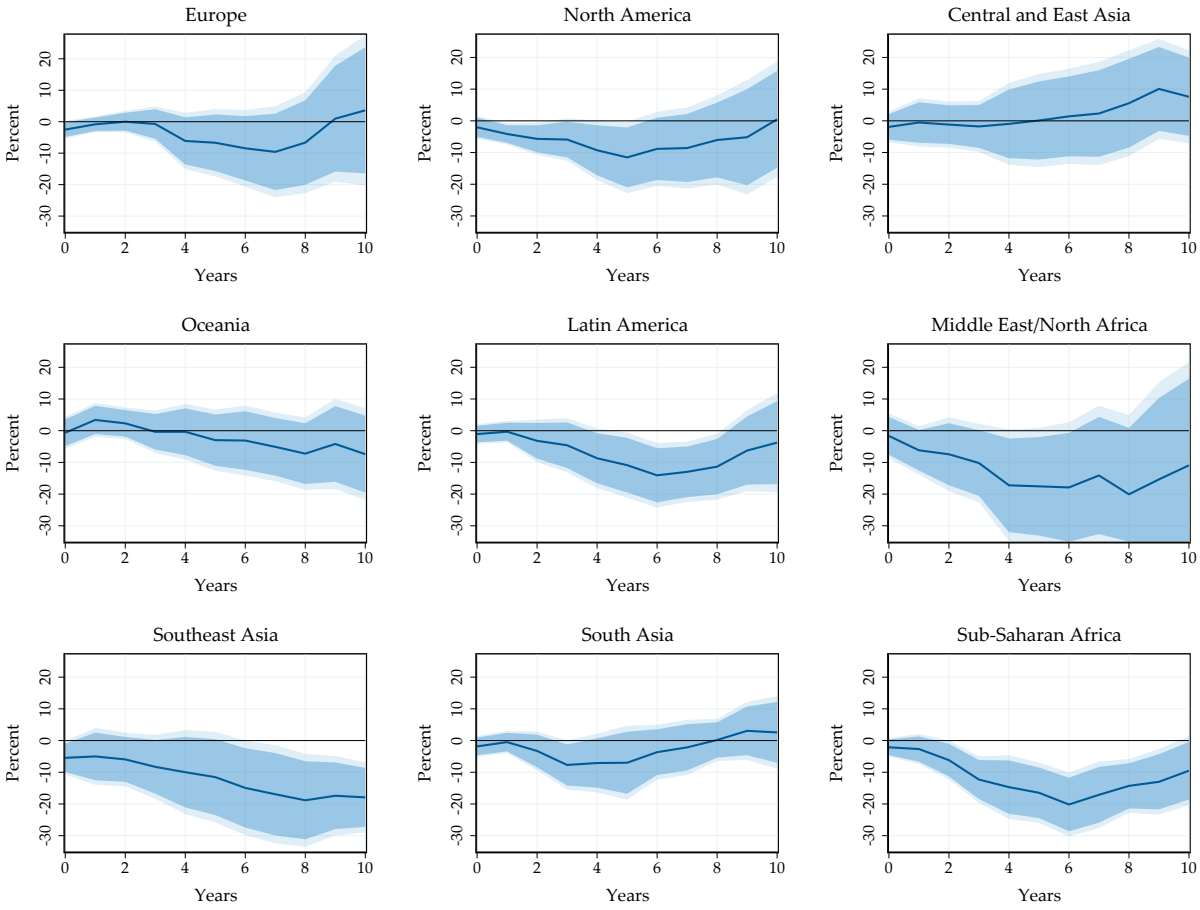

Impulse responses of GDP per capita to global temperature shocks for different regions across the world based on (3) over PWT sample 1960-2019, conditioning on the different regions. Solid lines: point estimate. Dark and light shaded areas: 90 and 95% confidence bands. Impulse responses of local temperature to global temperature shocks by region in Figure C.10, Appendix C.7.

et al., 2012; Burke et al., 2015). Quantitatively, however, global temperature shocks have larger and more uniformly detrimental effects than local temperature shocks.

So far we established the reduced-form impact of global temperature shocks on economic activity at the world and country level in the medium run. We now turn to our structural model to convert these estimates into long-run impacts, and calculate welfare losses and the Social Cost of Carbon.

5 A Model of Climate Change Across the World

Our framework closely follows the standard neoclassical growth model. As such, it mirrors the backbone of the Dynamic Integrated Climate Economy (DICE) model introduced by Nordhaus (1992) and developed in Barrage and Nordhaus (2024). Our key innovation is to use our reduced-form estimates of the impact of global temperature shocks to structurally estimate damage functions in the model.

5.1 Model Description

Setup. Time is continuous and runs forever. There is a unit continuum of infinitely-lived identical households who populate the world economy. Households have Constant Relative Risk Aversion flow preferences: $U(C) = \frac{C^{1-\gamma}-1}{1-\gamma}$. Labor supply is exogenous and set to $L_t = 1$. The pure rate of time preference of households is ρ.

Firms produce according to a Cobb-Douglas production function in capital K_t and labor L_t with time-dependent TFP Z_t: $Y_t = Z_t K_t^{\alpha} L_t^{1-\alpha}$. They hire labor and rent capital from households in competitive factor markets. Capital depreciates at rate δ, which is constant over time and covered by firms. The path of productivity Z_t is perfectly foreseen.

Households earn wages w_t, hold capital K_t and rent it out to firms for production. The net interest rate is r_t. Firms make zero profits given constant returns to scale, so we omit profits in the budget constraint of the household, which writes: $C_t + \dot{K}_t = w_t + r_t K_t$. Households are endowed with an initial capital stock K_0.

A competitive equilibrium of our economy is a collection of sequences $\{C_t, K_t, r_t, w_t\}_{t=0}^{\infty}$ such that households optimize given prices $\{r_t, w_t\}_{t=0}^{\infty}$:

$$\max_{\{C_t, K_t\}_t} \int_0^{\infty} e^{-\rho t} U(C_t) dt \quad \text{subject to} \quad C_t + \dot{K}_t = w_t + r_t K_t \quad \text{given } K_0;$$

firms optimize given prices $\{r_t, w_t\}_t$: $\max_{K_t^D, L_t^D} Z_t (K_t^D)^{\alpha} (L_t^D)^{1-\alpha} - (r_t + \delta) K_t^D - w_t L_t^D$; and factor markets clear: $K_t = K_t^D$ and $1 = L_t^D$.

Climate change. We model climate change as changes in TFP Z_t over time, relative to its baseline value Z_0. This representation follows existing work (Nordhaus, 1992; Nordhaus

and Yang, 1996; Moore and Diaz, 2015; Kahn et al., 2021) and parsimoniously but comprehensively captures the combined effects of the rich set of weather extremes described in Section 4.2 on world economic activity. We leave a richer representation based on natural disasters at the country level for future work (Barro, 2006; Barro, 2009).

We take the path of global mean temperature T_t relative to a reference level T_0 as given, and denote by $\widehat{T}_t \equiv T_t - T_0$ the path of excess temperature. Global mean temperature affects TFP through the structural damage function $\{\zeta_s\}_{s\geq 0}$:

$$Z_t = Z_0 \exp\left(\int_0^t \zeta_s \widehat{T}_{t-s} ds\right). \tag{6}$$

The structural damage function ζ_s governs the persistence of the effect of transitory global temperature shocks on TFP. When ζ_s is a Dirac mass point at $s = 0$, global temperature shocks have purely transitory level effects. When ζ_s is a positive function that asymptotes to zero, global temperature shocks have persistent level effects. When ζ_s is a positive function that asymptotes to a positive value, global temperature shocks have growth effects.

When temperature $T_t \equiv \overline{T}$ is constant, the economy converges to its steady-state with the corresponding value of TFP $\overline{Z} = Z_0 \exp\left((\overline{T} - T_0)\int_0^\infty \zeta_s ds\right)$. This expression highlights that the cumulative damage function $\int_0^\infty \zeta_s ds$ determines the long-run impact of global temperature changes. In that case, ζ_s needs to be integrable to obtain a well-defined steady-state. Hence, under growth effects, there is no well-defined steady-state and the economy asymptotes to zero for any amount of permanent warming. Yet, in Figure 3 we do not find statistically significant evidence supporting growth effects.

We do not model the feedback between the economy and emissions, and associated externalities, because we focus on climate damages. Thus, the competitive equilibrium is efficient as is standard in the neoclassical growth model.

Social Cost of Carbon. In our framework, we define the Social Cost of Carbon as the one-time dollar amount $\mathcal{C}$ that households would pay at time 0 that would make them indifferent between a world with an additional ton of CO2 emitted at time 0, and a world starting in steady-state, without emissions, but having paid $\mathcal{C}$.

Given that we do not model emissions directly, we must map a one-time CO2 pulse into a temperature path in order to calculate the SCC. We follow Folini et al. (2024) and use the temperature response of global mean temperature to a CO2 pulse from Dietz et al. (2021a), itself based on Joos et al. (2013).

We denote by $\{\widehat{T}_t^{\text{SCC}}\}_{t\geq 0}$ the path of excess warming implied by a one-time pulse of one ton of CO2 emitted at time 0. The median response in Dietz et al. (2021a) indicates that after a 1 gigaton pulse of carbon, temperature rises steadily and eventually stabilizes at 0.002°C after 15 years.[11] Our welfare numbers do not depend on the temperature response to a CO2 pulse, but instead on a particular warming scenario.

We then construct a productivity path $\{Z_t^{\text{SCC}}\}_{t\geq 0}$ according to equation (6) in which we use the temperature path $\{\widehat{T}_t^{\text{SCC}}\}_{t\geq 0}$ rather than a global warming scenario. The model delivers a path of value functions $\{V_t^{\text{SCC}}(K)\}_{t\geq 0}$, equilibrium capital stocks $\{K_t^{\text{SCC}}\}_{t\geq 0}$ with initial condition $K_0^{\text{SCC}} = K^{ss}$, leading to a path of realized values $\{V_t^{\text{SCC}}(K_t^{\text{SCC}})\}_{t\geq 0}$, in response to this CO2 pulse-induced warming. Our definition requires that the SCC $\mathcal{C}$ be given implicitly by:

$$V^{ss}(K^{ss} - \mathcal{C}) = V_0^{\text{SCC}}(K^{ss}), \tag{7}$$

where *ss* superscripts denote initial steady-state quantities.

To gain intuition, consider the case when the SCC is not too large. Then, a first order perturbation implies that the SCC satisfies $\mathcal{C} = \int_0^\infty e^{-\rho t} u'(C^{ss})(C^{ss} - C_t^{\text{SCC}})dt = \frac{1}{\rho}\frac{C^{ss} - \overline{C}^{\text{SCC}}}{C^{ss}}$, where $\frac{C^{ss} - \overline{C}^{\text{SCC}}}{C^{ss}}$ is the consumption-equivalent welfare loss from the warming implied by the CO2 pulse. These identities highlight that the SCC is equal to the present stock valuation of flow consumption-equivalent welfare losses from the warming induced by the CO2 pulse. While these conditions are useful to gain intuition, in our quantification we always use the nonlinear definition (7) that accounts for a time-varying marginal rate of substitution.

[11] For brevity, we refer to the 'best fit CMIP5 ensemble' response in Dietz et al. (2021a) as 'median response'.

5.2 Estimation Strategy

Our next step is to estimate the structural damage function ζ_s. To do so, we match the reduced-form impulse response functions of output to global temperature shocks from Figure 7(a). We proceed in two steps.

In the first step, we calibrate our model based on standard values from the literature, with the exception of our damage function. We set risk-aversion to $\gamma = 1$. The capital share is $\alpha = 0.33$. The annual capital depreciation rate is $\delta = 0.08$. Our choice of annual pure rate of time preference $\rho = 0.02$ follows Rennert et al. (2022) and is consistent with a 2% annual interest rate in steady-state. Of course, the equilibrium path of consumption in the model determines the effective consumption-based discount rate. We assess the robustness of our results with respect to the rate of time preference in Section 6.4 below.[12]

In the second step, we invert our model to estimate the sequence of TFP that corresponds to a temperature shock. We leverage that the actual temperature shocks that arise during our sample are small as in Figure C.1 and therefore imply output and capital fluctuations of the order of 1%. Therefore, we can use a first-order perturbation of the model around the initial steady-state for estimation. For any sequence of excess temperature $\widehat{T}_t$, we denote by $\widehat{z}_t$ the resulting log deviation in TFP, and by $\widehat{y}_t$ the log deviation in output along the transition. We emphasize that we use log-linearization for estimation only, not for counterfactuals.

Proposition 1. *(Model inversion)*
There exists $\mathcal{K}_{t,s}$ given in Appendix D.3, that only depends on steady-state objects and is independent from $\{\zeta_s\}_{s\geq 0}$, such that, to a first order in $\{\widehat{T}_t\}_{t\geq 0}$:

$$\widehat{y}_t = \widehat{z}_t + \alpha \int_0^\infty \mathcal{K}_{t,s}\widehat{z}_s ds.$$

Proof. See Appendix D.3. □

Proposition 1 delivers an identification result. Given observed output response $\widehat{y}_t$,

[12] This framework immediately accommodates balanced productivity growth. Provided we adjust the the rate of time preference and the baseline capital depreciation rate, standard rescaling arguments ensure that allocations and welfare would be identical in counterfactuals when the baseline economy is in steady-state or on a balanced growth path. See Weitzman (1998), Stern (2006), Nordhaus (2007), Dasgupta (2008), and Kelleher and Wagner (2018) for additional discussion of the discount rate.

we can recover the underlying sequence of productivity shocks $\widehat{z}_t$. The first component in Proposition 1 corresponds to the direct effect of productivity on output. The second component corresponds to the equilibrium response of capital. It is an integral over all times because investment is forward-looking and capital accumulates slowly over time.

The main content of Proposition 1 lies in this second component. By log-linearizing equilibrium conditions and solving explicitly for the equilibrium sequence of capital, we relate capital deviations to the sequence of productivity shocks through the sequence-space Jacobian $\mathcal{K}_{t,s}$ (Auclert et al., 2021; Bilal and Goyal, 2023). In the context of the neoclassical growth model, this Jacobian admits a closed-form expression as a function of parameters and steady-state objects. When $\mathrm{Id} - \alpha\mathcal{K}$ is invertible—where Id denotes the identity map, for instance when α is small enough—productivity shocks are identified. Proposition 1 allows us to obtain the sequence of TFP $\widehat{z}_t$ that correspond to any sequence of temperature shocks $\widehat{T}_t$.

We use Proposition 1 to estimate ζ_s. We consider the response of output to an observed temperature shock in Figure 3(b), that corresponds to the underlying temperature path $\widehat{T}_t$ in Figure 3(a). Proposition 1 delivers the corresponding sequence of productivity shocks $\widehat{z}_t$. We then identify ζ_t as the innovations to these sequences as per equation (6).

This approach is consistent with households having rational expectations about future temperature shocks: after a temperature shock, households expect temperature to remain persistently elevated as in Figure 3(a). One advantage of this approach is that we identify damage functions from empirical impulse responses to a shock that is itself persistent. Thus, counterfactuals that focus on a permanent increase in temperature build on moments identified from responses to a persistent shock—though not a fully permanent shock—rather than a purely transitory shock.

In practice, we face two additional challenges. We address both of them by imposing a smooth functional form for our structural damage function. We constrain ζ_s to be of the form $A\left(e^{-Bs} - e^{-Cs}\right)$.

The first challenge that our constrained estimation addresses is that we can only estimate the impulse response functions $\widehat{y}_t$ up to a finite horizon. By contrast, Proposition 1 requires the entire impulse response function. We cannot simply set the output impulse response to 0 from year 11 onwards, as this may imply a large underlying capital

windfall gain or loss for the economy. By constraining the shape of the structural damage functions, we use our 11 data points to estimate the 3 damage function parameters.

The second challenge is to discipline the long-run effects of temperature shocks. By constraining the structural damage functions, we ensure that the effects of transitory temperature changes vanish in the very long run. If we estimated the structural damage functions entirely unconstrained and with a longer horizon, temperature shocks could potentially have longer-ranging but extremely imprecisely estimated effects. Therefore, our approach is conservative in that it limits the long-run impact of a one-time transitory temperature shock.

Hence, instead of exactly inverting the model, we estimate A, B and C for ζ_s using Non-Linear Least Squares to minimize the squared deviations from the equation in Proposition 1 for the first 10 years only.

5.3 Estimation Results

Figure 12 shows our estimation results. We target PWT impulse response functions in the main analysis to maximize comparability to existing work that evaluates the impact of local temperature. We show that, if anything, the impact of global temperature is larger when using the BU impulse response functions in Section 6.4.

Panel (a) reproduces the underlying temperature path from Figure 3. Panel (b) reveals that the estimated model closely fits the empirical response of output given its limited degrees of freedom. Of course, the model fit relies on our constrained functional form: if we did not constrain the damage function, the fit would be one-to-one.

Panel (c) depicts the estimated structural damage function ζ_s. It coincides with the productivity responses to a one-time transitory global temperature shock of 1°C. It implies a short-run productivity loss of 4% that takes place two years after the temperature shock. Despite the corresponding temperature shock being transitory, the impact on productivity decays only slowly and persists for up to 10 years. We compute confidence bands with the Delta-method as detailed in Appendix D.4. The damage function is statistically significant at the 5% level, and reflects the confidence bands around our empirical output response.[13]

[13]While our focus is on global climate damages, we study the implied regional damage functions associ-

Figure 12: Output, Capital and Productivity Global Temperature Shocks

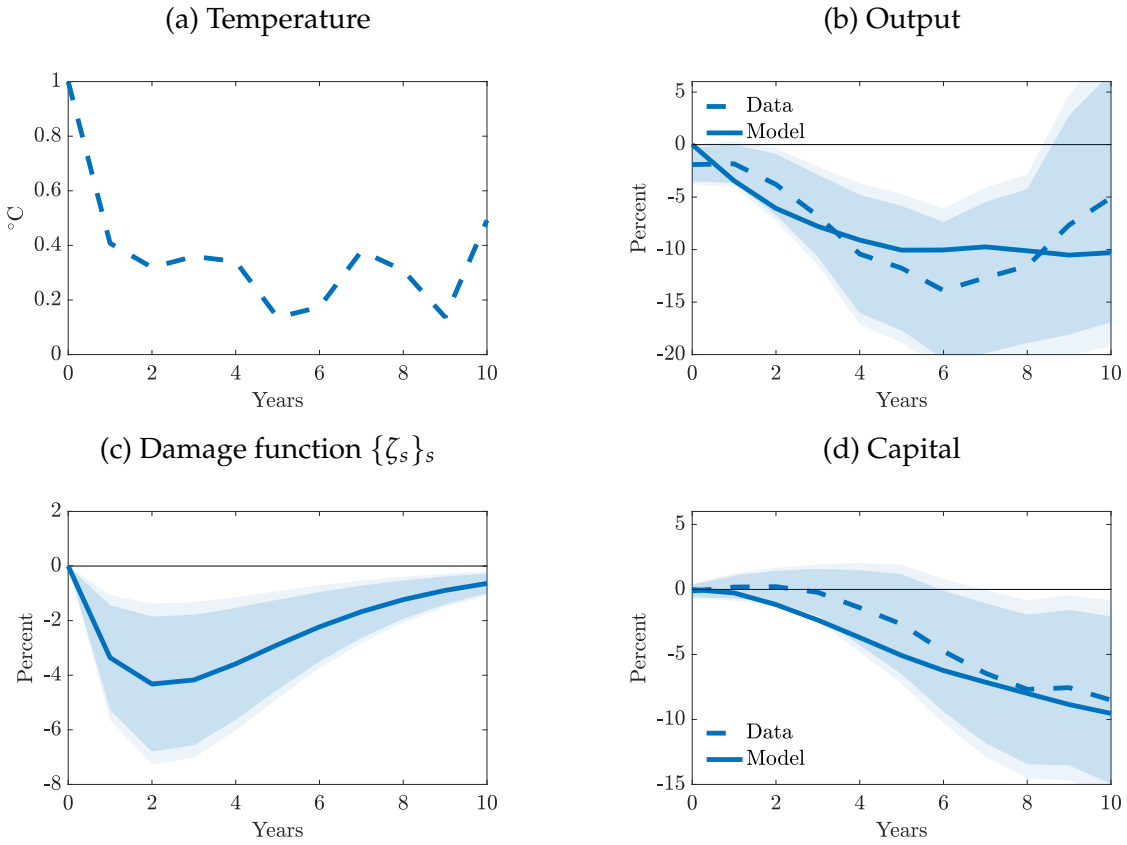

Estimation results from matching the model impulse response to the empirical response of output to global temperature shocks in the PWT data. Panel (a): underlying temperature path. Panel (b): output responses to this internally persistent temperature path. Panel (c): implied productivity shocks; confidence intervals based on the Delta-method as detailed in Appendix D.4. Panel (d): non-targeted capital responses to internally persistent temperature path. Dashed lines: data. Solid lines: model fit. Dark and light shaded areas: 90 and 95% confidence bands.

We test whether the estimated model also delivers empirically plausible implications for capital. In the estimation, we have not used any information about the empirical impulse response of capital to a global temperature shock. Panel (d) compares the prediction of our estimated model to the data from Figure 10. Despite being non-targeted, the response of capital in the model is close to its empirical counterpart.

How do the productivity effects of global temperature shocks compare to those associated with local temperature shocks? Given that the empirical responses for local temperature shocks are closer to zero as shown in Figure 7, such shocks likely also imply smaller damages. To answer this question quantitatively, we repeat our estimation but targeting

ated with our global temperature shocks in Appendices C.7 and D.5. Figure D.2 displays regional damage functions. Figure D.3 depicts counterfactual paths of GDP per capita for each region.

the impulse response of output to local temperature shocks.

Figure D.1 in Appendix D.5 displays the productivity effects of local temperature shocks. The damage function peaks at 0.5%, is not statistically different from zero at the 5% level, and the implied cumulative productivity effect is more than eight times smaller than under global temperature shocks. We conclude that climate damages associated with global temperature shocks are larger than those implied by local temperature shocks.

6 The Macroeconomic Impact of Climate Change

6.1 Representing Climate Change

To evaluate the consequences of climate change, we specify a path for global mean temperature. The baseline year $t = 0$ corresponds to 2024. The world subsequently warms by 3°C above preindustrial levels by 2100, after which temperature asymptotes to 3.3°C. This scenario is broadly consistent with IPCC business-as-usual scenarios that imply 3 to 4°C of warming by 2100 (Hausfather and Peters, 2020; Lee et al., 2023). Given that the world has warmed by approximately 1°C since preindustrial times, this scenario implies 2°C of additional warming since $t = 0$ (2024) by year $t = 76$ (2100).

We construct two counterfactuals to highlight the role of global temperature. In the first counterfactual, we use the structural damage function estimated under global temperature shocks ζ_s^{global} in Figure 12(c) to construct productivity changes using equation (6) together with excess temperature $\widehat{T}_t$. In the second counterfactual, we instead use the structural damage function estimated under local temperature shocks ζ_s^{local} in Figure D.1(c), Appendix D.5, using again equation (6) together with the same excess temperature path $\widehat{T}_t$.

Our counterfactuals compare allocations and welfare in an economy that warms according to $\widehat{T}_t$, to allocations and welfare in an economy that remains in steady-state under $\widehat{T}_t \equiv 0$. Welfare losses from climate change are defined as an equivalent percent decline in steady-state consumption. The SCC, which we report in 2024 international dollars, is defined in equation (7) and is independent from the global warming scenario because

it relies on the temperature response to a given CO2 pulse $\{\widehat{T}_t^{\text{SCC}}\}_{t\geq 0}$. Conversely, the welfare calculations are independent from $\{\widehat{T}_t^{\text{SCC}}\}_{t\geq 0}$. To solve for counterfactuals, we use standard global numerical methods to obtain the global solution—we only use log-linearization for estimation.

These counterfactuals assess the impact of gradually rising temperatures by multiple degrees using damage functions estimated under temperature shocks of smaller magnitude. In our framework, households can adjust to large anticipated temperature changes by shifting their consumption and investment behavior. Nevertheless, the parsimonious nature of our framework necessarily abstracts from other possible changes in behavior.

6.2 Economic Activity, Welfare and the Social Cost of Carbon

Figure 13 presents our main results. Panel (A) depicts the path of global mean temperature. Panel (B) reveals that output drops rapidly as global temperature rises, relative to a world that is not warming. In 2050, output declines by 28%. In 2100, output is 53% below what it would have been without climate change. This decline reflects accumulated productivity losses that reach 40%. These impacts are statistically significant at the 5% level.

Panel (C) highlights the adverse impact of lower productivity on capital accumulation. Initially, investment rises as households anticipate lower income going forward and therefore save, following standard permanent income logic. Capital starts decumulating rapidly thereafter under the pressure of lower output. By 2100, capital is 51% below what it would have been without climate change.

Panel (D) indicates that consumption drops, eventually reaching a 53% loss by 2100. This decline in consumption translates into substantial welfare losses. Panel (E) shows that the 2024 welfare impact of climate change amounts to a 35% loss in consumption equivalent percent. This welfare loss exceeds the initial consumption impact as households discount but value future declines in consumption as well. As temperature keeps rising, welfare continues to decline and reaches a 56% loss. All these values are statistically significant at the 5% level.

Our results point to significant economic costs of climate change. They are comparable to the U.S. Great Depression of 1929, but experienced permanently. They also correspond

Figure 13: Transitional Dynamics Under Climate Change

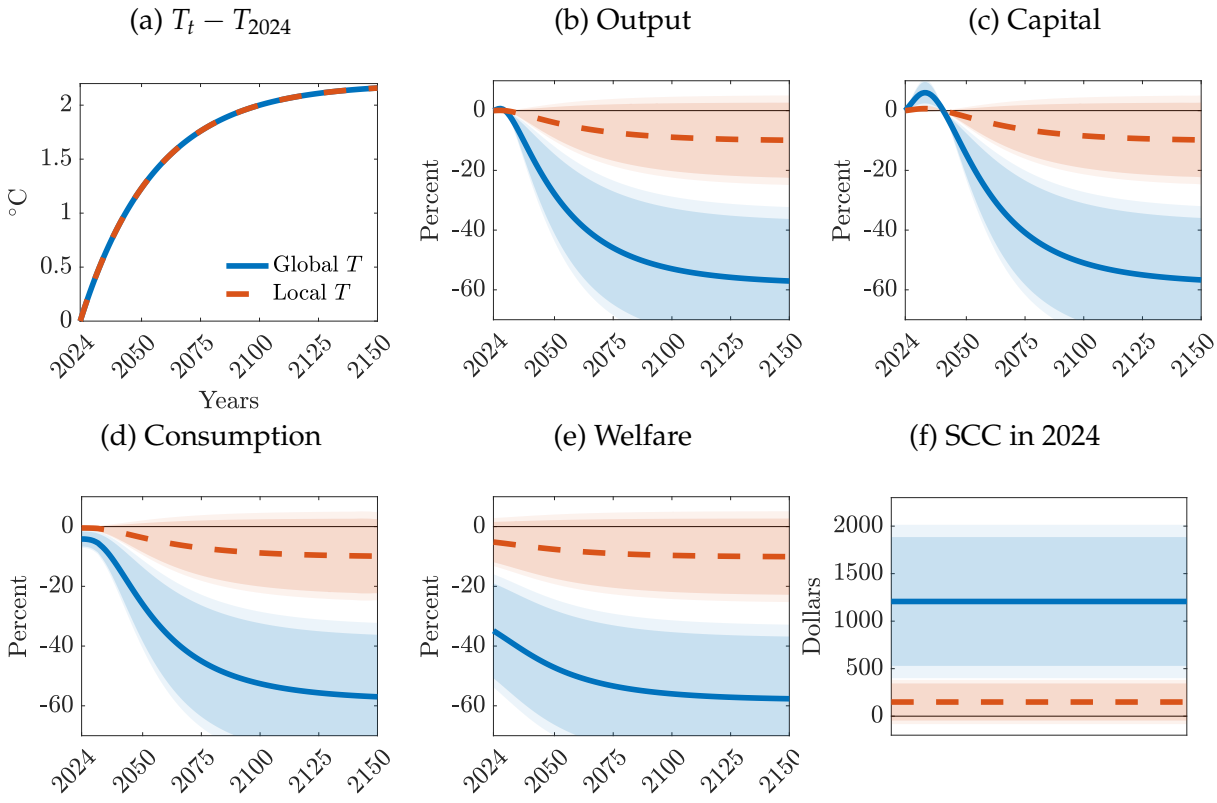

Transitional dynamics of the estimated model under the scenario in Panel (A). Solid blue lines: model estimated under global temperature. Shaded blue: 90 and 95% confidence intervals. Dashed red lines: model estimated under local temperature. Shaded red: 90 and 95% confidence intervals. Confidence intervals based on the Delta-method as detailed in Appendix D.4. Damage functions estimated in PWT data.

to approximately ten times the losses from moving from today's trade relations to complete autarky (Arkolakis et al., 2012). Of course, the cost of climate change is relative to a benchmark economy without climate change in which background economic growth may still take place.

Panel (F) uses our structural damage function to construct the SCC. We obtain a SCC of $1,207 per ton. This value is more than six times larger than the $185 per ton value in Rennert et al. (2022). The 95% confidence interval for the SCC ranges from $399 per ton to $2,015 per ton. Despite non-trivial uncertainty, even the lower bound of that confidence interval is several times larger than conventional SCC estimates.

Our focus on global temperature shocks is the main driver of these conclusions. Under local temperature damage functions, Figure 13 shows that climate change implies a 9% long-run output decline, a 5% present value welfare cost and a SCC of $149 per ton. None

Figure 14: Growth Accounting With Climate Change

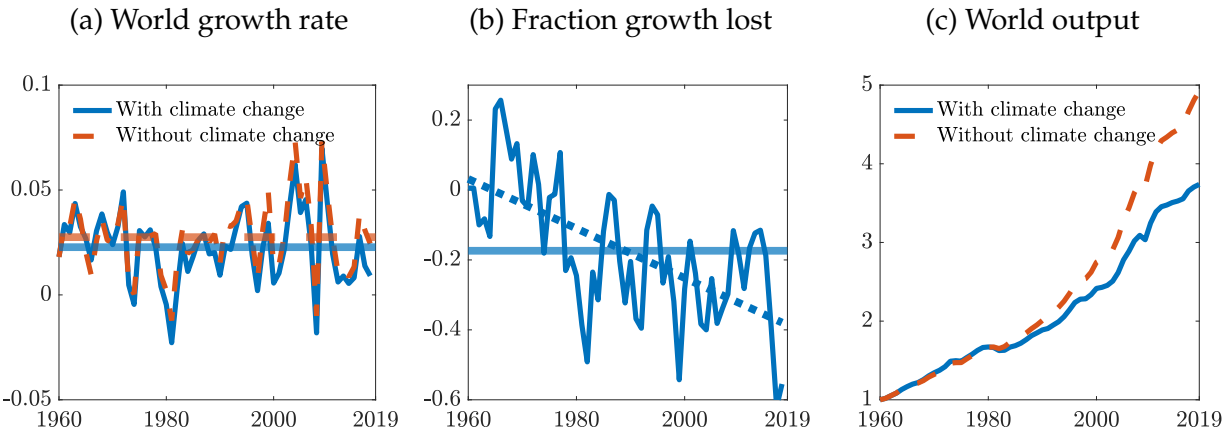

Impact of past climate change on world GDP. Panel (A): world output growth rate with (solid blue) and without (dashed red) climate change. Horizontal lines: sample averages. Panel (B): fraction of growth rate lost to climate change (annual growth loss out of 1960-2019 mean). Horizontal line: sample average. Dashed line: linear regression fit. Panel (C): world output with (solid blue) and without (dashed orange) climate change, normalized to one in 1960. Damage function estimated under global temperature in PWT data.

of these effects are statistically significant at the 5 or 10% level. These values and the associated uncertainty are consistent with results in Nordhaus (1992), Dell et al. (2012), Burke et al. (2015), Rennert et al. (2022), Barrage and Nordhaus (2024), and Nath et al. (2024). We conclude that global temperature effects are both larger and more precisely estimated than local temperature effects.

6.3 Growth Accounting

If the economic effects of global temperature are so large, why were they not noticed after nearly 1°C of global warming since 1960? We answer this question by analyzing the historical impact of climate change. We start the economy in 1960 and consider the realized path of warming until 2019, after which we impose constant temperature. We construct counterfactual changes in output relative to a baseline economy that remains in steady-state. We then add these changes directly to the data.

Figure 14 displays the results. Panel (A) reveals that climate change is responsible for moderate but persistent reductions in the world's annual growth rate. In the 1960s, there is little warming and thus little effect on economic growth. Between 1980 and 2019, potential growth without climate change deviates more systematically from realized growth with climate change. These results highlight that historical warming occurs in small incre-

ments. Warming shocks thus have moderate economic year-to-year effects in comparison to other economic shocks. The analysis in Sections 2 and 3 detects these effects that are otherwise hidden behind background economic variation.

Panels (B) and (C) show that the annual growth effects of climate change eventually accumulate because climate change is a permanent shift, despite having an initially moderate effect on growth. Panel (B) indicates that climate change reduces the world growth rate by as much as a third of baseline growth in the 21st century. Panel (C) shows that this growth slowdown implies that world GDP per capita would be 25% higher today had no warming occurred between 1960 and 2019. Even though in this counterfactual we hold temperature constant at its 2019 level in all subsequent years, economic losses continue to accumulate after 2019. These delayed impacts are due to the lagged productivity effects embedded in our estimated damage functions $\{\zeta_s\}_s$ and to the internal transitional dynamics of the neoclassical growth model. By 2040, output is 32% below its potential due to climate change: one quarter of the economic losses caused by past warming are yet to materialize.

6.4 Sensitivity

Given the magnitude of our results, we investigate which parameters may be particularly important for them. Figure 15 displays how our results depend on five key choices: the rate of time preference ρ, 2100 global mean temperature, the estimation sample, the climate sensitivity, and our treatment of expectations.

Panel (A) shows 2024 welfare losses as a function of the rate of time preference ρ, and panel (B) shows the corresponding SCC. As expected, a higher rate of time preference lowers welfare losses and the SCC: households then discount more damages that are far in the future. Our baseline rate of time preference $\rho = 0.02$ is consistent with Rennert et al. (2022) and with the secular decline in interest rates. However, welfare losses still exceed 20% at rates of time preference above 0.04. The corresponding SCC remains three times as large as the high end of previous estimates, and still seven times larger than the SCC based on local temperature under the same rate of time preference. By contrast, as we approach very low discount rates consistent with Stern (2006), welfare losses exceed 40% and the SCC rises above $2,500 per ton. Welfare losses are less sensitive to the discount

Figure 15: Welfare and the Social Cost of Carbon under Alternative Choices

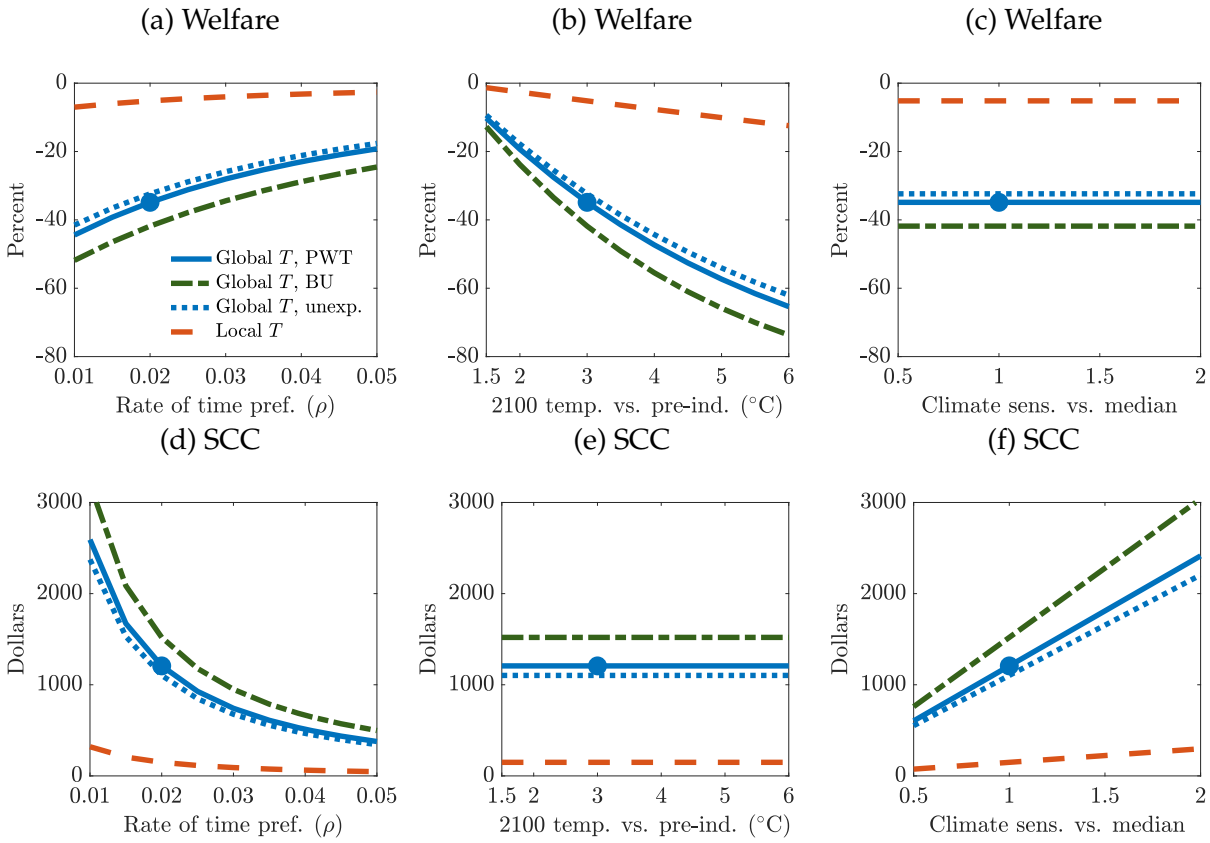

Sensitivity of welfare costs and Social Cost of Carbon in 2024 with respect to the rate of time preference (ρ), 2100 global mean temperature relative to preindustrial levels, the climate sensitivity, estimation sample, and treatment of expectations. Solid blue lines: model estimated using global temperature shocks under baseline expectations and PWT data. Dashed-dotted green lines: model estimated using global temperature shocks under baseline expectations and BU data. Dotted blue lines: model estimated using global temperature shocks with temperature shock surprises and PWT data. Dashed red lines: model estimated using local temperature shocks under baseline expectations and PWT data.

rate than the SCC because welfare losses represent an annualized flow of losses, while the SCC is a discounted stock valuation.

Panels (C) and (D) show welfare losses and the SCC when we vary 2100 temperature relative to preindustrial levels. Welfare losses under 15% materialize only at very low warming scenarios of 1.5°C since preindustrial levels by 2100. The IPCC evaluates that the world is on track for 3°C to 4°C above preindustrial levels under business as usual: global mean temperatures already largely exceed 1°C since preindustrial levels, and in 2023 reached 1.45°C since preindustrial levels. By contrast, scenarios under which global mean temperatures reach 6°C since preindustrial levels in 2100 lead to present value welfare losses of 60%. In Panel (D), the 2024 SCC is independent from the warming scenario

because it only depends on the temperature response to a CO2 pulse given our definition.

Panels (E) and (F) display how the climate sensitivity affect our conclusions. The climate sensitivity governs how carbon emissions map into current and future warming. Consequently, welfare losses to a given warming scenario in as in panel (E) are independent from the climate sensitivity. However, as shown in panel (F), the SCC is not. Our main analysis uses the median climate sensitivity from Dietz et al. (2021a) and Ricke and Caldeira (2014). When we halve or double the climate sensitivity—corresponding to the range across climate models from Dietz et al. (2021a)—the SCC varies from \$600 to \$2,400 per ton.

Figure 15 also depicts how these results shift when we estimate damage functions using the BU data instead of the PWT data. As we estimate larger GDP effects in the BU sample, we obtain larger damage functions and more pronounced counterfactuals. Welfare losses rise to 42%, 2100 GDP losses grow to 61% and the SCC increases to over \$1,500 per ton.

Finally, we show how our conclusions change when we treat household expectations differently. In our main estimation, we assume that households have rational expectations about the temperature path following a temperature shock. An alternative is to assume that households are surprised every period by persistently elevated temperatures following a temperature shock. Under this assumption, we linearly combine our estimated impulse response functions to obtain the output responses to a one-time transitory temperature shock. We then target these responses to a transitory shock to estimate structural damage functions, instead of estimating damage functions first as in our baseline. We provide more details in Appendix D.5. The dotted lines in Figure 15 display our results under this alternative treatment of expectations. The results are very close to our baseline, highlighting that our baseline treatment of expectations is not driving our results. Collectively, these sensitivity exercises indicate that significant climate damages occur over a wide range of specification choices.

7 Conclusion

In this paper, we show that the impact of climate change on economic activity is likely an order of magnitude larger than previously thought. We leverage natural climate variability in global mean temperature to obtain time-series estimates that are informative of the overall impact of global warming. Of course, identification is more challenging in the time series because of global confounders at high and low frequencies. While no set of sensitivity analyses is ever entirely exhaustive, our estimates remain stable across a wide range of specifications that vary the set of controls, sample periods, source of global temperature fluctuations and adjust for reverse causality. Collectively, these exercises suggest that our specification captures the causal effect of global temperature on economic activity.

Quantitatively, we find that a permanent 1°C rise in global temperature causes global GDP to persistently decline by over 20%. These impacts are due to ocean temperatures and an associated surge in extreme climatic events. By contrast, local temperature shocks used in the conventional panel literature lead to a minimal rise in extreme events and to smaller economic effects. Together, our results imply a SCC in excess of $1,200 per ton, a welfare loss of more than 30% and a GDP per capita loss in excess of 50% by the end of the century under a moderate warming scenario.

Our results also have salient consequences for decarbonization policy, which we discuss further in a companion paper (Bilal and Känzig, 2025). Most decarbonization interventions cost $80 per ton of CO2 abated on average (Bistline et al., 2023). Consider a conventional SCC value based on local temperature variation of $149 per ton. Decarbonization policies are then cost-effective only if governments internalize benefits to the entire world, as captured by the SCC.

However, a government that only internalizes domestic benefits evaluates decarbonization policies with a DCC, which is always lower than the SCC because losses to a given country are lower than for the world. Under conventional estimates based on local temperature variation, the DCC of the United States is below policy costs. Unilateral emissions reduction are then prohibitively expensive. By contrast, under our estimates based on global temperature variation, the DCC of the United States exceeds policy costs.

Unilateral decarbonization policy then becomes cost-effective for large economies such as the United States.

References

Arkolakis, Costas, Arnaud Costinot, and Andrés Rodríguez-Clare (2012). "New Trade Models, Same Old Gains?" *American Economic Review* 102.1, 94–130.

Auclert, Adrien, Bence Bardóczy, Matthew Rognlie, and Ludwig Straub (2021). "Using the Sequence-Space Jacobian to Solve and Estimate Heterogeneous-Agent Models". *Econometrica* 89.5, pp. 2375–2408.

Bansal, Ravi and Marcelo Ochoa (2011). "Temperature, Aggregate Risk, and Expected Returns". *National Bureau of Economic Research Working Paper Series 17575*.

Barrage, Lint and William Nordhaus (2024). "Policies, projections, and the social cost of carbon: Results from the DICE-2023 model". *Proceedings of the National Academy of Sciences of the United States of America* 121.13, e2312030121.

Barro, Robert J. (2006). "Rare Disasters and Asset Markets in the Twentieth Century". *The Quarterly Journal of Economics* 121.3, pp. 823–866.

— (2009). "Rare Disasters, Asset Prices, and Welfare Costs". *American Economic Review* 99.1, 243–64.

Barro, Robert J. and José F. Ursúa (2008). "Macroeconomic Crises since 1870". *Brookings Papers on Economic Activity* 1, pp. 255–335.

Berg, Kimberly A., Chadwick C. Curtis, and Nelson C. Mark (2024). "GDP and temperature: Evidence on cross-country response heterogeneity". *European Economic Review* 169, p. 104833.

Bilal, Adrien and Shlok Goyal (2023). "Some Pleasant Sequence-Space Arithmetic in Continuous Time". *Social Science Research Network Working Paper 4634993*.

Bilal, Adrien and Diego R. Känzig (2025). "Does Unilateral Decarbonization Pay For Itself?" *In preparation for the American Economic Association Papers and Proceedings*.

Bilal, Adrien and Esteban Rossi-Hansberg (2023). "Anticipating Climate Change Across the United States". *National Bureau of Economic Research Working Paper 31323*.

Bistline, John, Neil R. Mehrotra, and Catherine Wolfram (2023). "Economic Implications of the Climate Provisions of the Inflation Reduction Act". *Brookings Papers on Economic Activity*.

Burke, Marshall, Solomon M. Hsiang, and Edward Miguel (2015). "Global non-linear effect of temperature on economic production". *Nature* 527.7577, pp. 235–239.

Burke, Marshall, Mustafa Zahid, Noah Diffenbaugh, and Solomon M Hsiang (2023). "Quantifying Climate Change Loss and Damage Consistent with a Social Cost of Greenhouse Gases". *National Bureau of Economic Research Working Paper Series 31658*.

Burke, Marshall, Mustafa Zahid, Mariana C. M Martins, Christopher W Callahan, Richard Lee, Tumenkhusel Avirmed, Sam Heft-Neal, Mathew Kiang, Solomon M Hsiang, and David Lobell (2024). "Are We Adapting to Climate Change?" Working Paper Series 32985.

Callahan, Christopher W. and Justin S. Mankin (2023). "Persistent effect of El Niño on global economic growth". *Science* 380.6649, pp. 1064–1069.

Cerra, Valerie and Sweta Chaman Saxena (2008). "Growth Dynamics: The Myth of Economic Recovery". *American Economic Review* 98.1, pp. 439–57.

Cruz, José-Luis and Esteban Rossi-Hansberg (2023). "The Economic Geography of Global Warming". *The Review of Economic Studies* 91.2, pp. 899–939.

Dasgupta, Partha (2008). "Discounting climate change". *Journal of Risk and Uncertainty* 37.2, pp. 141–169.

Dell, Melissa, Benjamin F. Jones, and Benjamin A. Olken (2012). "Temperature shocks and economic growth: Evidence from the last half century". *American Economic Journal: Macroeconomics* 4.3, pp. 66–95.

— (2014). "What Do We Learn from the Weather? The New Climate–Economy Literature". *Journal of Economic Literature* 52.3, pp. 740–798.

Deryugina, Tatyana (2013). "The role of transfer payments in mitigating shocks: Evidence from the impact of hurricanes". *Social Science Research Network Working Paper 2314663*.

Deschênes, Olivier and Michael Greenstone (2011). "Climate Change, Mortality, and Adaptation: Evidence from Annual Fluctuations in Weather in the US". *American Economic Journal: Applied Economics* 3.4, pp. 152–85.

Desmet, Klaus, Robert E. Kopp, Scott A. Kulp, Dávid Krisztián Nagy, Michael Oppenheimer, Esteban Rossi-Hansberg, and Benjamin H. Strauss (2021). "Evaluating the Economic Cost of Coastal Flooding". *American Economic Journal: Macroeconomics* 13.2, pp. 444–86.

Dietz, Simon, Frederick van der Ploeg, Armon Rezai, and Frank Venmans (2021a). "Are Economists Getting Climate Dynamics Right and Does It Matter?" *Journal of the Association of Environmental and Resource Economists* 8.5, pp. 895–921.

Dietz, Simon, James Rising, Thomas Stoerk, and Gernot Wagner (2021b). "Economic impacts of tipping points in the climate system". *Proceedings of the National Academy of Sciences* 118.34, e2103081118.

Dingel, Jonathan I., Kyle C. Meng, and Solomon M. Hsiang (2023). "Spatial correlation, trade, and inequality: Evidence from the global climate". *National Bureau of Economic Research Working Paper Series 25447*.

Domeisen, Daniela I. V., Elfatih A. B. Eltahir, Erich M. Fischer, Reto Knutti, Sarah E. Perkins-Kirkpatrick, Christoph Schär, Sonia I. Seneviratne, Weisheimer Antje, and Heini Wernli (2023). "Prediction and Projection of Heatwaves". *Nature Reviews Earth and Environment* 4, 36–50.

Driscoll, John C. and Aart C. Kraay (1998). "Consistent covariance matrix estimation with spatially dependent panel data". *Review of Economics and Statistics* 80.4, pp. 549–560.

Folini, Doris, Aleksandra Friedl, Felix Kübler, and Simon Scheidegger (2024). "The Climate in Climate Economics". *The Review of Economic Studies*.

Granger, C.W.J. and P. Newbold (1974). "Spurious regressions in econometrics". *Journal of Econometrics* 2.2, pp. 111–120.

Hamilton, James D. (2018). "Why you should never use the Hodrick-Prescott filter". *Review of Economics and Statistics* 100.5, pp. 831–843.

Hausfather, Zeke and Glen P. Peters (2020). "Emissions – the 'business as usual' story is misleading". *Nature* 577.7792, pp. 618–620.

Hsiang, Solomon M. and Amir S. Jina (2014). "The Causal Effect of Environmental Catastrophe on Long-Run Economic Growth: Evidence From 6,700 Cyclones". *National Bureau of Economic Research Working Paper Series 20352*.

Hsiang, Solomon M., Kyle C. Meng, and Mark A. Cane (2011). "Civil conflicts are associated with the global climate". *Nature* 476, 438–441.

Joos, F., R. Roth, J. S. Fuglestvedt, G. P. Peters, I. G. Enting, W. von Bloh, V. Brovkin, E. J. Burke, M. Eby, N. R. Edwards, T. Friedrich, T. L. Frölicher, P. R. Halloran, P. B. Holden, C. Jones, T. Kleinen, F. T. Mackenzie, K. Matsumoto, M. Meinshausen, G.-K. Plattner, A. Reisinger, J. Segschneider, G. Shaffer, M. Steinacher, K. Strassmann, K. Tanaka, A. Timmermann, and A. J. Weaver (2013). "Carbon dioxide and climate impulse response functions for the computation of greenhouse gas metrics: a multi-model analysis". *Atmospheric Chemistry and Physics* 13.5, pp. 2793–2825.

Jordà, Òscar (2005). "Estimation and inference of impulse responses by local projections". *American Economic Review* 95.1, pp. 161–182.

Jordà, Òscar, Moritz Schularick, and Alan M. Taylor (2020). "The effects of quasi-random monetary experiments". *Journal of Monetary Economics* 112, pp. 22–40.

Kahn, Matthew E., Kamiar Mohaddes, Ryan N.C. Ng, M. Hashem Pesaran, Mehdi Raissi, and Jui-Chung Yang (2021). "Long-term macroeconomic effects of climate change: A cross-country analysis". *Energy Economics* 104, p. 105624.

Kaufmann, Robert K., Heikki Kauppi, and James H. Stock (2006). "Emissions, concentrations, & temperature: a time series analysis". *Climatic Change* 77, pp. 249–278.

Kelleher, J. Paul and Gernot Wagner (2018). "Ramsey discounting calls for subtracting climate damages from economic growth rates". *Applied Economics Letters* 26.1, pp. 79–82.

Kose, M. Ayhan, Naotaka Sugawara, and Marco E. Terrones (2020). "Global recessions".

Krusell, Per and Anthony A. Smith (2022). "Climate change around the world". *National Bureau of Economic Research Working Paper Series 30338*.

Lee, Hoesung, Katherine Calvin, Dipak Dasgupta, Gerhard Krinner, Aditi Mukherji, Peter Thorne, Christopher Trisos, José Romero, Paulina Aldunce, Ko Barret, et al. (2023). "IPCC, 2023: Climate Change 2023: Synthesis Report, Summary for Policymakers. Contribution of Working Groups I, II and III to the Sixth Assessment Report of the Intergovernmental Panel on Climate Change [Core Writing Team, H. Lee and J. Romero (eds.)]. IPCC, Geneva, Switzerland."

Montiel Olea, José Luis, Mikkel Plagborg-Moller, Eric Qian, and Christian K. Wolf (2024). "Double Robustness of Local Projections and Some Unpleasant VARithmetic". *National Bureau of Economic Research Working Paper Series 32495*.

Moore, Frances C. and Delavane B. Diaz (2015). "Temperature impacts on economic growth warrant stringent mitigation policy". *Nature Climate Change* 5.2, pp. 127–131.

Moore, Frances C., Moritz A. Drupp, James Rising, Simon Dietz, Ivan Rudik, and Gernot Wagner (2024). "Synthesis of Evidence Yields High Social Cost of Carbon Due to Structural Model Variation and Uncertainties". *Proceedings of the National Academy of Sciences of the United States of America* 121.52.

Nath, Ishan B., Valerie A. Ramey, and Peter J. Klenow (2024). "How Much Will Global Warming Cool Global Growth?" *National Bureau of Economic Research Working Paper Series 32761*.

National Oceanic and Atmospheric Administration (2005). *Volcanos and Climate*. Online Resource.

— (2009). *Climate Change: Incoming Sunlight*. Online Resource.

— (2023). *What are El Niño and La Niña?* Online Resource.

Neal, Timothy, Ben R. Newell, and Andy Pitman (2025). "Reconsidering the macroeconomic damage of severe warming". *Environmental Research Letters* 20.4, p. 044029.

Newell, Richard G., Brian C. Prest, and Steven E. Sexton (2021). "The GDP-temperature relationship: implications for climate change damages". *Journal of Environmental Economics and Management* 108, p. 102445.

Nordhaus, William D. (1992). "An optimal transition path for controlling greenhouse gases". *Science* 258.5086, pp. 1315–1319.

— (2007). "A Review of the Stern Review on the Economics of Climate Change". *Science* 317.5835, pp. 201–202.

— (2013). "Integrated economic and climate modeling". *Handbook of Computable General Equilibrium Modeling*. Vol. 1. Elsevier, pp. 1069–1131.

Nordhaus, William D. and Zili Yang (1996). "A Regional Dynamic General-Equilibrium Model of Alternative Climate-Change Strategies". *The American Economic Review* 86.4, pp. 741–765. (Visited on 09/17/2025).

Reinhart, Carmen M. and Kenneth S. Rogoff (2009). "The aftermath of financial crises". *American Economic Review* 99.2, pp. 466–472.

Rennert, Kevin, Frank Errickson, Brian C. Prest, Lisa Rennels, Richard G. Newell, William Pizer, Cora Kingdon, Jordan Wingenroth, Roger Cooke, Bryan Parthum, et al. (2022). "Comprehensive evidence implies a higher social cost of CO2". *Nature* 610.7933, pp. 687–692.

Ricke, Katharine L. and Ken Caldeira (2014). "Global surface temperature change". *Environ. Res. Lett.* 9, p. 124002.

Seneviratne, S. I., X. Zhang, M. Adnan, W. Badi, C. Dereczynski, A. Di Luca, S. Ghosh, I. Iskandar, J. Kossin, S. Lewis, F. Otto, I. Pinto, M. Satoh, S.M. Vicente-Serrano, M. Wehner, and B. Zhou (2021). "Chapter 11: Weather and Climate Extreme Events in a Changing Climate". *In Climate Change 2021: The Physical Science Basis. Contribution of Working Group I to the Sixth Assessment Report of the Intergovernmental Panel on Climate Change; Masson-Delmotte, V., P. Zhai, A. Pirani, S.L. Connors, C. Péan, S. Berger, N. Caud, Y. Chen, L. Goldfarb, M.I. Gomis, M. Huang, K. Leitzell, E. Lonnoy, J.B.R. Matthews, T.K. Maycock, T. Waterfield, O. Yelekçi, R. Yu, and B. Zhou (eds.). Cambridge University Press, Cambridge, United Kingdom and New York, NY, USA*, 1513–1766.

Seneviratne, Sonia I., Markus G. Donat, Andy J. Pitman, Reto Knutti, and Robert L. Wilby (2016). "Allowable CO2 Emissions Based on Regional and Impact-Related Climate Targets". *Nature* 529, 477–483.

Sims, Christopher A. (1986). "Are forecasting models usable for policy analysis?" *Quarterly Review* 10, pp. 2–16.

Stern, N. (2006). *Stern Review: The Economics of Climate Change*.

Stern, Nicholas, Joseph Stiglitz, and Charlotte Taylor (2022). "The economics of immense risk, urgent action and radical change: towards new approaches to the economics of climate change". *Journal of Economic Methodology* 29.3, pp. 181–216.

Tran, Brigitte Roth and Daniel J. Wilson (2023). "The local economic impact of natural disasters". *Federal Reserve Bank of San Francisco Working Paper*.

Wartenburger, R., M. Hirschi, M. G. Donat, P. Greve, A. J. Pitman, and S. I. Seneviratne (2017). "Changes in Regional Climate Extremes as a Function of Global Mean Temperature: an Interactive Plotting Framework". *Geoscientific Model Development* 10, 3609–3634.

Weitzman, Martin L. (1998). "Why the Far-Distant Future Should Be Discounted at Its Lowest Possible Rate". *Journal of Environmental Economics and Management* 36.3, pp. 201–208.

Online Appendix

The Macroeconomic Impact of Climate Change: Global vs. Local Temperature

Adrien Bilal[†]
Diego R. Känzig[‡]

Contents

[†]Stanford University, CEPR and NBER. E-mail: adrienbilal@stanford.edu.
[‡]Northwestern University, CEPR and NBER. E-mail: dkaenzig@northwestern.edu.

A Data

A.1 Economic Data

We rely on two complementary sources for our macroeconomic data. First, we obtain data on real GDP and population from the Penn World Tables (PWT; Feenstra et al., 2015). This data is available for a comprehensive selection of countries around the world, however, it only has historical coverage back to the 1960s. Our main output measure is real GDP per capita from the national accounts (rgdpna/pop). Based on this data, we construct a measure of world real GDP, by chain-weighting country-level growth rates. We complement this data with information from the World Bank, which also provides information on GDP and population for the same sample period.

Second, we obtain alternative data on GDP and population from Barro and Ursúa (2008). This data set is only available for a smaller set of countries but has much longer historical coverage, going back to the 19th century (with reliable coverage since 1860). The online dataset only features real GDP per capita indices. Robert Barro kindly shared the underlying data for real GDP in dollars and population with us. This allowed us to construct real GDP per capita (in dollars). We also construct a chain-weighted world real GDP series based on this data.

While our focus is on real GDP per capita, we are also interested in the effects on other variables such as consumption, investment and productivity. This information is unfortunately not available in the Barro and Ursúa (2008) data, therefore we focus here on the more recent sample period. For this period, such data is readily available for a large set of countries in the PWT. For capital, we use the capital stock from national accounts (rnna). Investment, we compute using data on capital and capital depreciation (delta) based on the capital accumulation equation $I_t = K_t - (1 - \delta_t)K_{t-1}$. For total factor productivity, we also use the measure based on national accounts (rtfpna). We compute a measure of labor productivity based on output and employment data (rgdpna/emp).[1] For our country comparisons by income, we use (expenditure-side) real GDP per capita at chained PPPs (rgdpe/pop).

[1] We use employment as a proxy for the labor input because the data on average hours is not very well populated.

A.2 Climate Data

Global temperature. We obtain global temperature anomalies (land and ocean surface, in degrees Celsius) at an annual frequency between 1850 and 2022 from NOAA National Centers for Environmental Information (2023a). Temperature anomalies are deviations from the climatology, which is measured as the 1901-2000 mean temperature, 13.9 degree Celsius (NOAA National Centers for Environmental Information, 2023b). Temperature levels are constructed by adding the climatology to the anomaly series.

Alternatively, we obtain the global temperature anomalies (land and ocean surface, in degrees Celsius) at an annual frequency between 1880 and 2022 from Lenssen et al. (2019) and NASA Goddard Institute for Space Studies (2023). Temperature anomalies are deviations from the climatology, which is measured as the 1951-1980 mean temperature, approximately 14 degree Celsius (NASA Earth Observatory, 2020). Temperature levels are similarly constructed by adding the climatology to the anomaly series.

Figure A.1: Global Average Temperature Since 1860

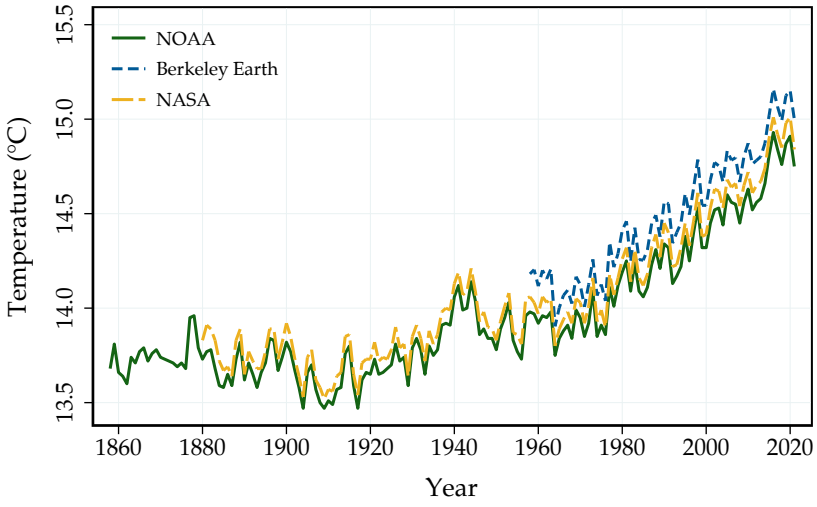

Evolution of global average temperature. The NOAA and NASA measures are constructed by adding the climatology to the official anomaly series. The Berkeley Earth measure is constructed by first, obtaining grid-level temperature levels by adding the grid-level climatology to the grid-level anomaly series, and second, aggregating the grid-level temperature levels using area weights. We plot the Berkeley Earth series starting 1956, after which the percentage of monthly grid-level missing observations is consistently below ≈2%.

Gridded temperature and weather datasets. Our primary gridded temperature dataset is Berkeley Earth, due to its geographic coverage, temporal coverage, and update frequency.

We obtain gridded temperature anomalies (using air temperatures at sea ice) at a daily and monthly frequency between 1850 and 2022 from Berkeley Earth (2023), at a resolution of $1^\circ \times 1^\circ$ latitude-longitude grid. Temperature anomalies are deviations from the climatology, which is measured as the 1951-1980 mean temperature (Rohde and Hausfather, 2020). Grid-level temperature levels are constructed by adding the grid-level climatology to the grid-level anomaly series.

We also obtain gridded estimates of temperature, wind, and precipitation at a daily frequency between 1901 and 2019 from the Inter-Sectoral Impact Model Intercomparison Project (ISIMIP), at a 0.5° spatial resolution (Lange et al., 2023).

Because the granular weather data is more reliably measured in the more recent period, we restrict our attention to the data starting in 1960.

To assess the sensitivity of the results to the gridded temperature data used, we obtain alternate, prominent datasets used in the literature. We obtain gridded temperature levels (surface air temperature) at a monthly frequency between 1948 and 2014 from the Princeton Global Forcing Dataset (version 2) constructed by Sheffield et al. (2006), a later version of which was used, for instance, by Nath et al. (2024). Additionally, we obtain the gridded temperature levels (surface air temperatures) at a monthly frequency between 1900 and 2014 from the Willmott and Matsuura, University of Delaware Dataset (version 4.01) (Matsuura and National Center for Atmospheric Research Staff, 2023), earlier versions of which were used, for instance, by Dell et al. (2012) and Burke et al. (2015).

Aggregation of gridded temperature datasets. To aggregate the gridded temperature datasets to the global or country level we consider two different type of weights. One approach is to use area weights. Specifically, we use the area of the grid, calculated using the latitude and longitude. Alternatively, we use population weights. In that case, we use the grid-level population count in 2000 as weights, obtained from the Center for International Earth Science Information Network (CIESIN), Columbia University (2018).

As a quality check of the gridded temperature data, we compute population- and area-weighted global temperature measures and compare them to the official measures from NOAA and NASA. Note that both official measures follow an area-weighted aggregation scheme. Reassuringly, aggregating the Berkeley Earth gridded temperature data using area weights to obtain a global temperature measure produces a series that is virtually perfectly correlated with both the NOAA and NASA global temperature series: we find

that the measures based on all these different data sets align very well, as shown in Figure A.1.

Country-level temperatures. Using the approach outlined above, we construct population- and area-weighted country-level mean temperatures, based on the Berkeley Earth data. In our analyses, we use population-weighted temperature as the baseline, however, using area-weighted measures produces very similar results. To assess the sensitivity of the results with respect to the gridded temperature data used, we similarly compute the population- and area-weighted country-level mean temperatures using the Princeton Global Forcing Dataset and the University of Delaware Dataset. We find that the results are consistent across different temperature datasets.

Extreme climatic events. We use the ISIMIP gridded estimates of temperature, wind, and precipitation at a daily frequency between 1901 and 2019 to construct extreme events indicators for each latitude-longitude grid. To define a threshold for extreme events, we use the percentiles of the distribution of the variables between 1950 and 1980, and define an extreme event as one where the realization of a variable was above a given percentile of its distribution. Specifically, we use the percentiles of the worldwide distribution to construct "absolute" extreme events indicators, and the percentiles of a country's distribution for "relative" indicators. We use the relative indicators as our baseline, however, our results are robust to using the absolute indicators.

To aggregate the variables across the grids to construct country-level measures, we use two methods. First, we construct the daily average of the variable for the country, and then compute the fraction of days in the year when the variable was above the threshold percentile (i.e., "country-level" extreme events indicator). We define these threshold percentiles such that the extreme heat, drought, extreme precipitation and extreme wind indices have a baseline probability of 0.05, 0.25, 0.01 and 0.01, respectively. Alternatively, we also compute the fraction of days in the year when the variable was above the threshold percentile *at the grid-level*, and then aggregate this indicator for the country (i.e., "cell-level" extreme events indicator). Of course, the threshold percentile changes across the definitions: for the former, we use the distribution of daily country-level averages, and for the latter, the distribution of daily grid-level observations between 1950 and 1980. As a robustness exercise, we used alternative thresholds computed based on data from 1900 to 1930, yielding very similar results. Note that similar to the aggregation of gridded tem-

perature datasets, we consider both area- and population-weights in both methods above. We use the country-level, area-weighted indicators as our baseline. However, the results are similar when using our alternative measures (cell-level and/or population-weighted).

Table A.1: Descriptive Statistics

	Obs	Mean	SD	Median	Min	Max
PWT: Global variables						
Global temperature anomaly	60	0.35	0.33	0.33	-0.24	1.04
Global temperature shock	60	0.00	0.13	-0.01	-0.29	0.30
World real GDP per capita growth	59	2.06	1.47	2.13	-1.74	6.36
Oil price change	59	8.55	30.32	1.70	-47.79	167.83
US Treasury yield	60	5.04	3.31	5.00	0.12	14.78
PWT: Country-level variables						
Local temperature anomaly	10379	0.40	0.57	0.35	-1.89	3.33
Local temperature shock	10379	0.01	0.46	0.00	-2.59	2.89
Real GDP per capita growth	9090	2.07	6.31	2.23	-67.01	94.17
Investment per capita growth	8938	6.58	23.61	4.68	-98.36	499.01
TFP growth	5716	0.33	4.90	0.47	-65.22	83.10
Labor productivity growth	8353	1.75	6.63	1.79	-67.31	142.17
Extreme heat days	10379	0.10	0.08	0.08	0.00	0.87
Drought days	10033	0.29	0.10	0.27	0.05	0.91
Extreme precipitation days	10033	0.01	0.01	0.01	0.00	0.08
Extreme wind days	10033	0.01	0.01	0.01	0.00	0.06
BU: Global variables						
Global temperature anomaly	160	0.04	0.33	-0.06	-0.43	1.03
Global temperature shock	160	0.00	0.11	-0.00	-0.30	0.27
World real GDP per capita growth	159	1.78	2.75	2.15	-13.78	7.20
Commodity price change	160	1.10	20.11	1.65	-120.39	60.10
US Treasury yield	160	4.47	2.26	3.68	1.73	13.92
BU: Country-level variables						
Real GDP per capita growth	6051	2.05	6.11	2.16	-66.06	67.15

Descriptive statistics for our global and country-level variables in PWT and BU datasets. We report the number of non-missing observations, the mean, standard deviation, median, and min and max for the main variables used in our analysis over the PWT sample (1960-2019) and BU sample (1860-2019), respectively.

Sample restrictions. In the PWT data, we drop countries for which we have fewer than 20 non-missing observations of temperature and real GDP per capita. This leaves us with 173 countries. Our results are robust to restricting the selection of countries further. We do not impose any additional restrictions in the BU data.

Descriptive statistics. The PWT dataset spans 173 countries over the period from 1960 to 2019 while the BU dataset covers 43 countries from 1860 to 2019.

In Table A.1, we present some descriptive statistics on the main variables of interest. The table shows, statistics on our global time-series variables and the country-level variables in the panel, for the PWT and the BU datasets, respectively. Specifically, we report the number of non-missing observations, the mean, median, standard deviation as well as the minimum and the maximum observation.

B Additional Results for Global Temperature Shocks

B.1 Statistical Properties of Global Temperature Shocks

In this appendix, we discuss some of the statistical properties of global temperature shocks in more detail. We perform all the diagnostics on the PWT and the BU sample.

Serial correlation. Figure B.1 shows the autocorrelation function of the global temperature shocks. The shocks are weakly autocorrelated. This is not too surprising, given that we construct the shocks as multi-step forecast errors. To account for this serial correlation, we therefore include lags of the global temperature shock in our local projections. However, as we show in Appendix B.9, our results are robust with respect to the number of lags for the temperature shock.

Forecastablility. A desirable feature of "shocks" is that they should not be forecastable by past information (Ramey, 2016). In our context, if global tempreature shocks were forecastable by economic variables, this could point to reverse causality or other endogeneity threats. Thus, we check whether our temperature shocks are forecastable, considering a wide set of past macroeconomic or financial variables in a series of Granger-causality tests. To account for the long and variable lags between emissions and warming, we conservatively include up to 8 years worth of lags in the PWT sample and 16 lags in the BU

Figure B.1: Autocorrelation of Global Temperature Shock

(a) PWT sample: 1960-2019

(b) BU sample: 1860-2019

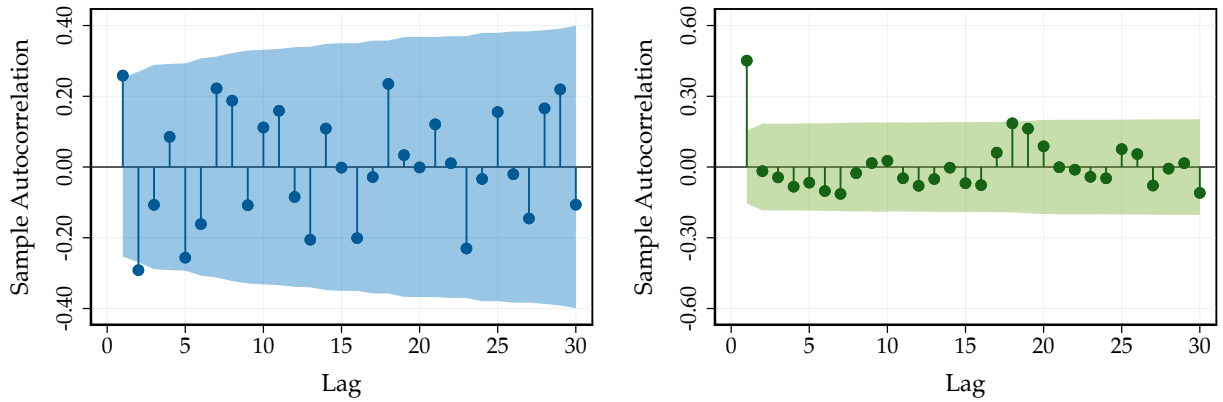

Autocorrelation function of global temperature shocks, together with the 95% confidence bands, computed based on Bartlett's formula for MA(q).

sample.[2] Table B.1 reports the results. We find no evidence that macroeconomic or financial variables have any power in forecasting global temperature shocks. None of the selected variables Granger cause the series at conventional significance levels. The joint test is also insignificant.

Table B.1: Granger-causality Tests

(a) PWT sample: 1960-2019

Variable	p-value
Real GDP	0.808
Population	0.763
WTI price	0.727
Commodity price index	0.682
Treasury 1Y	0.798
Overall	0.945

(b) BU sample: 1860-2019

Variable	p-value
Real GDP	0.341
Population	0.789
WTI price	0.316
Commodity price index	0.308
Treasury 10Y	0.747
Overall	0.266

p-values of a series of Granger causality tests of the global temperature shock series using a selection of macroeconomic and financial variables. Non-stationary variables are transformed to growth rates. We allow for up to 8 lags in the PWT and 16 lags in the BU sample.

[2] In the PWT sample, it is unfortunately not possible to control for more than 8 lags because we run out of degrees of freedom.

B.2 Accounting for Estimation Uncertainty in Temperature Shocks

Our baseline specifications take the global temperature shock as given and do not take estimation uncertainty in the shock into account. To assess the potential role of estimation uncertainty in the shock, we alternatively construct confidence bands using bootstrapping techniques. We implement this approach as follows. We assume that the data generating process (DGP) is our estimated local projections model at $h = 0$:

$$\Delta y_t = \alpha_h + \theta_h T_t^{\text{shock}} + \rho(L)\Delta y_{t-1} + \widetilde{\mathbf{x}}_t'\boldsymbol{\beta}_h + \varepsilon_t, \tag{B.1}$$

where $\widetilde{\mathbf{x}}_t$ includes our deterministic controls (recession dummy and linear trend).

Having estimated that model, we resample T_t^{shock} and ε_t under the assumption that $E[T_t^{\text{shock}}\varepsilon_t] = 0$—the exclusion restriction underlying our approach. Specifically, we use a Wild bootstrap, keeping the deterministic controls fixed.

Based on the drawn $\varepsilon_t^{(b)}$ and $T_t^{\text{shock},(b)}$, we obtain bootstrapped draws of $\Delta y_t^{(b)}$ based on (B.1), starting from the initial values $\Delta y_0, \ldots, \Delta y_p$ at the beginning of our sample. We cumulate this series starting from y_0 to get $y_t^{(b)}$.

In a next step, we estimate our local projections model (2) based on the bootstrapped series for real GDP, $y_t^{(b)}$, and the temperature shock, $T_t^{\text{shock},(b)}$. We repeat this procedure 4,000 times and obtain confidence bands for the impulse responses based on their bootstrapped distribution.

Figure B.2 compares the confidence bands based on our baseline HAC errors with the bootstrapped confidence bands. The coverage is similar, suggesting that taking estimation uncertainty in the global temperature shock into account turns out to be inconsequential in the context of our application.

Figure B.2: The Role of Estimation Uncertainty in Temperature Shocks

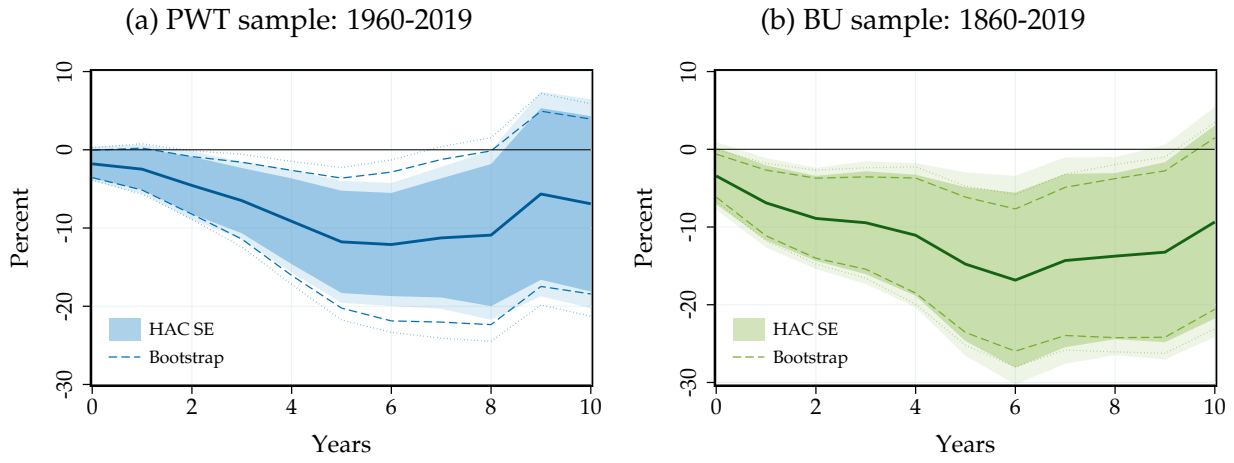

Impulse responses of world real GDP per capita to a global temperature shock, estimated based on (2). Left panel: PWT sample, 1960-2019. Right panel: BU sample, 1860-2019. Solid black line: point estimate. Dark and light shaded areas are 90 and 95% confidence bands based on HAC errors. Dotted and dashed lines: 90 and 95% confidence bands based on bootstrap, taking estimation uncertainty in the temperature shock into account.

In the next appendix, we also present alternative estimators which take the estimation uncertainty in the temperature shock into account.

B.3 Alternative Estimation Models

In this appendix, we explore the sensitivity of our results with respect to alternative estimation models.

One-step local projection. Recall, our baseline empirical model consists of a two-step approach: (i) estimate temperature shocks using the Hamilton (2018) filter and (ii) estimate the impulse responses using local projections.

Here, we present results if we instead estimate the responses directly, projecting cumulative changes in GDP directly on temperature. This is closer to the distributed lag models commonly used in the literature (Dell et al., 2012; Burke et al., 2015):

$$y_{t+h} - y_{t-1} = \alpha_h + \theta_h T_t + \mathbf{x}_t' \boldsymbol{\beta}_h + \varepsilon_{t+h}, \tag{B.2}$$

where y_t is the outcome variable of interest, T_t is global temperature and θ_h is the dynamic causal effect of interest at horizon h. Importantly, $\mathbf{x}_t$ contains sufficient lags of GDP growth and temperature to account for the serial correlations in both variables. We use

5 lags of temperature in the PWT sample, and 9 lags of temperature in the BU sample. These choices match the implied number of lags when we plug in the Hamilton-filtered temperature shocks into our baseline model (2). To more flexibly account for the kink in the temperature series, we also include a quadratic time trend.

Figure B.3 shows the results. The responses are very similar to our baseline. This should not come as a surprise. In fact, if we rely on one-step ahead forecast errors as the relevant temperature shock measure and include the same set of controls in the shock regression (1) and the local projection (2), the two approaches yield the exact same results by the Frisch–Waugh–Lovell theorem. This discussion also highlights that the previous literature implicitly relied on "temperature shocks", i.e. deviations from the temperature trend, even when not explicitly detrending.

Figure B.3: Impulse Responses based on One-Step Estimation

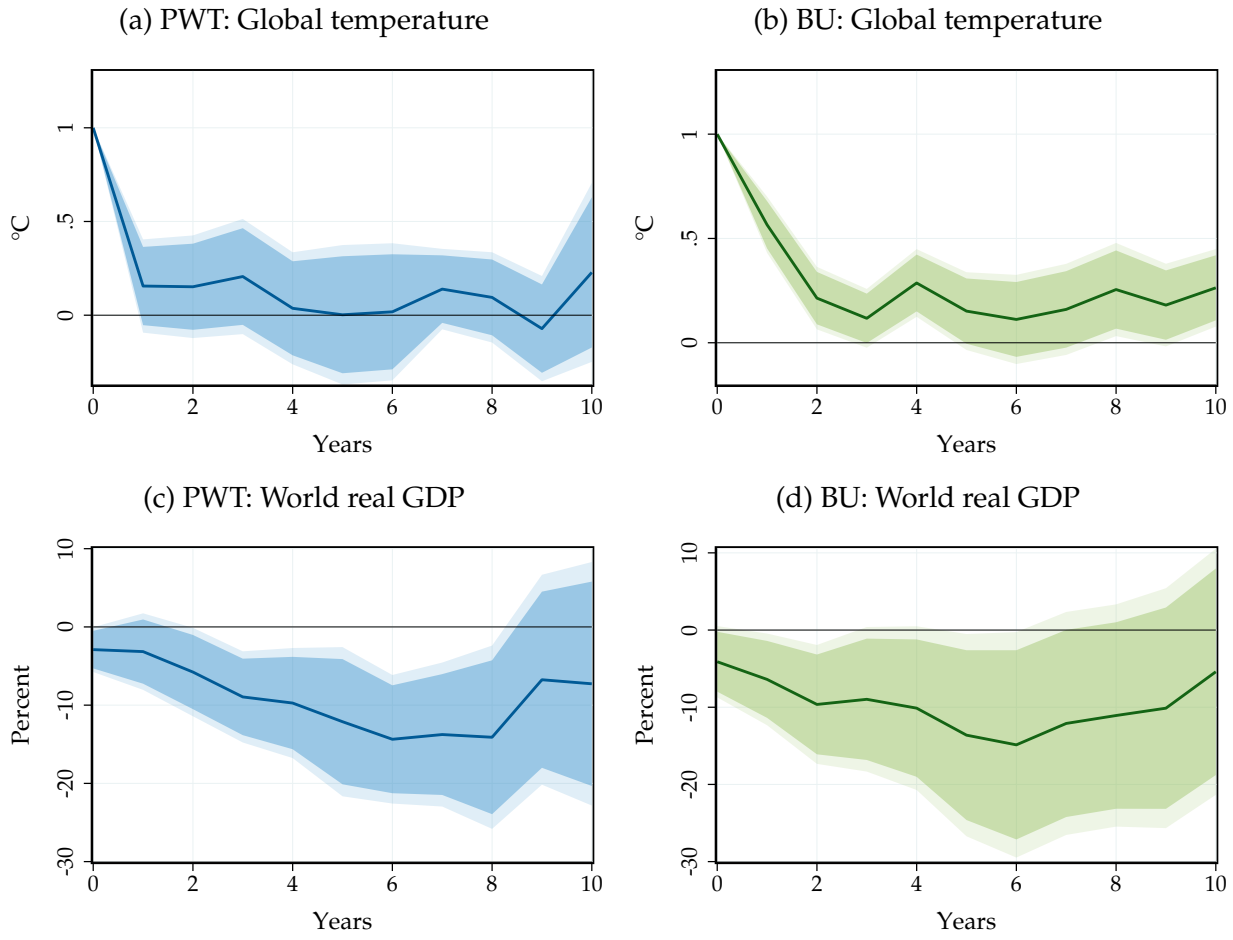

Impulse responses of global mean temperature and world real GDP per capita to a global temperature shock, estimated based on (B.2). Left panel: PWT sample, 1960-2019. Right panel: BU sample, 1860-2019. Solid line: point estimate. Dark and light shaded areas: 90 and 95% confidence bands.

Vector autoregression model. Our main empirical specification relies on local projection techniques. In this appendix, we alternatively estimate the responses based on VAR methods. Starting point is the following structural vector moving-average representation

$$\mathbf{Y}_t = \mathbf{B}(L)\mathbf{S}\boldsymbol{\varepsilon}_t, \tag{B.3}$$

where $\mathbf{Y}_t$ is a $k \times 1$ vector of annual time series, $\boldsymbol{\varepsilon}_t$ is a vector of structural shocks driving the economy with $\mathbb{E}[\boldsymbol{\varepsilon}_t \boldsymbol{\varepsilon}_t'] = \mathbf{I}$, $\mathbf{B}(L) \equiv \mathbf{I} + \mathbf{B}_1 L + \mathbf{B}_2 L^2 + \ldots$ is a matrix lag polynomial, and $\mathbf{S}$ is the structural impact matrix.

Assuming that the vector-moving average process (B.3) is invertible, it admits the fol-

lowing VAR representation:

$$\mathbf{A}(L)\mathbf{Y}_t = \mathbf{S}\boldsymbol{\varepsilon}_t = \mathbf{u}_t, \tag{B.4}$$

where $\mathbf{u}_t$ is a $k \times 1$ vector of reduced-form innovations with variance-covariance matrix $\mathbb{E}[\mathbf{u}_t\mathbf{u}_t'] = \boldsymbol{\Sigma}_u$ and $\mathbf{A}(L) \equiv \mathbf{I} - \mathbf{A}_1 L - \ldots$ is a matrix lag polynomial. Truncating the VAR to order p, we can estimate the model using standard techniques and recover an estimate of $\mathbf{B}(L)$.

The main identification problem is then to find the structural impact matrix $\mathbf{S}$. From the linear relation between the structural shocks and the reduced-form innovations, we obtain the following covariance restrictions $\mathbf{S}\mathbf{S}' = \boldsymbol{\Sigma}_u$. We assume that temperature shocks can impact all variables in the VAR contemporaneously, while other shocks only affect temperature with a lag. This is motivated by the fact that emissions increases usually translate into temperature with a substantial lag. The identifying restriction can be implemented via the Cholesky decomposition of $\boldsymbol{\Sigma}_u$, denoted by $\widetilde{\mathbf{S}}$.

In terms of model specification, $\mathbf{Y}_t$ includes global temperature and real GDP growth. To mitigate concerns about non-invertibility, we also include oil/commodity price growth and the U.S. treasury yield. The lag order is set to 4 in the PWT sample and 8 in the BU sample. In addition, we include the global recession dummy as an exogenous variable.

Figure B.4 shows the results. The estimated impacts turn out to be consistent with our local projection evidence. As expected, the shape of the impulse response is not exactly as in Figure 3 because the VAR extrapolates from the first four autocovariances between GDP and temperature to obtain impacts at higher horizons, while the local projection in Figure 3 directly estimates these impacts at higher horizons.

Figure B.4: VAR Responses

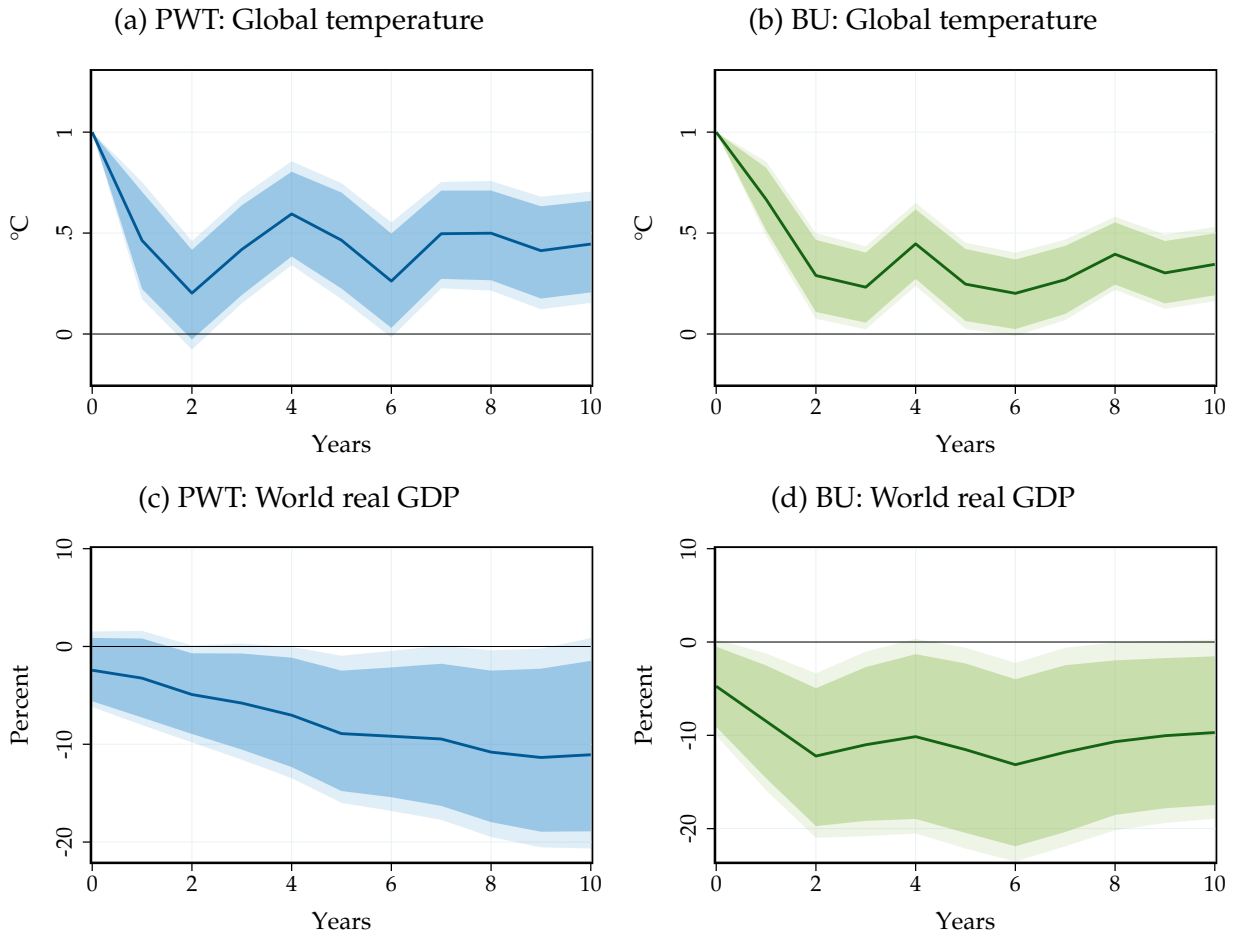

Impulse responses of global temperature and real GDP per capita to a global temperature shock, estimated based on our VAR model (B.4). Left panel: PWT sample, 1960-2019. Right panel: BU sample, 1860-2019. Solid lines: point estimates. Dark and light shaded areas: 90 and 95% confidence bands.

B.4 Accounting for the Persistence in the Temperature Response

As described in the main text, global temperature shocks lead to a relatively persistent increase in temperature. We estimate this increase based on the following model:

$$T_{t+h} - T_{t-1} = \alpha_h + \phi_h^T T_t^{\text{shock}} + \mathbf{x}_t' \boldsymbol{\beta}_h + \varepsilon_{t+h}, \tag{B.5}$$

where $\{\phi_h^T\}_{h=0,\dots H}$ is the global temperature response to a global temperature shock.

Approach. To account for the persistence in the temperature response, we construct the response to a counterfactual scenario where the global temperature increase is purely

transitory, i.e. temperature increases by 1°C on impact and zero after. Following Sims (1986), we achieve this by introducing a series of shocks T_h^{shock} at each horizon h to impose the desired temperature response $\widetilde{\boldsymbol{\phi}}^T$. The series of shocks $\mathbf{T}^{\text{shock}}$ can then be obtained through

$$\underbrace{\begin{pmatrix} T_0^{\text{shock}} \\ T_1^{\text{shock}} \\ \vdots \\ T_H^{\text{shock}} \end{pmatrix}}_{\mathbf{T}^{\text{shock}}} = \underbrace{\begin{pmatrix} 1 & 0 & \cdots & 0 \\ \phi_1^T & 1 & \cdots & 0 \\ \vdots & \vdots & \ddots & \vdots \\ \phi_H^T & \phi_{H-1}^T & \cdots & 1 \end{pmatrix}^{-1}}_{(\boldsymbol{\Phi}^T)^{-1}} \underbrace{\begin{pmatrix} 1 \\ 0 \\ \vdots \\ 0 \end{pmatrix}}_{\widetilde{\boldsymbol{\phi}}^T}.$$

With the shock series $\mathbf{T}^{\text{shock}}$ implying a purely transitory temperature response at hand, the impulse responses of GDP, $\widetilde{\boldsymbol{\theta}}_h$, can be obtained through

$$\underbrace{\begin{pmatrix} \widetilde{\theta}_0 \\ \widetilde{\theta}_1 \\ \vdots \\ \widetilde{\theta}_H \end{pmatrix}}_{\widetilde{\boldsymbol{\theta}}} = \underbrace{\begin{pmatrix} T_0^{\text{shock}} & 0 & \cdots & 0 \\ T_1^{\text{shock}} & T_0^{\text{shock}} & \cdots & 0 \\ \vdots & \vdots & \ddots & \vdots \\ T_H^{\text{shock}} & T_{H-1}^{\text{shock}} & \cdots & T_0^{\text{shock}} \end{pmatrix}}_{\boldsymbol{\mathcal{T}}^{\text{shock}}} \underbrace{\begin{pmatrix} \boldsymbol{\theta}_0 \\ \boldsymbol{\theta}_1 \\ \vdots \\ \boldsymbol{\theta}_H \end{pmatrix}}_{\boldsymbol{\theta}}.$$

The obtained impulse responses $\widetilde{\boldsymbol{\theta}}$ correspond to the effects on GDP following global temperature shock that leads to a one-time, purely transitory increase in global temperature. Based on these responses it is then straightforward to compute the responses to global temperature shocks of arbitrary persistence. For inference, we rely on bootstrapping techniques.

It is important to note that this method is not robust to the Lucas critique. The underlying assumption is that the effects of a series of unanticipated temperature shocks are equivalent to an anticipated path announced at time zero. However, given that economic agents have historically paid little attention to temperature shocks, this assumption may be less restrictive than in other contexts.

Results. Figure B.5 shows the results. Once accounting for the internal persistence of temperature, the effects on GDP become much less pronounced and persistent. This holds

true in both the PWT and the BU sample.

Figure B.5: The Effect of a Transitory Global Temperature Shock

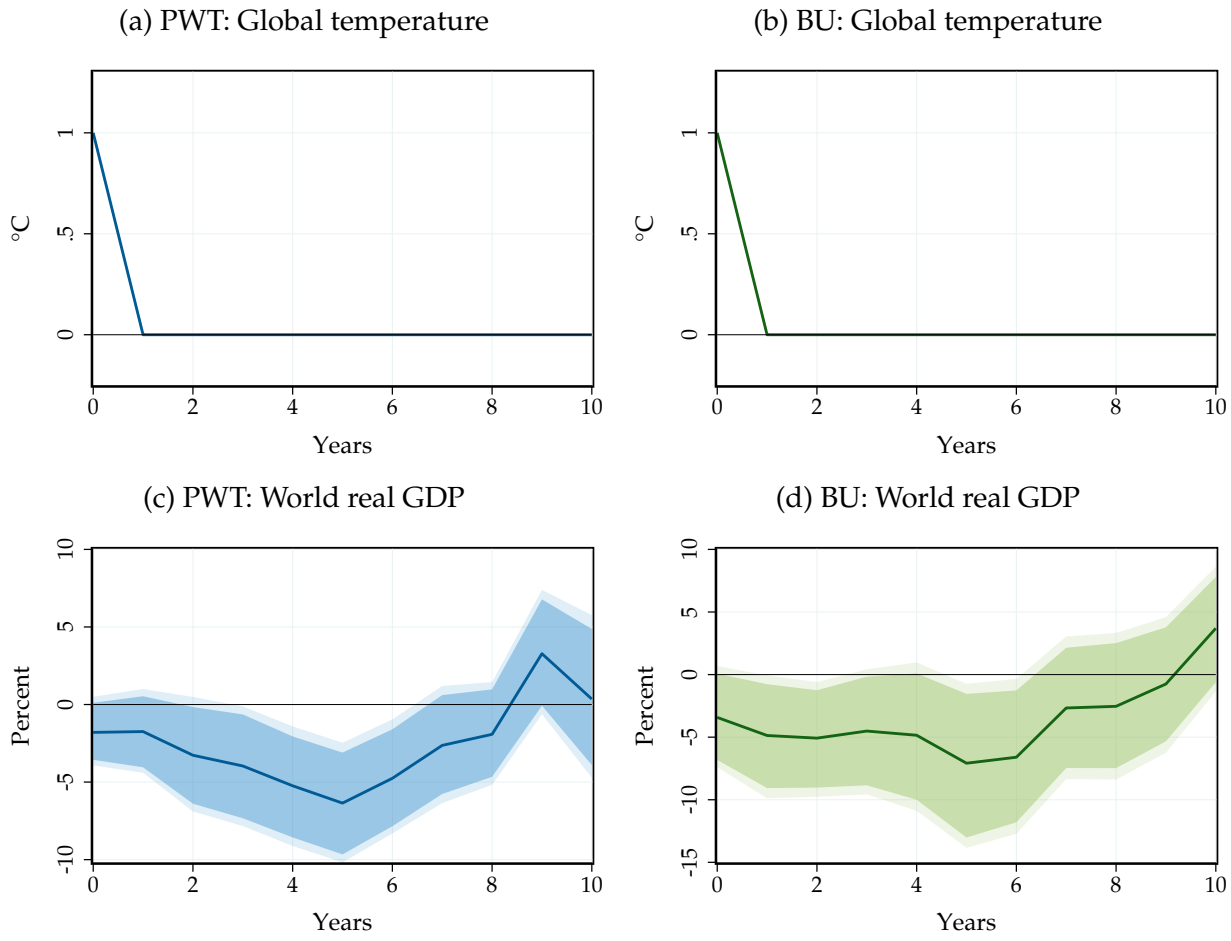

Impulse responses of global mean temperature and world real GDP per capita to a global temperature shock, estimated based on (2), transformed to a counterfactual responses to a completely transitory temperature shock computed using Sims (1986) method. Left panel: PWT sample, 1960-2019. Right panel: BU sample, 1860-2019. Solid line: point estimate. Dark and light shaded areas: 90 and 95% confidence bands.

B.5 Nonlinearities in the Impact of Temperature Shocks

In this appendix, we investigate the role of potential non-linearities for the impact of temperature shocks. Our baseline model relies on the assumption of linearity. We motivate this feature by the fact that we only observe relatively small global temperature shocks in our sample. To further support this assumption, we estimate a local projection model, allowing for differential impacts of small and larger temperature shocks. Specifically, we consider temperature shocks below and above a given percentile p of the global tempera-

ture shock distribution, in absolute terms. In the PWT sample, we use the 90th percentile and in the BU sample the 95th, as we have more observations for the shocks in the longer sample. The percentiles in the two samples are both near 0.2°C. The model we estimate is the following:

$$y_{t+h} - y_{t-1} = \alpha_h + \theta_h^{\text{small}} T_t^{\text{shock}} I(|T_t^{\text{shock}}| \leq z_p) + \theta_h^{\text{big}} T_t^{\text{shock}} I(|T_t^{\text{shock}}| > z_p) + \mathbf{x}_t' \boldsymbol{\beta}_h + \varepsilon_{t+h}, \quad \text{(B.6)}$$

where θ_h^{small} are the dynamic causal effects of small and θ_h^{big} are the dynamic causal effects of big temperature shocks.

The results are shown in Figures B.6(a)-(b). The impact of small and large global temperature shocks is roughly comparable. However, the responses are less precisely estimated. These observations motivate the use of both small and large shocks in our baseline specification.

We also investigate potential asymmetries in the impact of temperature shocks. Arguably, positive temperature shocks are more informative of future climate change than negative temperature shocks. How do the effects of positive shocks compare to our baseline? We consider a specification that allows for differential impacts of positive and negative shocks:

$$y_{t+h} - y_{t-1} = \alpha_h + \theta_h^{\text{pos}} T_t^{\text{shock}} I(T_t^{\text{shock}} > 0) + \theta_h^{\text{neg}} T_t^{\text{shock}} I(T_t^{\text{shock}} \leq 0) + \mathbf{x}_t' \boldsymbol{\beta}_h + \varepsilon_{t+h}, \quad \text{(B.7)}$$

where θ_h^{pos} are the dynamic causal effects of positive global temperature shocks.

Figures B.6(c)-(d) present the results. Positive shocks have comparable impacts to our baseline responses. If at all, the effects of positive shocks are somewhat more pronounced, even though they are less precisely estimated than when we include all shocks. The increased precision motivates our baseline specification, which includes both positive and negative shocks.

Figure B.6: The Role of Nonlinearities

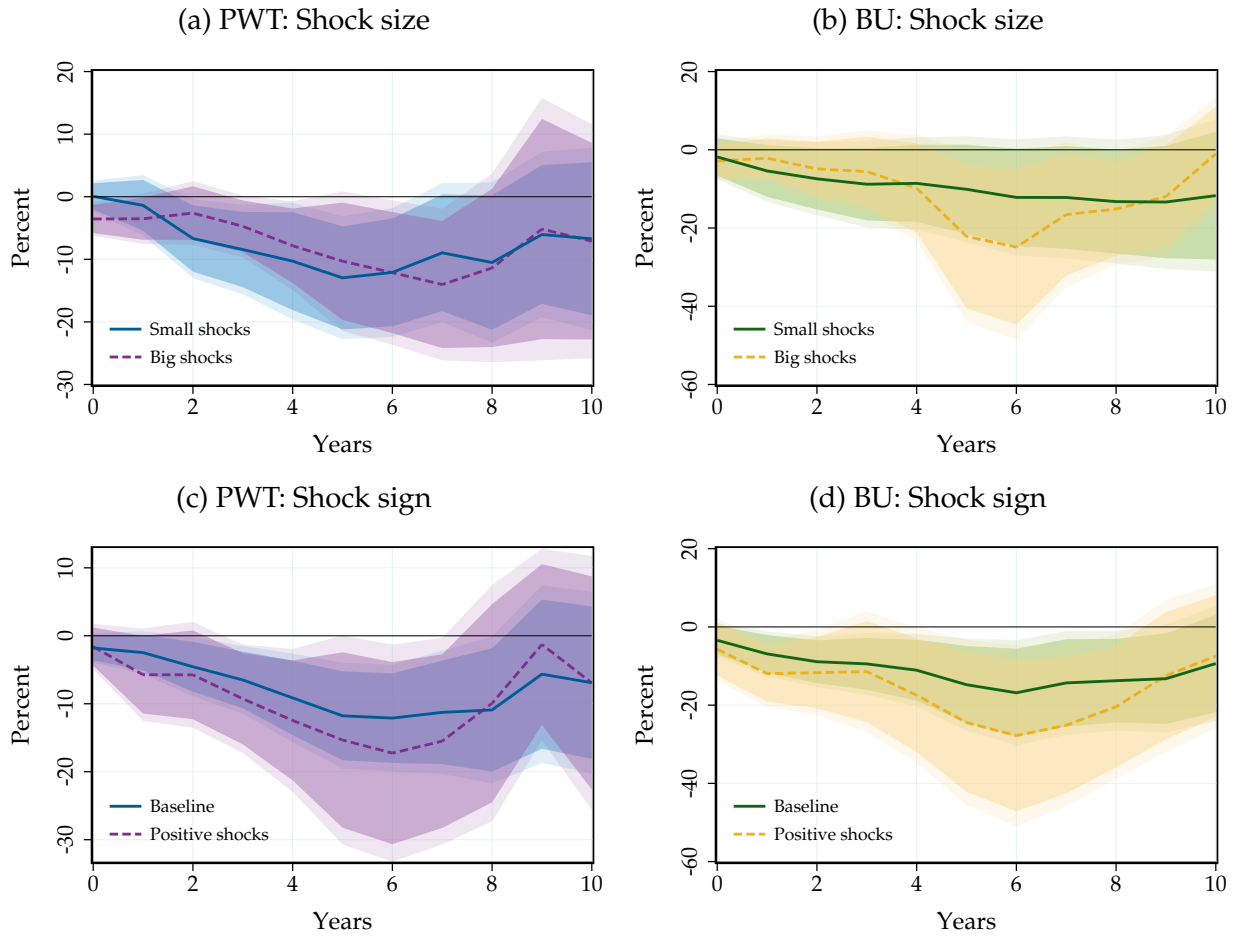

Nonlinearities in the response of world real GDP per capita to a global temperature shock. Left column: PWT sample, 1960-2019. Right column: BU sample, 1860-2019. Top row: allowing for differential impacts of small shocks and large shocks based on (B.6). Bottom row: allowing for differential impacts of positive shocks against baseline based on (B.7). Lines: point estimates. Dark and light shaded areas: 90 and 95% confidence bands.

B.6 Additional Robustness in the Time Series

In Section 3.2, we perform a comprehensive set of robustness checks in our panel local projections model (3) to alleviate concerns about omitted variable bias and sample stability.

In this appendix, we re-do these robustness exercises in the framework of our time-series local projections model (2). Figure B.7 shows that the results also turn out to be robust in the time series.

Figure B.7: Sensitivity of the Effect of Global Temperature Shocks in the Time Series

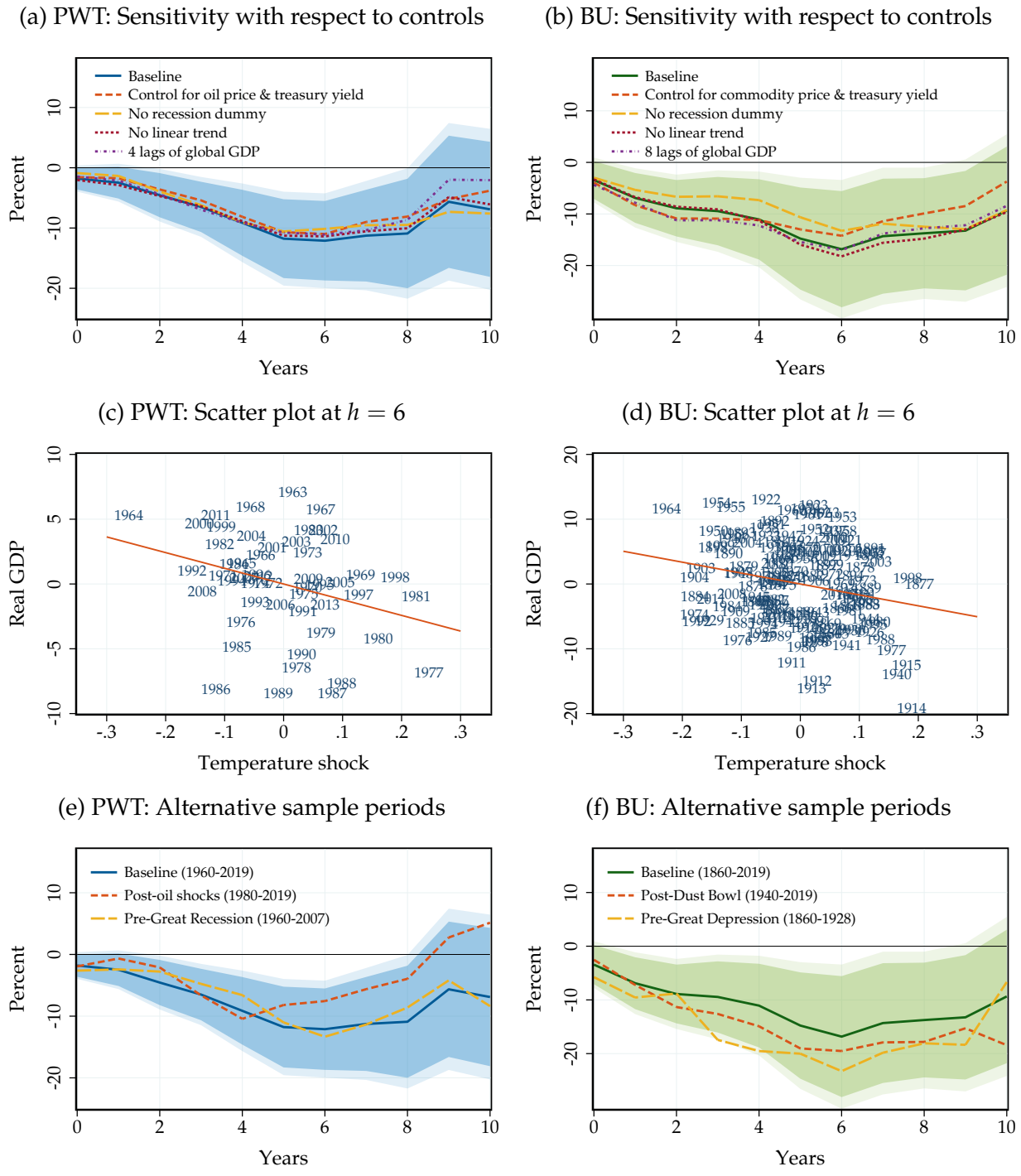

Impulse responses of world real GDP per capita to a global temperature shock, estimated from (2). Left column: PWT sample, 1960-2019. Right column: BU sample, 1860-2019. Top row: sensitivity to controls included. Baseline controls for lags of dependent variable, temperature shock, world real GDP growth, current and lagged recession dummies, and linear time trend. Middle row: scatter plot of temperature shocks against the cumulative change in real GDP per capita 6 years out, after residualizing our set of controls. Bottom row: results for alternative subsamples; PWT: 1980-2019 and 1960-2007; BU: 1940-2019 and 1860-1928. Lines: point estimate. Dark and light shaded areas: baseline 90 and 95% confidence bands.

B.7 Searching for Influential Observations

Section 3 displays the identifying variation in a scatter plot. The negative relationship between temperature and GDP turns out to be a robust one and does not appear to be driven by a particular set of extreme observations.

Nevertheless, there were a few potentially influential temperature shocks: in the PWT sample, there is a large positive temperature shock in 1977, just preceeding the second oil shock and the following Volker disinflation. In the BU sample, there is a large positive temperature in 1940, preceeding the post-World War II contraction. In our baseline specification, we try to control as well as possible for these global economic contractions using our set of recession dummies. However, it is still important to assess the role of these potentially influential observations.

To formally assess influential observations, we perform a jackknife exercise. Specifically, we censor one shock value at a time to zero, and re-run our local projection. To account for the differential impact on our controls, we also include a dummy variable for the year we censor.

Figure B.8: Sensitivity of the Response to Global Temperature Shocks

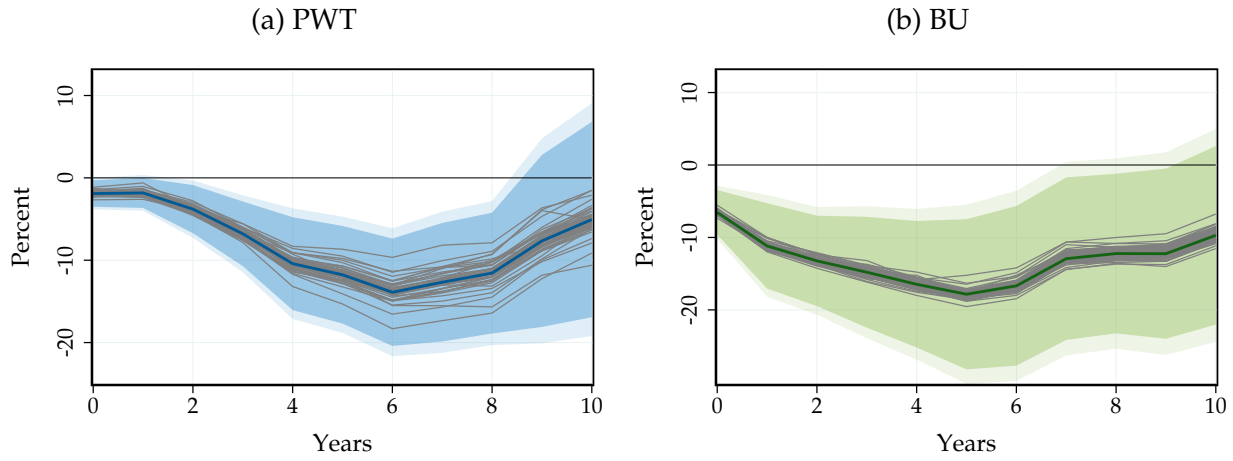

Baseline response of real GDP per capita to a global temperature shock (bold line), together with the responses obtained from the jackknife, censoring one shock value at a time (in gray). Left panel: PWT sample, 1960-2019. Right panel: BU sample, 1860-2019. Dark and light shaded areas: baseline 90 and 95% confidence bands.

Figure B.8 shows our baseline response as the bold blue and green lines, respectively, together with the responses from the jackknife exercise in gray. The estimated impact of temperature on GDP is not driven any single extreme shock. When censoring certain shocks we can get even bigger impacts, while when dropping others the effects can be

somewhat attenuated. In all cases, the peak effect is always close to 10% and within the confidence bands. It is also interesting to note that the dispersion of responses is much smaller in the BU sample. This illustrates the advantages of employing a longer estimation sample in our time-series approach.

B.8 Reverse Causality

In this appendix, we describe how we account for reverse causality. To ease notation, we assume that we start from detrended, stationary variables. We specify, for GDP: $y_t = \sum_{s=-\infty}^{t} T_s \theta_{t-s} + \varepsilon_t$, where T_s is the temperature deviation, and ε_t is a possibly autocorrelated shock. We are interested in estimating the vector θ. For temperature, we specify: $T_t = \sum_{s=-\infty}^{t} y_s \gamma_{t-s} + \tau_t$, where τ_t is a possibly autocorrelated shock, and we know γ. Without loss of generality, We normalize the variance of T_t and y_t to 1. The local projection estimates:

$$P_h^{YT} \equiv \mathbb{C}\text{ov}[y_{t+h} - y_{t-1}, T_t | \mathbf{x}_{t-1}] \equiv \mathbb{C}\text{ov}_{t-1}[y_{t+h} - y_{t-1}, T_t],$$

where $\mathbf{x}_{t-1}$ is our vector of controls, and we denote $\mathbb{C}\text{ov}_{t-1}[\bullet, \bullet] \equiv \mathbb{C}\text{ov}[\bullet, \bullet | \mathbf{x}_{t-1}]$. We obtain, after some algebra and imposing that we include sufficiently many lags of temperature and GDP in our vector of controls to cover the moving average structure:

$$P_h^{YT} = \sum_{s=0}^{h} \theta_{h-s} \mathbb{C}\text{ov}_{t-1}\left[T_{t+s}, T_t\right] + \mathbb{C}\text{ov}_{t-1}\left[\varepsilon_{t+h}, T_t\right]$$

There are two sources of reverse causality: internal persistence (first term), and residual shocks to GDP (second term). Of course, residual shocks can also affect the covariance in the first term, but one can condition this channel out with the deconvolution procedure that conditions on the realized temperature path after a shock.

We start with the second term. After some algebra:

$$\mathbb{C}\text{ov}_{t-1}\left[\varepsilon_{t+h}, T_t\right] = \gamma_0 \mathbb{C}\text{ov}_{t-1}[\varepsilon_t, \varepsilon_{t+h}] + \gamma_0 \theta_0 \mathbb{C}\text{ov}_{t-1}[\varepsilon_{t+h}, T_t].$$

Re-arranging, we obtain:

$$\mathbb{C}\text{ov}_{t-1}\left[\varepsilon_{t+h}, T_t\right] = \frac{\gamma_0}{1 - \gamma_0 \theta_0} \mathbb{C}\text{ov}_{t-1}[\varepsilon_t, \varepsilon_{t+h}].$$

We now denote by $P_s^{TT} = \mathbb{C}\text{ov}_{t-1}\left[T_{t+s}, T_t\right]$ the (observed) autocovariance function of the temperature process. We also denote by $E_s = \mathbb{C}\text{ov}_{t-1}[\varepsilon_t, \varepsilon_{t+s}]$ the (unobserved) autocovariance function of the GDP residuals. We have shown that our local projection estimator is:

$$P_h^{YT} = \sum_{s=0}^{h} \theta_{h-s} P_s^{TT} + \frac{\gamma_0}{1-\gamma_0\theta_0} E_h.$$

The first term represents how internal persistence of the temperature process affects our estimator. We start our discussion by abstracting from the bias in the second term.

If we are only interested in the response to a purely transitory temperature shock—i.e. the θ's—then we can directly correct our estimator for this internal persistence using the observed autocovariance P_s^{TT}. However, if we want to reconstruct the unbiased GDP response to a temperature shock with the same amount of persistence as in the data, i.e.: $\widetilde{\theta}_h = \sum_{s=0}^{h} \theta_{h-s} \mathbb{C}\text{ov}_{t-1}[\tau_t, \tau_{t+s}]$, we need to construct the autocovariance function of the structural temperature shocks $\mathcal{V}_s \equiv \mathbb{C}\text{ov}_{t-1}[\tau_t, \tau_{t+s}]$. Since we assumed that we know the γ's, we can simply residualize the temperature process using lagged GDP and the known γ's and obtain the τ's.

Now we turn to the second term. This term is the classic reverse causality bias. However, since we assume that we know γ_0, we can construct E_h as a function of θ and known covariances, and then solve for θ. Indeed, we obtain after some algebra:

$$E_h = P_h^{YY} - \theta_0 P_h^{YT} - \sum_{s=0}^{h} \theta_{h-s} P_s^{TY} + \theta_0 \sum_{s=0}^{h} \theta_{h-s} P_s^{TT},$$

where we defined $P_h^{YY} = \mathbb{C}\text{ov}_{t-1}[y_t, y_{t+h}]$ the known autocovariance function of output and $P_s^{TY} = \mathbb{C}\text{ov}_{t-1}[y_t, T_{t+s}]$ the local projection of temperature on output (the "reverse" of our baseline local projection).

Hence, we obtain the collection of equations (some nonlinear) indexed by h:

$$P_h^{YT} = \sum_{s=0}^{h} \theta_{h-s} P_s^{TT} + \frac{\gamma_0}{1-\gamma_0\theta_0} \left\{ P_h^{YY} - \theta_0 P_h^{YT} - \sum_{s=0}^{h} \theta_{h-s} P_h^{TY} + \theta_0 \sum_{s=0}^{h} \theta_{h-s} P_s^{TT} \right\}$$

The θ's are the unknowns. Everything else is known or observable. The only nonlinearity comes from θ_0. Conditional on θ_0, these are linear equations. Hence, we examine the equation for θ_0 separately. We obtain: $P_0^{YT} = \theta_0 + \frac{\gamma_0}{1-\gamma_0\theta_0} \left\{1 - \theta_0 P_0^{YT} - \theta_0 P_0^{TY} + \theta_0^2\right\}$,

where recall that we normalized $V_0 = 1$ and $Y_0 = 1$. We also note that $P_0^{YT} = P_0^{TY}$ by definition (but not at higher lags). Multiplying by $1 - \gamma_0\theta_0$: $P_0^{YT}(1 - \gamma_0\theta_0) = \theta_0(1 - \gamma_0\theta_0) + \gamma_0\left\{1 - 2\theta_0 P_0^{YT} + \theta_0^2\right\}$. Re-arranging, we observe that the quadratic terms cancel out. Hence the equation for θ_0 is actually also linear. We obtain an unbiased estimator of θ_0:

$$\theta_0 = \frac{P_0^{YT} - \gamma_0}{1 - \gamma_0 P_0^{YT}}.$$

Given θ_h, we construct θ_{h+1} by induction. We obtain after more algebra:

$$\begin{aligned}\theta_{h+1} = &\frac{1}{1 - \gamma_0 P_0^{YT}} P_{h+1}^{YT} - \frac{1 - \gamma_0\theta_0}{1 - \gamma_0 P_0^{YT}} \sum_{s=0}^{h} \theta_s P_{h+1-s}^{TT} \\ &- \frac{\gamma_0}{1 - \gamma_0 P_0^{YT}} \left\{ P_{h+1}^{YY} - \sum_{s=0}^{h} \theta_s P_{h+1-s}^{TY} + \theta_0 \sum_{s=0}^{h} \theta_s P_{h+1-s}^{TT} \right\}.\end{aligned}$$

This correction delivers the θ's after adjusting for reverse causality. We observe that the "classic" reverse causality adjustment scales with γ_0.

We can then construct $\widetilde{\theta}_h$, the response to a persistent temperature shock τ_t. We start from the unbiased θ's. Then, we construct the autocovariance function of the τ's, i.e. $\mathcal{V}$. We obtain after some algebra: $\mathcal{V}_h = P_h^{TT} - \gamma_0 P_h^{TY} - \sum_{s=0}^{h} \gamma_{h-s}\left(P_s^{YT} - \gamma_0 P_s^{YY}\right)$. Then, we construct: $\widetilde{\theta}_h = \sum_{s=0}^{h} \theta_{h-s}\mathcal{V}_s$.

Implementation. In practice, we need a sequence γ. We construct a central case, and some alternatives for robustness.

The central case uses the following parameters. We use $\eta = 1$ for CO2, CH4 and SO2: emissions move one-for-one with output, which is consistent with a Cobb-Douglas production function.

Average world CO2 emissions during our 1960-2019 sample are $\overline{E}^{\text{CO2}} = 22.5\,\text{Gt/y}$.[3] The temperature response in Celsius to a 100 Gt pulse in Dietz et al. (2021) is well-approximated by:

$$\begin{aligned}100 \times \phi_h^{\text{CO2}} &= a_{100}^{\text{CO2}} \times (e^{-b^{\text{CO2}} \times h} - e^{-c^{\text{CO2}} \times h}) + d_{100}^{\text{CO2}} \times (1 - e^{-f^{\text{CO2}} \times h}) \\ a_{100}^{\text{CO2}} &= 0.1878,\ b^{\text{CO2}} = 0.083,\ c^{\text{CO2}} = 0.2113,\ d_{100}^{\text{CO2}} = 0.1708,\ f^{\text{CO2}} = 0.2113.\end{aligned}$$

[3] See `https://ourworldindata.org/co2-emissions`.

Then we define: $\gamma_h^{\text{CO2}} = \eta \times \overline{E}^{\text{CO2}} \times \phi_h^{\text{CO2}}$.

We use CH4 emissions of $\overline{E}^{\text{CH4}} = 125$ Mt/y.[4] The temperature response in Celsius to a 1 Mt pulse in Azar et al. (2023) is well-approximated by:

$$\phi_h^{\text{CH4}} = a^{\text{CH4}} \times (e^{-b^{\text{CH4}} \times h} - e^{-c^{\text{CH4}} \times h}) + d^{\text{CH4}} \times (1 - e^{-f^{\text{CH4}} \times h})$$
$$a^{\text{CH4}} = 4.9970,\ b^{\text{CH4}} = 0.1230,\ c^{\text{CH4}} = 0.1376,\ d^{\text{CH4}} = 0.0109,\ f^{\text{CH4}} = 0.0019.$$

Then we define: $\gamma_h^{\text{CH4}} = \eta \times \overline{E}^{\text{CH4}} \times \phi_h^{\text{CH4}}$.

We use SO2 emissions of $\overline{E}^{\text{SO2}} = 100$ Mt/y.[5] The temperature response in Celsius to a 1 Mt pulse in Albright et al. (2021) is well-approximated by:

$$\phi_h^{\text{SO2}} = F^{\text{SO2}} \times (A_1^{\text{SO2}} e^{-h/\tau_1^{\text{SO2}}} + A_2^{\text{SO2}} e^{-h/\tau_2^{\text{SO2}}} + A_3^{\text{SO2}} e^{-h/\tau_3^{\text{SO2}}})$$
$$F^{\text{SO2}} = -0.0051$$
$$A_1^{\text{SO2}} = 0.2537,\ \tau_1^{\text{SO2}} = 0.6700,\ A_2^{\text{SO2}} = 0.0269,\ \tau_2^{\text{SO2}} = 12,\ A_3^{\text{SO2}} = 0.0010,\ \tau_3^{\text{SO2}} = 352$$

Then we define: $\gamma_h^{\text{SO2}} = \eta \times \overline{E}^{\text{SO2}} \times \phi_h^{\text{SO2}}$.

Finally, we define $\gamma = \gamma^{\text{CO2}} + \gamma^{\text{CH4}} + \gamma^{\text{SO2}}$. Alternative, plausible choices of emissions-to-GDP elasticities or temperature sensitivity do not affect the reverse causality correction materially because it is small to begin with.

B.9 Additional Robustness Checks in Panel

In this appendix, we perform a number of additional sensitivity checks on the effect of global temperature shocks based on our panel local projections.

Overall, these results further illustrate the robustness of our finding that global temperature shocks lead to a persistent and statistically significant fall in economic output.

The role of El Niño and other temperature variability. Are our results are driven by specific sources of temperature variability such as El Niño events or volcanic eruptions? To answer this question, we source data on El Niño, proxied by the Oceanic Niño Index (ONI), from NOAA and Webb and Magi (2022), and data on volcanic eruptions from the NOAA.

[4] See `https://www.iea.org/reports/global-methane-tracker-2023/overview`.
[5] See `https://ourworldindata.org/grapher/so-emissions-by-world-region-in-million-tonnes`.

To shed light on the role of El Niño, we control for the ONI in our main specification. The results are shown in Figure B.9. The responses are similar to our baseline estimates, suggesting that our main results capture a common effect of global temperature on economic activity that does not depend heavily on being driven by El Niño or other sources of climate variability.

A related concern is that major volcanic eruptions may affect world real GDP through other channels than temperature, for instance by limiting air travel. Controlling for volcanic eruptions also yields virtually unchanged results.

Figure B.9: The Role of El Niño and Other Temperature Variability

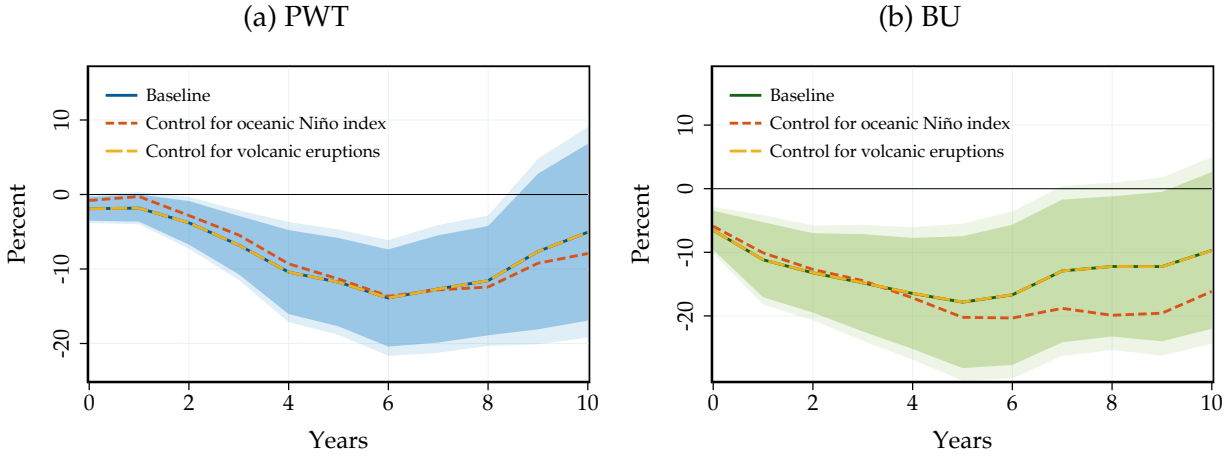

Impulse responses of real GDP per capita to a global temperature shock estimated based on (2), controlling for El Niño and volcanic eruptions. Left column: PWT dataset (173 countries, 1960-2019. Right column: BU dataset (43 countries, 1860-2019). Dark and light shaded areas: 90 and 95% confidence bands for our baseline estimates.

Weighting and pre-trends. In our panel local projections, we estimate an average effect. One concern is that small countries with extreme responses to temperature shocks may have a disproportionate weight in the estimate. Reassuringly, our time series local projection estimates are close to our panel estimates. To further assess this, we estimate a GDP-weighted panel local projection, using GDP as a share of world GDP as weights.

Figure B.10 displays our results. Consistent with our time-series estimates, the GDP-weighted panel local projection exhibits similar impacts to the unweighted, baseline panel local projection in the PWT and BU samples.

Pre-trends are another potential concern. Thus, we assess how the pre-trends look in our baseline panel local projections. In both samples, we detect no economically meaningful or statistically significant pre-trends. Note that the pre-trends from $h =$

$-(p+1), \ldots, -1$ are zero by construction because of the lags included in our local projections.

Figure B.10: Weighting and Pre-trends

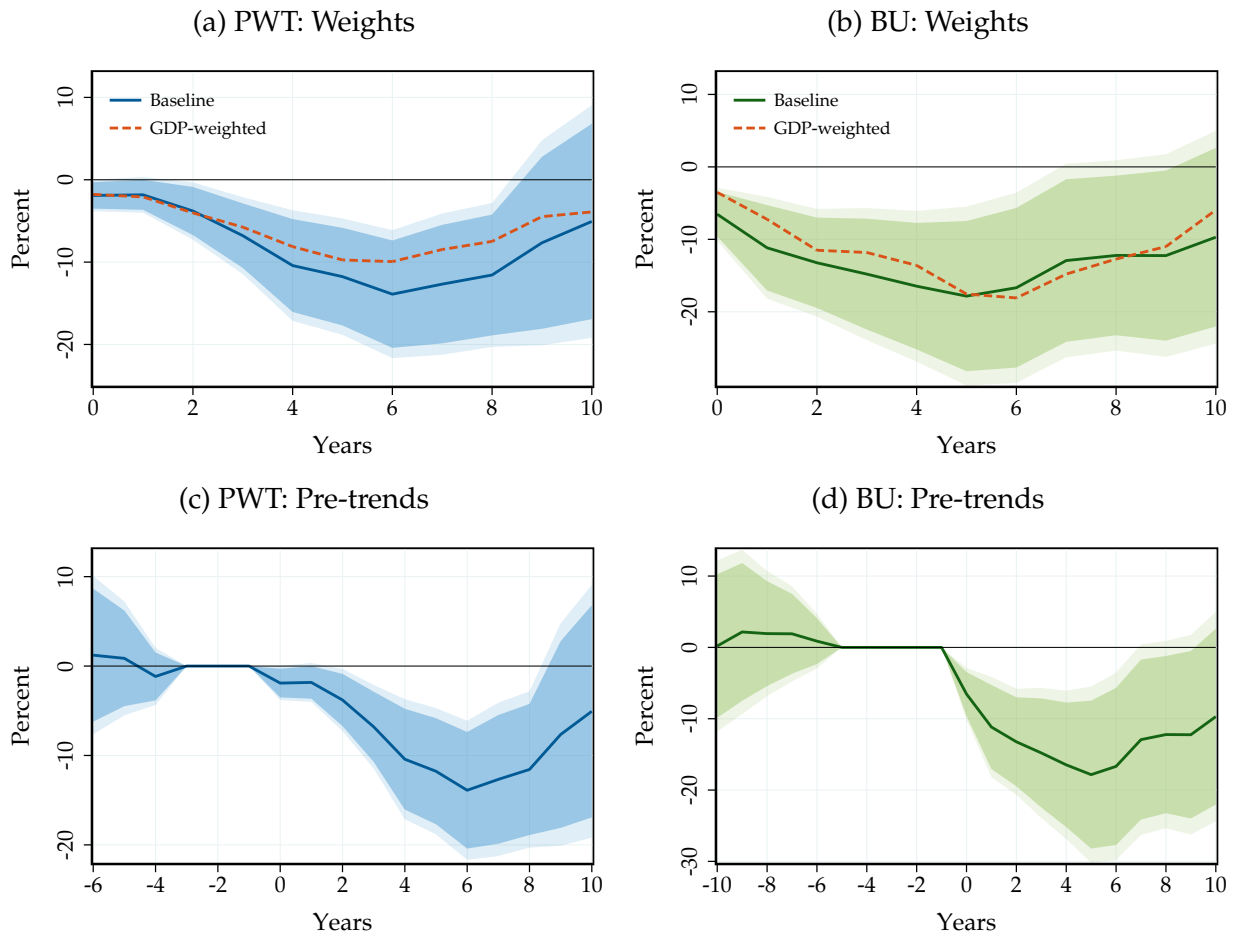

Impulse responses of real GDP per capita to a global temperature shock estimated in the panel using (3). Left column: PWT dataset (173 countries, 1960-2019. Right column: BU dataset (43 countries, 1860-2019). Top row: using uniform (baseline), population and GDP weights (3); weights defined at $t-1$ for the regression of outcome at $t+h$ onto the global temperature shock at time t. Bottom row: baseline response with pre-trends. Lines: point estimate. Dark and light shaded areas: 90 and 95% confidence bands.

Alternative GDP and temperature datasets. We also assess the robustness of our results to using alternative data sources. Figure B.11 collects the results. Panels (a)-(b) assess the sensitivity with respect to the GDP and temperature data we use. In the more recent sample, using real GDP per capita from the PWT or from the WDI produces very similar results. Similarly, using aggregated global mean temperature data from the Berkeley Earth dataset or off-the-shelf measures from NASA or NOAA produces virtually identical results. In our longer sample, we alternatively use GDP data from the Global Macro

Database (Müller et al., 2025). The results are very similar to our baseline with the Barro-Ursúa data.

Figure B.11: Data Sources and Other Specification Choices

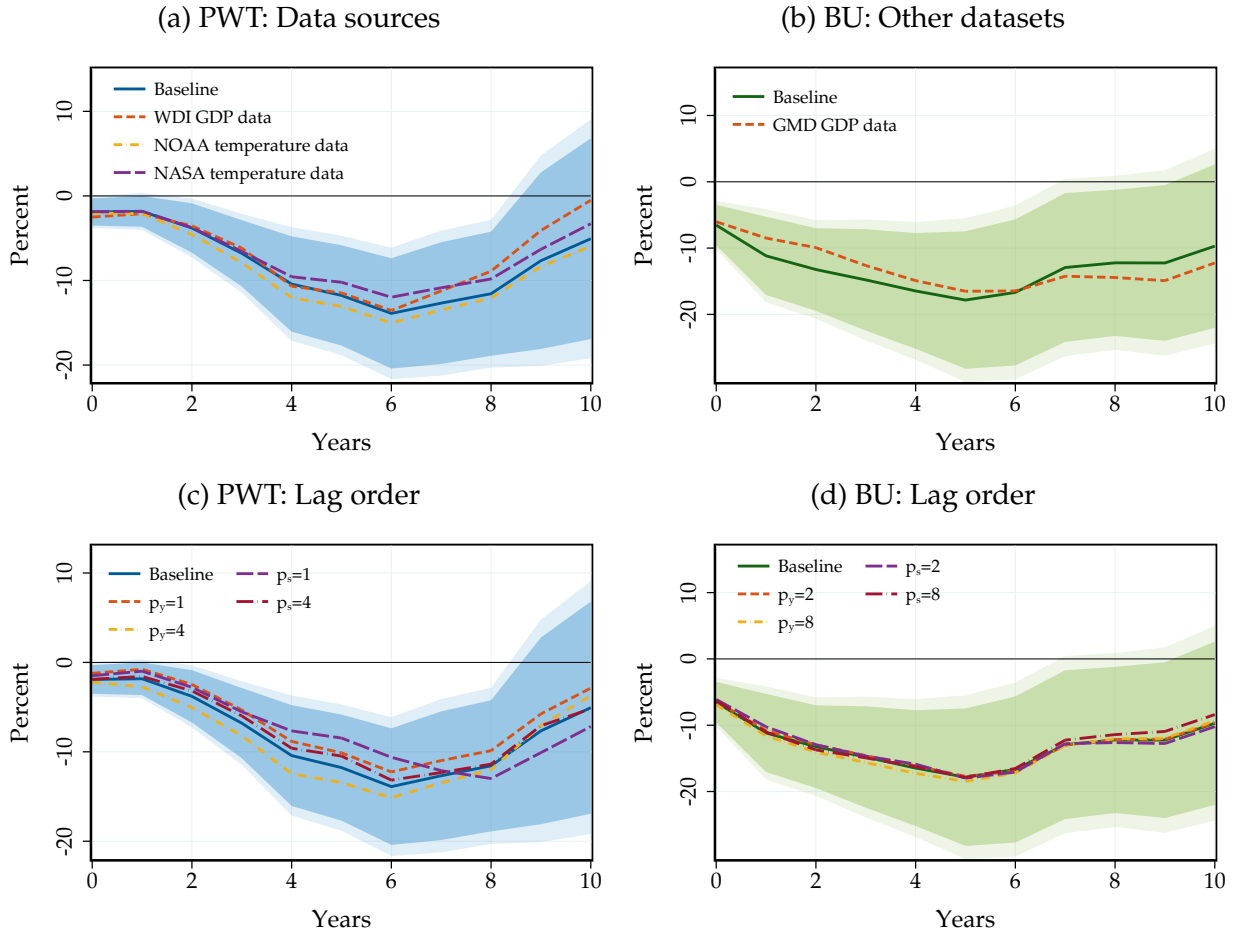

Sensitivity of the effects of global temperature shocks on real GDP per capita to a global temperature shock, with respect to data choices, and the number of lags included. Left column: PWT dataset (1960-2019). Right column: BU dataset (1860-2019). Lines: point estimate. Dark and light shaded areas: 90 and 95% confidence bands.

Number of lags. Panels (c)-(d) evaluate sensitivity with respect to the number of lags included for real GDP and temperature shocks. When varying the lag order of the dependent variable, we keep the lag order of our temperature shock at the baseline value and vice versa. Our results turn out to be robust with respect to the lag order.

Selection of countries. We also assess the sensitivity to the countries included in our panel. We focus here on the PWT data, as the BU data features only a more limited set of relatively larger countries. In our baseline analysis, we include countries in the PWT data

that we observe for at least 20 non-missing observations of temperature and real GDP per capita.

Figure B.12 shows how the results change if we vary the set of countries in our panel. We alternatively focus on the set of countries included in Dell et al. (2012), Burke et al. (2015), or exclude countries in Sub-Saharan Africa. Reassuringly, the results turn out to be very similar.

Figure B.12: Sensitivity to Selection of Countries

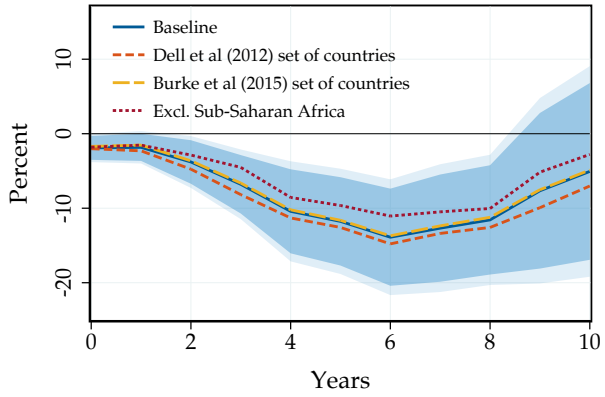

Sensitivity of the effects of global temperature shocks on real GDP per capita to selection of countries included in panel. Lines: point estimate. Dark and light shaded areas: 90 and 95% confidence bands. PWT dataset.

One-step Forecast Error Temperature Shocks. As our baseline, we measure the temperature shocks as two-step ahead forecast errors, motivated by the period of the climatic variation we aim to capture. A more common choice in the literature is to construct temperature shocks as one-step ahead forecast errors, as in Bansal and Ochoa (2011) and Nath et al. (2024). We have already showed that the point estimates of the GDP response are virtually identical when using the one- or two-step ahead forecast error as the relevant shock measure. For completeness, we present our main results with confidence bands based on the one-step ahead temperature forecast error. The results are shown in Figure B.13. The responses turn out to be virtually identical using this alternative shock measure.

Figure B.13: Results with One-step Ahead FE

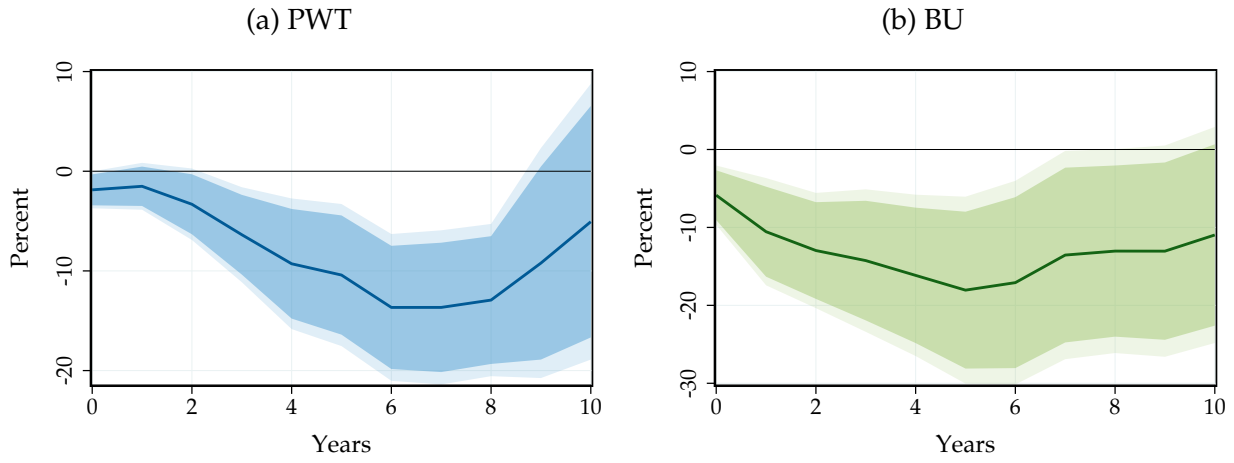

The effects of global temperature shocks on real GDP per capita to a global temperature shock, measured as one-step ahead forecast error. Left panel: PWT dataset (173 countries, 1960-2019. Right panel: BU dataset (43 countries, 1860-2019). Solid line: point estimate. Dark and light shaded areas: 90 and 95% confidence bands.

C Additional Results for Global vs. Local Temperature

C.1 Global vs. Local Temperature Shocks

To illustrate the identifying variation when estimating the effects of local temperature, we show in Figure C.1 the constructed local temperature shocks for two example countries: the United States and South Africa.

Figure C.1: Local and Global Temperature Shocks

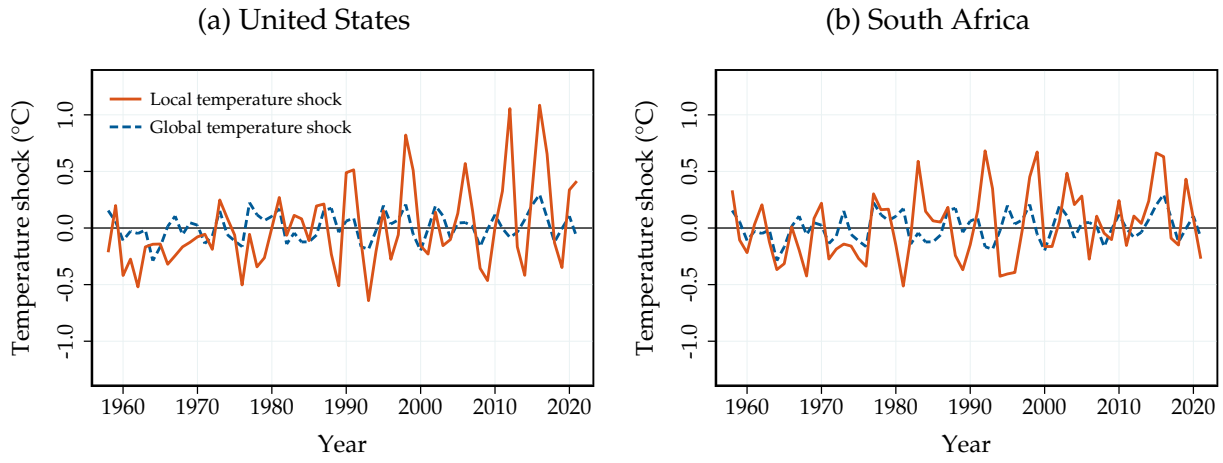

Local temperature shocks for the United States (left panel) and South Africa (right panel) in red together with the global temperature shocks as the blue dashed line. All the shocks are computed using the Hamilton (2018) filter with ($h = 2$, $p = 2$). Local shocks are based on population-weighted country-level temperature data. PWT dataset.

The standard deviation of local temperature shocks is approximately three times larger than that of global temperature shocks, which is apparent in the examples above. While local and global shocks have a correlation of 0.31, they frequently move in different directions. Thus, local shocks do not always correspond to global shocks and vice-versa.

C.2 Jointly Estimating Local and Global Shocks

As our baseline, we estimate the impacts of global and local temperature shocks separately, in individual models. In this appendix, we report the results when we estimate the impacts jointly in the same local projection specification (4a).

Figure C.2 displays the results. The jointly estimated responses are very similar to our baseline responses. This is especially true for the impulse responses to the global temperature shock. For the local temperature shock, the effects are slightly attenuated, and lie closer to the responses from the univariate model with time fixed effects than to the responses from the univariate model with global controls. This is intuitive as both, global temperature shocks and time fixed effects net out common variation in local temperature shocks.

Figure C.2: Joint Responses of Local and Global Temperature Shocks

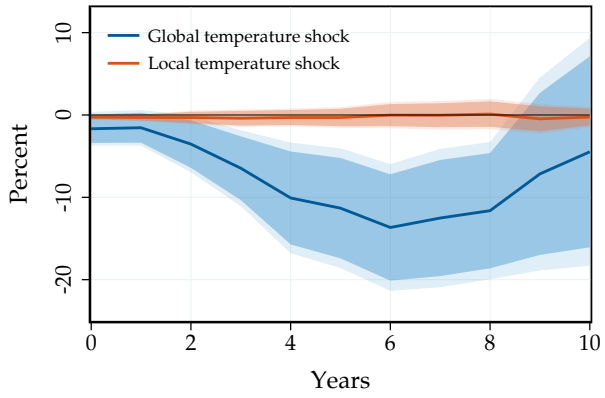

Impulse responses of GDP per capita to global and local temperature shocks, estimated based on (4a). Lines: point estimates. Dark and light shaded areas: 90 and 95% confidence bands. PWT dataset.

C.3 The Role of Time Fixed Effects

In this appendix, we shed further light on the role of time fixed effects. Figure C.3(a) compares the impulse responses of GDP to local temperature shocks with and without time fixed effects. The responses from the local temperature shock specification with time fixed effects are close to the baseline with global controls. The coverage of the confidence bands is also comparable. Overall, these results suggest that our controls successfully account for common economic shocks.

While we cannot include time fixed effects in our baseline specification with global temperature, we alternatively consider a specification based on an intermediate level of aggregation. Specifically, we construct distance-weighted external temperature shocks. To do so, we first construct an external temperature measure that weights temperature in the surrounding countries by their physical distance: $T_{i,t}^{\text{dist, ex}} = \sum_{j \neq i} d_{ij} T_{i,t}$, where d_{ij} is proportional to the inverse geodesic distance between countries i and j and are normalized to sum to one for each country i. We source these distances from the TRADHIST database. In a next step, we create a distance-weighted external temperature shock measure by applying the Hamilton (2018) filter.

These shocks are close in spirit to our land-based global temperature shocks, but because the weights differ by country, the shock measure will too. Therefore, we are able to control for time fixed effects in this setting.

Figure C.3(b) shows how the inclusion of time fixed effects affects the response of distance-weighted temperature shocks. In both cases, real GDP falls significantly with a

Figure C.3: The Role of Time Fixed Effects

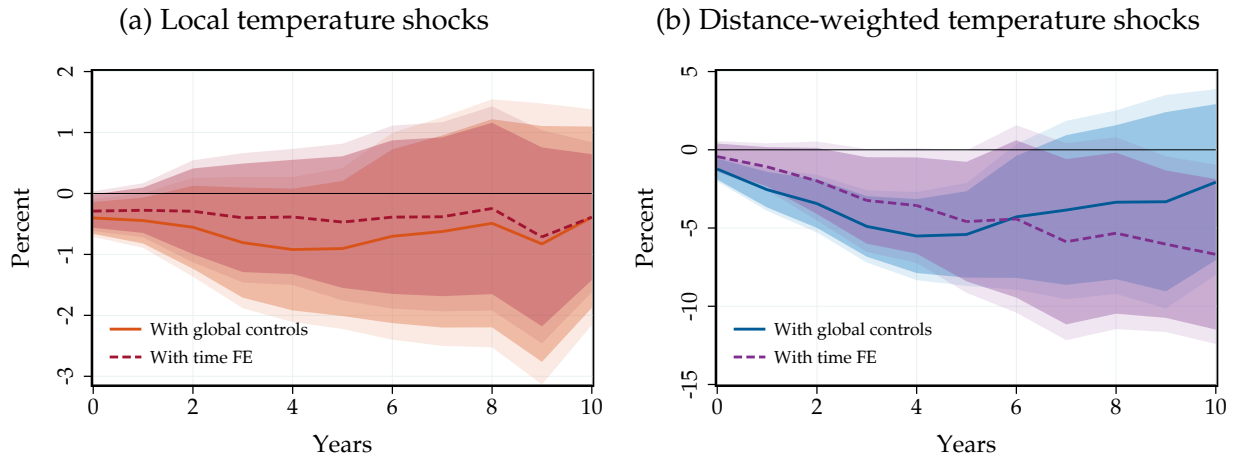

Impulse responses of real GDP per capita. Responses to a local temperature shock in Panel (a) and responses to a distance-weighted external temperature shock in Panel (b), estimated based on a specification with global controls (3) or with time FE (4b). Solid line: point estimate. Dark and light shaded areas/dashed and dotted lines: 90 and 95% confidence bands. Sample of countries differs from main analysis due to availability of trade data at the beginning of the sample. PWT dataset.

peak effect in excess of 5%. The shape of the responses is a bit different, with the model without time fixed effects generating more front-loaded impacts. However, the cumulative effect is very similar in both cases, suggesting that our larger impacts of global temperature shocks are not the consequence of an omitted control variable due to the omission of time fixed effects.

C.4 Impacts of Extreme Events

Figure 8 shows that global temperature shocks strongly correlate with the exposure to extreme weather events: extreme temperature, drought, extreme precipitation, and extreme wind. Here we project world real GDP on extreme event exposure directly, so that we can aggregate up the impact of global temperature on GDP through extreme events.

Because local temperature and extremes may be correlated, we estimate these impacts jointly, based on the following panel local projection specification:

$$y_{i,t+h} - y_{i,t-1} = \alpha_{i,h} + \sum_X \phi_h^X X_{i,t} + \mathbf{x}_t' \boldsymbol{\beta}_h + \mathbf{x}_{i,t}' \boldsymbol{\gamma}_h + \varepsilon_{i,t+h}, \tag{C.1}$$

where X_i are the country-level extreme event exposure indices (extreme heat, droughts, extreme precipitation, extreme wind) and local temperature changes. ϕ_h^X is the impact of an increase in country-level exposure for extreme event X_i on country-level GDP y_i at

horizon h. We include our expanded set of global controls, and also control for 4 lags of the extremes.

Figure C.4: The Impact of Extreme Events on GDP

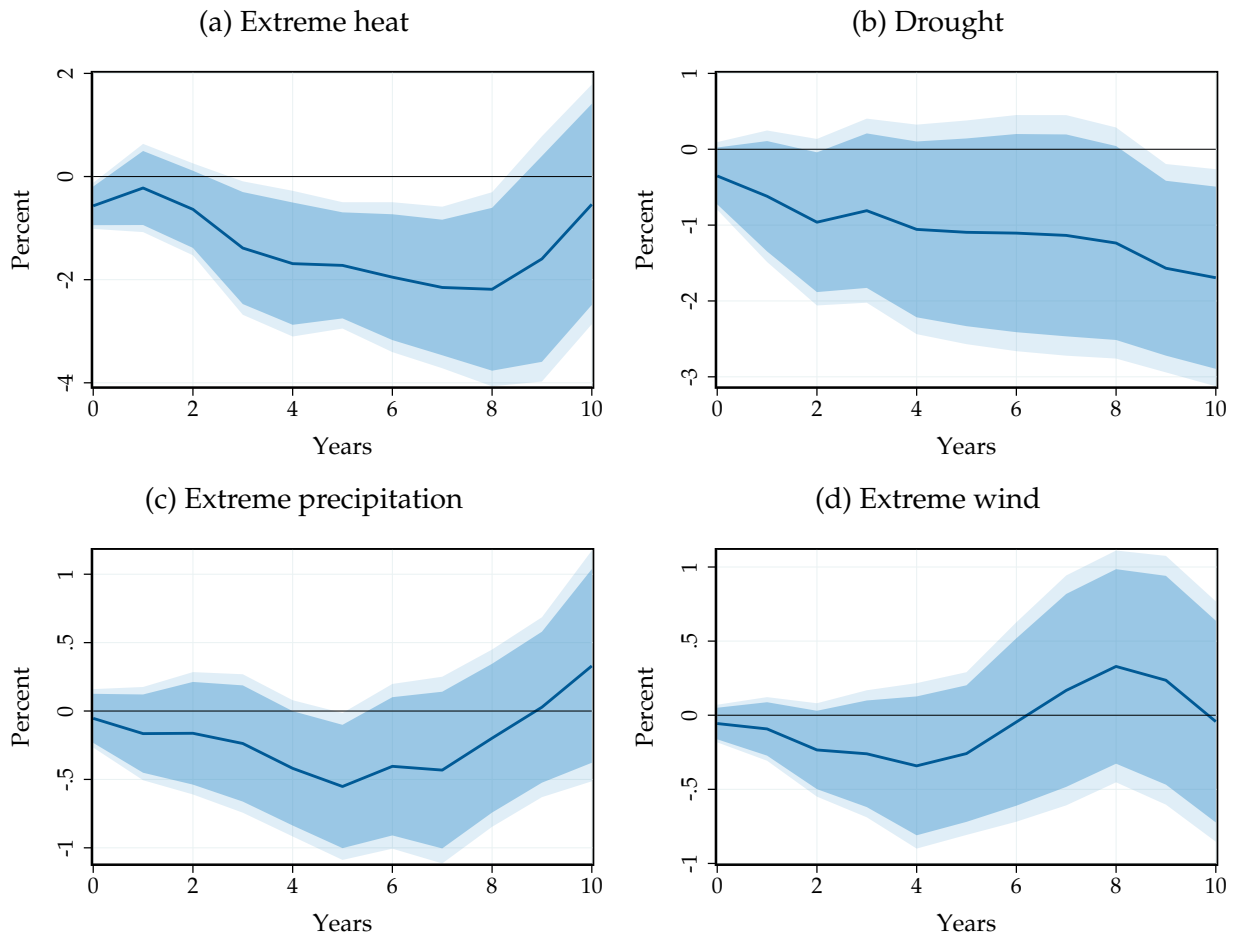

Impulse responses of world real GDP per capita to extreme events, estimated based on (C.1) with our expanded set of controls. Extreme weather variables record the share of cell-days in a given year and country where temperature, precipitation, or wind speed are above/below a threshold. We define threshold using the daily weather distribution in 1950-1980. Temperature: above 95th percentile. Drought: below 25th percentile. Extreme precipitation: above 99th percentile. Wind: above 99th percentile. Though not necessary for our results, we smooth the precipitation and wind measures with a backward-looking (current and previous two years) moving average to remove their inherent noise. Responses are normalized to the peak increase in frequency from Figure 8: graphical responses report $\psi_h^X/(\max_t \theta_t^X)$. Solid lines: point estimates. Dark and light shaded areas: 90 and 95% confidence bands. PWT dataset.

Figure C.4 displays our results. Graphically, we normalize the estimated impact normalized by the peak frequency rise in exposure from Figure 8 to ease interpretation: we report $\frac{\phi_h^X}{\max_t \theta_t^X}$. Extreme weather events lead to a significant and persistent fall in GDP. The response is pronounced for extreme heat, extreme precipitation and droughts. Extreme wind also has meaningful adverse effects, even though somewhat less precisely estimated.

To construct the aggregate impact of global temperature on GDP through extreme events, we further need to adjust the estimates ϕ_h^X for internal persistence. Underlying the estimates in Figure C.4, extreme event exposures turn out to have very low internal persistence. Thus, the estimates in Figure C.4 largely represent the GDP impact of a one-time increase in extreme events. Nevertheless, we convert the estimates ϕ_h^X in response to a realized rise in extreme event frequency to estimates in response to a one-time fully transitory surge in extreme event frequency using the method in Sims (1986). We denote those adjusted estimates by ψ_h^X. In practice, the ϕ_h^X and ψ_h^X are close. We then aggregate these estimates using the definition of Θ_h in Section 4.2.

C.5 Spillovers and External Temperature Shocks

When the trading partners of a given country are hit by adverse local temperature realizations, some of the resulting economic consequences may also be felt domestically as hypothesized by Neal et al. (2025) and shown in Dingel et al. (2023) and Zappalà (2023). How does explicitly accounting for such spillovers affect the comparison between global and local temperature shock estimates?

To gauge the relevance of economic spillovers, we exploit an intermediate level of spatial aggregation of local temperature shocks. We first construct an external temperature measure for each country that averages local temperature in surrounding countries, weighted by their respective trade share: $T_{i,t}^{\text{ex, trade}} = \sum_{j \neq i} \pi_{ij} T_{i,t}$, where π_{ij} denote trade shares based on imports plus exports between countries i and j in 1960 from TRADHIST. We then normalize total trade shares π_{ij} such that all weights sum to one for any given country. Next, we apply the same Hamilton (2018) filter to $T_{i,t}^{\text{ex, trade}}$ to construct an external temperature shock.

We expect the trade-weighted external temperature shock to have a substantial impact on GDP if economic spillovers explain the difference between local and global temperature impacts. In that case, the effect of global temperature shocks would also be largely absorbed by the external temperature shock when estimating the impacts jointly. We operationalize these ideas by estimating the impact of trade-weighted external temperature, both in isolation and jointly with global temperature and with local temperature.[6]

Figure C.5 shows the impulse responses of world real GDP to the two external tem-

[6]Because we largely leverage regional variation, we exclude the region-specific time trends from our set of controls. Omitting region-specific trends leaves our baseline results virtually unchanged.

Figure C.5: The Impact of External Temperature Shocks

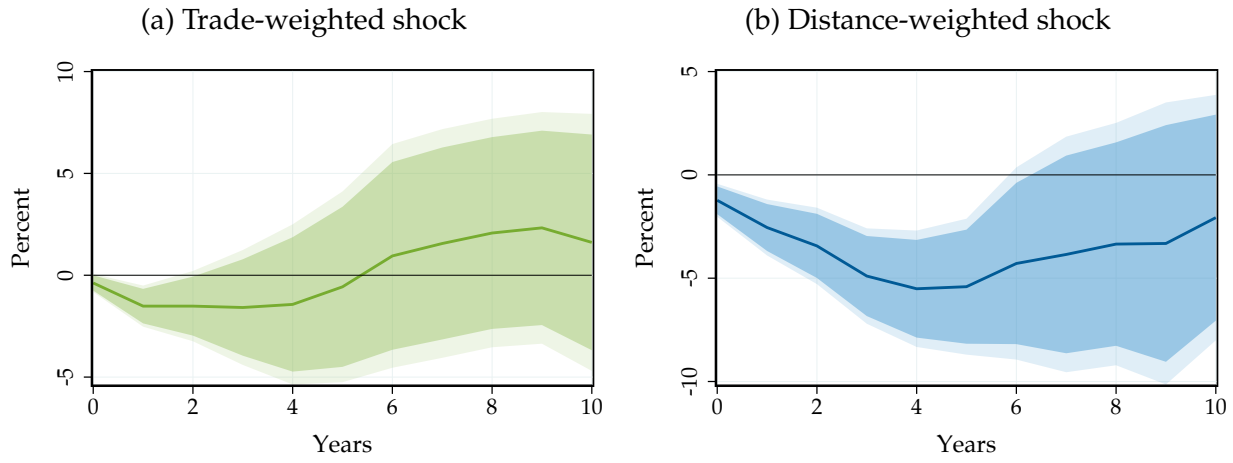

Impulse responses of world real GDP per capita to external temperature shocks, estimated based on (3). Left panel: response to a trade-weighted shock. Right panel: responses to a distance-weighted shock. Solid lines: point estimates. Dark and light shaded areas: 90 and 95% confidence bands. Sample of countries differs from main analysis due to availability of trade data at the beginning of the sample. PWT dataset.

perature shocks, estimated in separate specifications. In isolation, temperature shocks to a country's trading partners (trade-weighted external temperature shocks) turn out to moderately affect GDP. The fall is comparable to the impact of local, idiosyncratic temperature shocks at first. The response, however, turns out to be less persistent and reverses after 5 years.

Temperature shocks to a country's neighbors (distance-weighted external temperature shocks) have more pronounced effects on GDP. The peak effect materializes after 4 years and is near 5%. The response features also a considerable degree of persistence. Overall, the estimated impacts are comparable to the effects estimated for common land temperature shocks, and larger than for idiosyncratic local temperature shocks.

Figure C.6(a) shows the responses to a trade-weighted external temperature shock and a global temperature shock, jointly estimated in the same local projection model. The response to the trade-weighted temperature shock from the joint model is very close to the estimated impact from the individual model. Global temperature continues to have adverse impacts on GDP, even when controlling for trade-weighted external temperature.[7]

Figure C.6(b) indicates that the effects of local temperature shocks rises somewhat when controlling for trade-weighted temperature shocks. This change is consistent with

[7]The shape of the response to the global temperature shock is slightly different from our baseline response because we cannot obtain trade information for all countries at the beginning of our sample and must thus rely on a different set of countries.

Figure C.6: The Role of Economic Spillovers

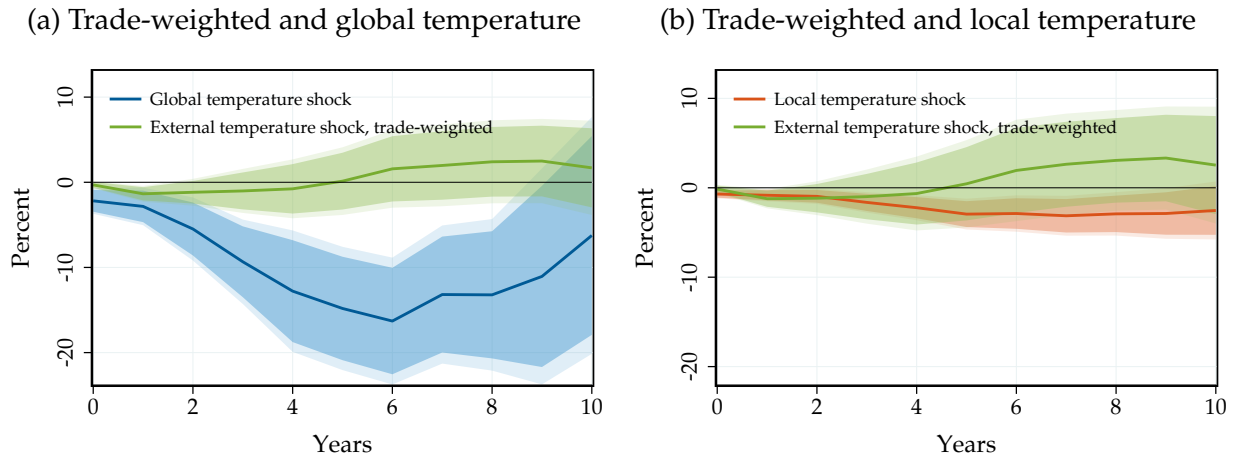

Impulse responses of world real GDP per capita to external temperature shocks. Left panel: response to a global and trade-weighted shock, estimated jointly in the same local projection specification. Right panel: response to a local and trade-weighted shock, estimated jointly in the same local projection specification. Solid lines: point estimates. Dark and light shaded areas: 90 and 95% confidence bands. Sample of countries differs from main analysis due to availability of trade data at the beginning of the sample. PWT dataset.

export-led spillover effects and spatially correlated temperature shocks. Quantitatively however, neither the direct effect of local temperature nor the indirect effect of trade-weighted external temperature are able to bridge the gap with global temperature impacts. Overall, these results suggest that economic spillovers do not play a major role in accounting for the difference between global and local temperature.

C.6 Additional Empirical Results

In this appendix, we present some additional empirical results on the effects of global and local temperature shocks.

Effect of global temperature shocks on ocean and land temperature. On average, global temperature shocks increase local temperature by nearly 1°C. How can this be reconciled with the fact that oceans warm by less and more slowly than land?

The answer lies in the weights. In our baseline specification, we use population-weighted local temperature and study the average effect across countries. In this appendix, we alternatively construct area-weighted time series of global ocean surface and land temperature. For our land temperature measure, we exclude Antarctica.

Figure C.7 shows the results. As expected given that land warms more than oceans, a global temperature shock of 1°C leads to an increase in ocean surface temperature by

Figure C.7: Effect on Ocean and Land Temperature

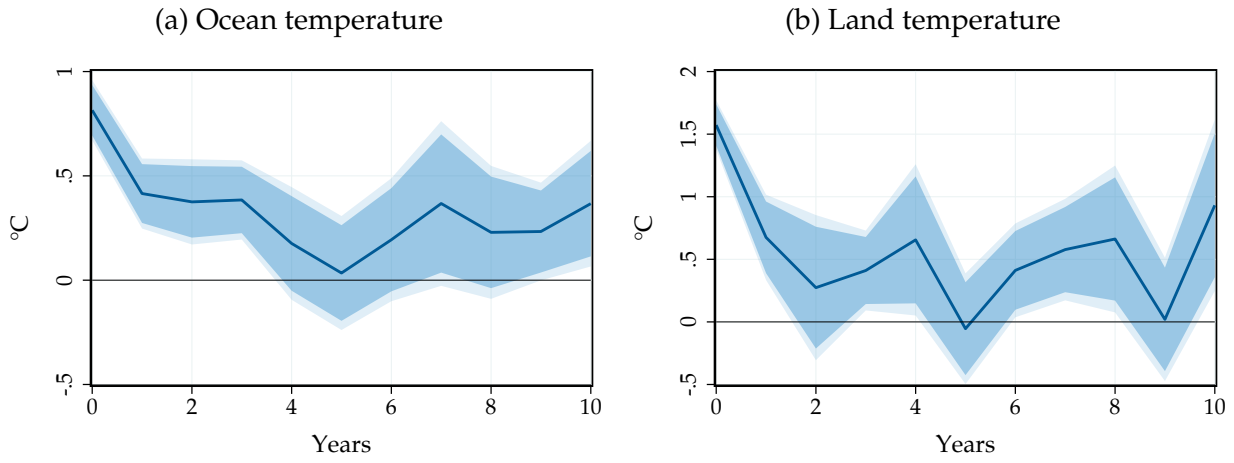

Impulse responses of ocean surface and land temperature to a global temperature shock, estimated based on (2). Solid line: point estimate. Dark and light shaded areas: 90 and 95% confidence bands. PWT dataset.

nearly 0.8°C and an increase in land temperature by about 1.5°C.

Additional local temperature shock responses. In Section 4.3, we study through which margins of GDP do global temperature shocks transmit, finding salient effects on investment, capital and productivity. Do local temperature shocks transmit differently?

Figure C.8 shows the responses of investment, capital and productivity to a local temperature shock. Local temperature shocks also lead to a fall in investment, capital and productivity. However, as for the output responses, these effects are by an order of magnitude smaller than for global temperature shocks. Controlling for time fixed effects makes again little difference.

C.7 Regional Impacts

Country heterogeneity by average temperature and income. We study how the impact of global temperature varies by average temperature and income. To this end, we bin countries into different groups based on temperature and income data. Specifically, we bin countries into three temperature and income groups, based on data from 1957-1959 to ensure that group characteristics are not influenced by the effects of the global temperature shocks.

Figure C.9 displays our results. Panel (a) shows the effects to a global temperature shock for cold countries (average temperature below 10°C), temperate climate countries

Figure C.8: Transmission of Local Temperature Shocks

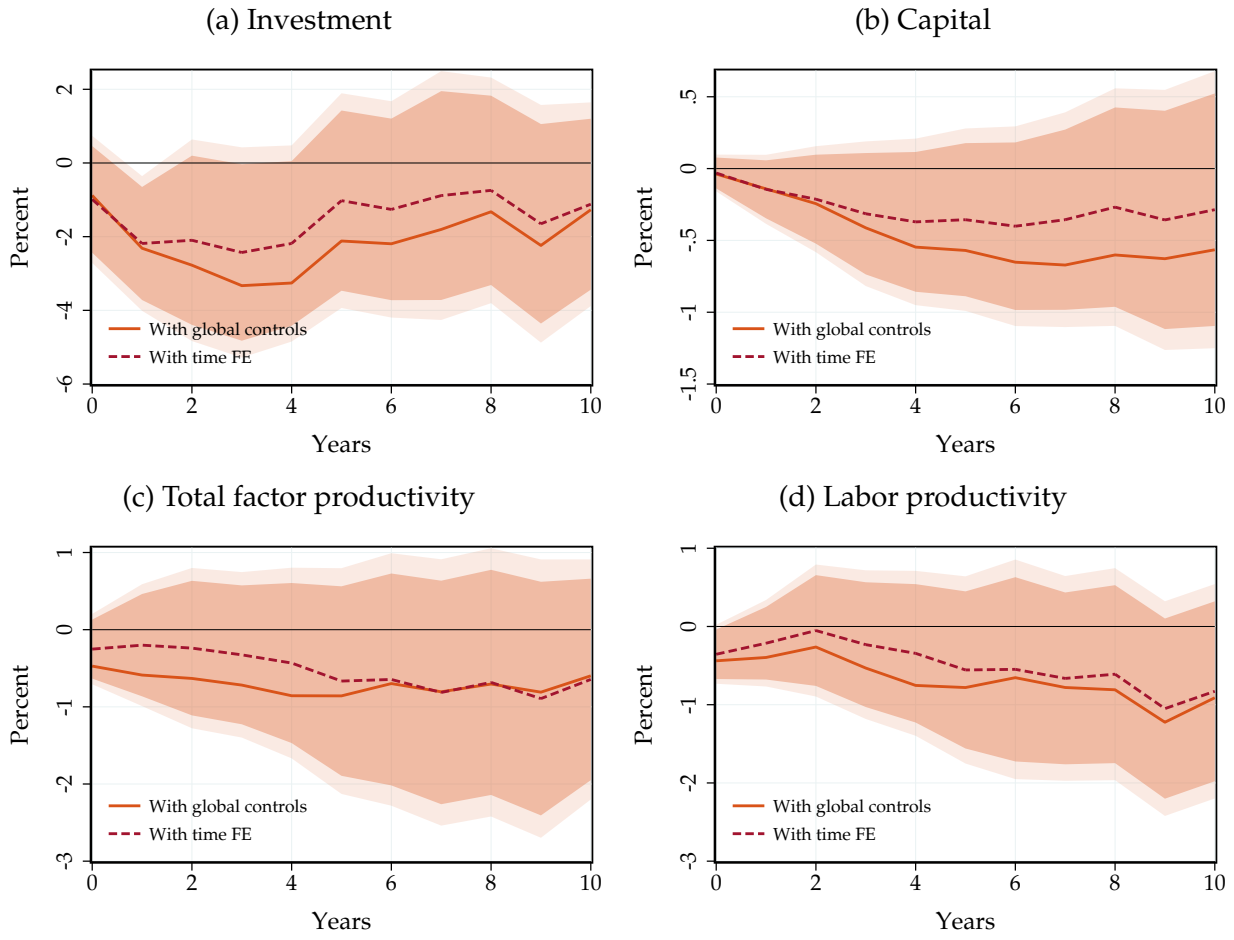

Impulse responses of investment per capita, the capital stock per capita, total factor productivity and labor productivity to a global temperature shock, estimated based on panel local projections (3). Labor productivity: output over employment. Total factor productivity: Penn World Tables. Solid line: point estimate from specification with global controls. Dark and light shaded areas: 90 and 95% confidence bands. Dashed line: point estimate based on model with time fixed effects. PWT dataset.

Figure C.9: Heterogeneous Effects of Global Temperature Shocks

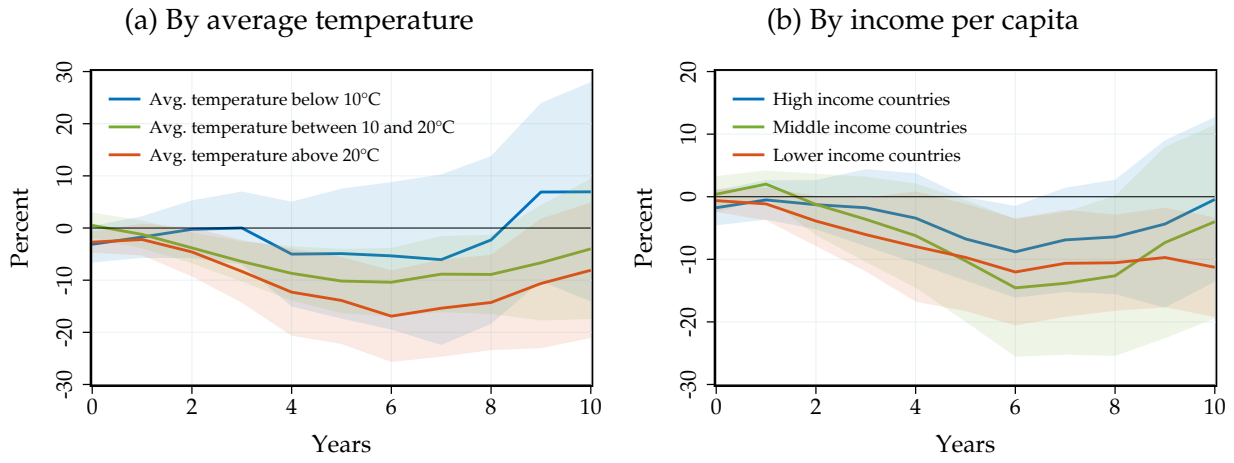

Impulse responses of real GDP per capita to a global temperature shock for different groups of countries. We estimate these responses based on (3), conditioning on the different groups. In Panel (a), we group countries by their average temperature in 1957-1959. In Panel (b), we group countries by their per capita income (in PPP terms) in 1957-1959. Solid line: point estimate. Dark and light shaded areas: 95% confidence bands. PWT dataset.

(average temperature between 10°C and 20°C) and hot countries (average temperature above 20°C). Hot countries display the strongest adverse effects of temperature shocks. This result is *qualitatively* consistent with previous evidence on local temperature shocks (Dell et al., 2012; Burke et al., 2015; Nath et al., 2024). *Quantitatively*, global temperature shocks have larger effects across all countries: they are more uniformly detrimental than local temperature shocks. Temperate countries also display a response that is economically large. Only colder countries display a somewhat smaller effect that is also not statistically significant.

Figure C.9(b) shows the responses by income per capita. We consider effects on poorer countries (real GDP per capita below 4,000 USD), middle income countries (real GDP per capita between 4,000 and 8,000 USD), and high income countries (real GDP per capita above 8,000 USD). Relative to the evidence based on local temperature, we find again more uniformly detrimental impacts: real GDP per capita falls across all income groups. Poor countries experience the most significant and persistent decline. Middle-income countries also see a considerable decrease in output. Only high-income countries are relatively more insulated, with a somewhat smaller and less enduring impact.

Regional temperature responses. How do global temperature shocks transmit to different regions? In Figure C.10, we show the local temperature response across different regions. Temperatures increase in all regions, however, there is notable heterogeneity

in terms of magnitude and persistence. Sub-Saharan Africa, Southeast-Asia and Latin America display more pronounced local temperature responses.

Figure C.10: Regional Temperature Response to Global Temperature Shocks

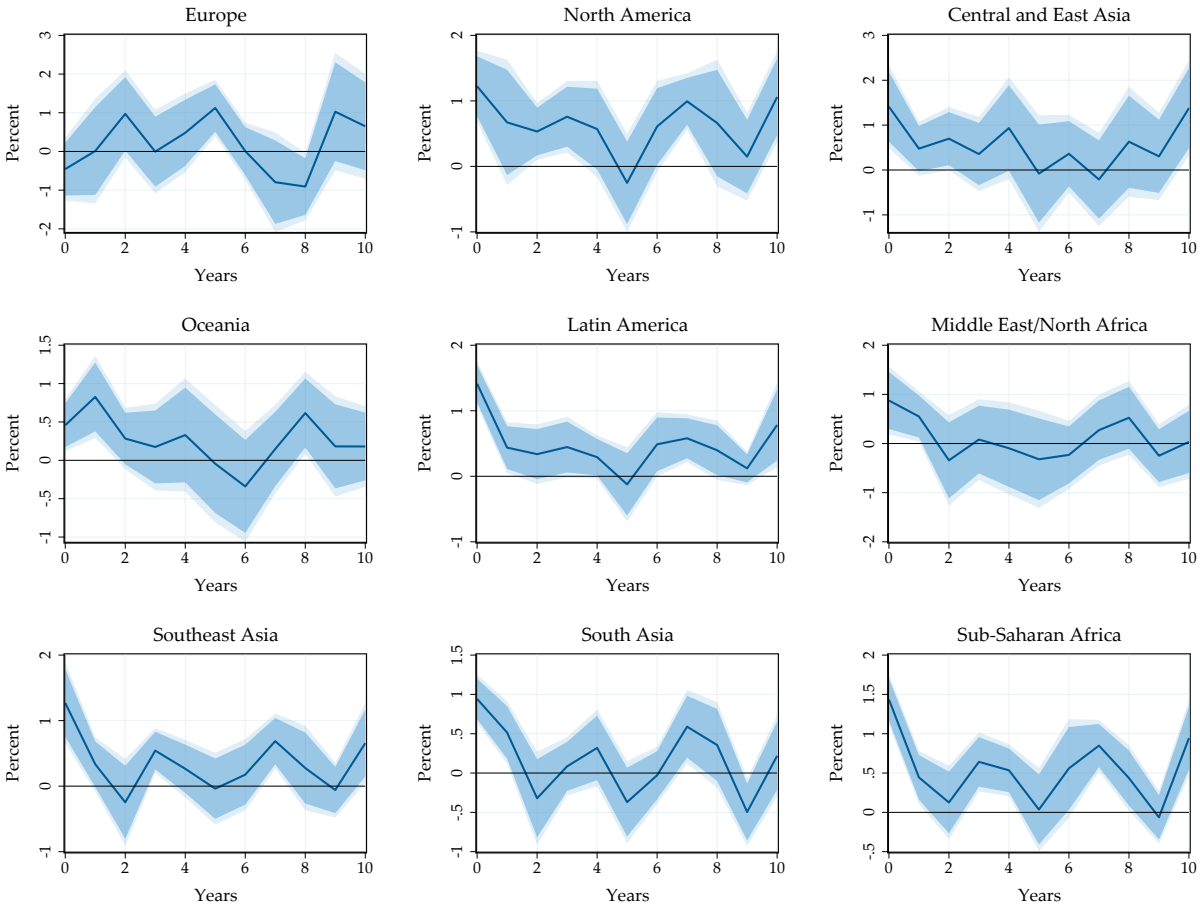

Impulse responses of local temperature per capita to global temperature shocks for different regions across the world based on (3) over PWT sample 1960-2019, conditioning on the different regions. Solid lines: point estimate. Dark and light shaded areas: 90 and 95% confidence bands.

D Model

Our solution to the neoclassical growth model is entirely standard and we present it for completeness.

D.1 Equilibrium

The resource constraint is:

$$\dot{K}_t = Z_t K_t^{\alpha} - C_t - \delta K_t.$$

Firm behavior and market clearing implies $r_t + \delta = \alpha Z_t K_t^{\alpha-1}$ and $w_t = (1-\alpha)K_t^{\alpha}$. The Euler equation is:

$$\dot{C}_t = \gamma^{-1}(\alpha Z_t K_t^{\alpha-1} - \delta - \rho)C_t.$$

In steady-state,

$$\begin{aligned} r = \alpha Z K^{\alpha-1} &= \rho + \delta \implies K = \left(\frac{\alpha Z}{\rho+\delta}\right)^{\frac{1}{1-\alpha}} \\ C &= ZK^{\alpha} - \delta K. \end{aligned}$$

D.2 Linearization

We denote steady-state variables without time subscripts. We denote deviations from steady-state with hats. We linearize the resource constraint:

$$\begin{aligned} \frac{d\widehat{K}_t}{dt} &= (\alpha Z K^{\alpha-1} - \delta)\widehat{K}_t - \widehat{C}_t + \widehat{Z}_t K^{\alpha} \\ &= \rho \widehat{K}_t - \widehat{C}_t + Y\widehat{z}_t. \end{aligned}$$

where we denoted $\widehat{z}_t = \widehat{Z}_t / Z$. Next, we linearize the Euler equation:

$$\begin{aligned} \frac{d\widehat{C}_t}{dt} &= \frac{C}{\gamma}\left(-\alpha(1-\alpha)ZK^{\alpha-2}\widehat{K}_t + \alpha K^{\alpha-1}\widehat{Z}_t\right) \\ &= \frac{C}{\gamma}\left(-\frac{(1-\alpha)r}{K}\widehat{K}_t + r\widehat{z}_t\right). \end{aligned}$$

We define:

$$X_t = \begin{pmatrix} \widehat{K}_t \\ \widehat{C}_t \end{pmatrix}.$$

We can summarize the linearized resource constraint and Euler equation as:

$$\dot{X}_t = AX_t + S_t,$$

where:

$$A = \begin{pmatrix} \rho & -1 \\ -\frac{(1-\alpha)rC}{\gamma K} & 0 \end{pmatrix} \ , \ S_t = \widehat{z}_t B \ , \ B = \begin{pmatrix} Y \\ \frac{rC}{\gamma} \end{pmatrix}.$$

We have an initial condition $\widehat{K}_0$, and a terminal condition $\widehat{C}_t \to 0$. We now apply standard Blanchard-Kahn arguments. Let $A = M^{-1}DM$, with D diagonal. For determinacy we require that parameters are such that D has a positive eigenvalue in the top left position, and a negative eigenvalue in the bottom right position. We denote by $\mathcal{X}_t = MX_t$, so that

$$\dot{\mathcal{X}}_t = D\mathcal{X}_t + MS_t.$$

We then solve explicitly for $\mathcal{X}_t$:

$$\mathcal{X}_t = e^{tD}\left[\mathcal{X}_0 + \int_0^t e^{-sD}(MS_t)ds\right].$$

Hence, long-run stability requires the top entry of the bracket to be zero as time grows. That is:

$$0 = \mathcal{X}_{0,1} + \int_0^\infty e^{-sD_1}(MS_s)_1 ds.$$

Therefore,

$$M_{1\bullet}X_0 = -\int_0^\infty e^{-sD_1}M_{1\bullet}S_s ds.$$

We can thus solve for initial consumption:

$$\widehat{C}_0 = -\frac{1}{M_{12}}\left[M_{11}\widehat{K}_0 + \int_0^\infty e^{-sD_1}M_{1\bullet}S_s ds\right].$$

We denote $\varepsilon_K = -\frac{M_{11}}{M_{12}}$, $\varepsilon_S = -\frac{1}{M_{12}}M_{1\bullet}$ and $\varepsilon_{S,s} = e^{-sD_1}\varepsilon_S$. We can write more compactly:

$$\widehat{C}_0 = \varepsilon_K \widehat{K}_0 + \int_0^\infty \varepsilon_{S,s} S_s ds.$$

Of course, this condition must hold at all times:

$$\widehat{C}_t = \varepsilon_K \widehat{K}_t + \int_0^\infty \varepsilon_{S,s} S_{t+s} ds.$$

D.3 Model Inversion: Proof of Proposition 1

We substitute the solution for linearized consumption into the law of motion of capital:

$$\frac{d\widehat{K}_t}{dt} = (L_{11} - \varepsilon_K)\widehat{K}_t + S_{1t} - \int_0^\infty \varepsilon_{S,s} S_{t+s} ds.$$

Denote $\kappa = -(L_{11} - \varepsilon_K)$ and $\mathcal{S}_t = S_{1t} - \int_0^\infty \varepsilon_{S,s} S_{t+s} ds$ so that:

$$\frac{d\widehat{K}_t}{dt} = -\kappa \widehat{K}_t + \mathcal{S}_t.$$

Assuming we start in steady-state, we obtain:

$$\widehat{K}_t = e^{-\kappa t}\int_0^t e^{\kappa s}\mathcal{S}_s ds.$$

In small log deviations:

$$\widehat{k}_t = \frac{e^{-\kappa t}}{K}\int_0^t e^{\kappa s}\mathcal{S}_s ds.$$

Since (in small log deviations):

$$\widehat{y}_t = \widehat{z}_t + \alpha \widehat{k}_t,$$

we are left with calculating $\widehat{k}_t$ as a function of the sequence $\widehat{z}$. We express:

$$\begin{aligned}\int_0^t e^{\kappa s}\mathcal{S}_s ds &= \int_0^t e^{\kappa s}\left(S_{1s} - \int_0^\infty \varepsilon_{S,r} S_{s+r} dr\right) ds \\ &= \int_0^t e^{\kappa s} S_{1s} ds - \iint_0^\infty \mathbb{1}[s \leq t]\varepsilon_{S,r} S_{s+r} e^{\kappa s} ds dr \\ &= \int_0^t e^{\kappa s} S_{1s} ds - \iint_0^\infty \mathbb{1}[s \leq t]\varepsilon_S S_{s+r} e^{\kappa s - D_1 r} ds dr.\end{aligned}$$

Changing variables to $\tau = s + r$ over r, we obtain

$$\begin{aligned}\int_0^t e^{\kappa s}\mathcal{S}_s ds &= \int_0^t e^{\kappa s} S_{1s} ds - \varepsilon_S \iint_0^\infty \mathbb{1}[s \leq t, s \leq \tau] S_\tau e^{\kappa s - D_1(\tau - s)} ds d\tau \\ &= \int_0^t e^{\kappa s} S_{1s} ds - \varepsilon_S \int_{\tau=0}^\infty e^{-D_1\tau} S_\tau \int_{s=0}^{\min\{t,\tau\}} e^{(D_1+\kappa)s} ds d\tau \\ &\equiv \int_0^t e^{\kappa s} S_{1s} ds - \varepsilon_S \int_{\tau=0}^\infty J_{t,\tau} S_\tau d\tau,\end{aligned}$$

where we defined:

$$J_{t,\tau} = e^{-D_1\tau}\int_{s=0}^{\min\{t,\tau\}} e^{(D_1+\kappa)s} ds = e^{-D_1\tau}\frac{e^{(D_1+\kappa)\min\{t,\tau\}} - 1}{D_1 + \kappa}.$$

Thus,

$$\widehat{k}_t = \frac{e^{-\kappa t}}{K}\int_0^\infty \left\{B_1 \mathbb{1}[s \leq t] e^{\kappa s} - (\varepsilon_S B) J_{t,s}\right\}\widehat{z}_s ds \equiv \int_0^\infty \mathcal{K}_{t,s}\widehat{z}_s ds,$$

where we defined:

$$\mathcal{K}_{t,s} = \frac{e^{-\kappa t}}{K}\left\{B_1 \mathbb{1}[s \leq t] e^{\kappa s} - (\varepsilon_S B) J_{t,s}\right\}.$$

Hence, we have obtained:

$$\widehat{y}_t = \widehat{z}_t + \alpha \int_0^\infty \mathcal{K}_{t,s}\widehat{z}_s ds.$$

These equations conclude the proof of Proposition 1.

D.4 Standard Errors

We compute standard errors around our counterfactuals using the Delta-method for the damage function scale parameter A and hold B and C fixed at their point estimates.

Specifically, we first estimate which values of A match the upper and lower ranges of the 95% confidence bands, on average across all horizons. Next, we compute the numerical derivative of model outcomes with respect to A. We combine this derivative with the values of A corresponding to the empirical confidence bands to construct confidence bands around the damage functions and counterfactuals.

D.5 Additional Estimation Results

D.5.1 Damages under local temperature

Figure D.1 displays the productivity effects of local temperature shocks, discussed in the main text.

D.5.2 Treatment of expectations

An alternative estimation strategy is to construct the impulse response function to a one-time transitory temperature shock with linear combinations of the impulse response function to the observed, persistent temperature shock *before* matching the model to the data. The interpretation of this approach is that households are surprised by elevated temperature each period after a global temperature shock.

We follow Sims (1986) to obtain the impulse response to one-time transitory temperature shocks. It is equivalent to using a recursive approach. Indeed, denote by $\widetilde{y}_t$ the unknown impulse response function of output to a transitory temperature shock. In discrete data and under linearity: $\widehat{y}_t = \sum_{s=0}^{t} \widehat{T}_{t-s}\widetilde{y}_s$. We then obtain $\widetilde{y}_t = \left(\widehat{y}_t - \sum_{s=0}^{t-1} \widehat{T}_{t-s}\widetilde{y}_s\right)/\widehat{T}_0$ recursively.

With the deconvoluted impulse response functions of output and capital to a one-time unit transitory temperature shock at hand, we use Proposition 1 and obtain the corresponding shocks $\widehat{z}_t$, $\widehat{\Delta}_t$. We then identify $\zeta_s = \widehat{z}_s$ and $\delta_s = \widehat{\Delta}_s/\Delta_0$.

Figure D.1: Output, Capital and Productivity After Local Temperature Shocks

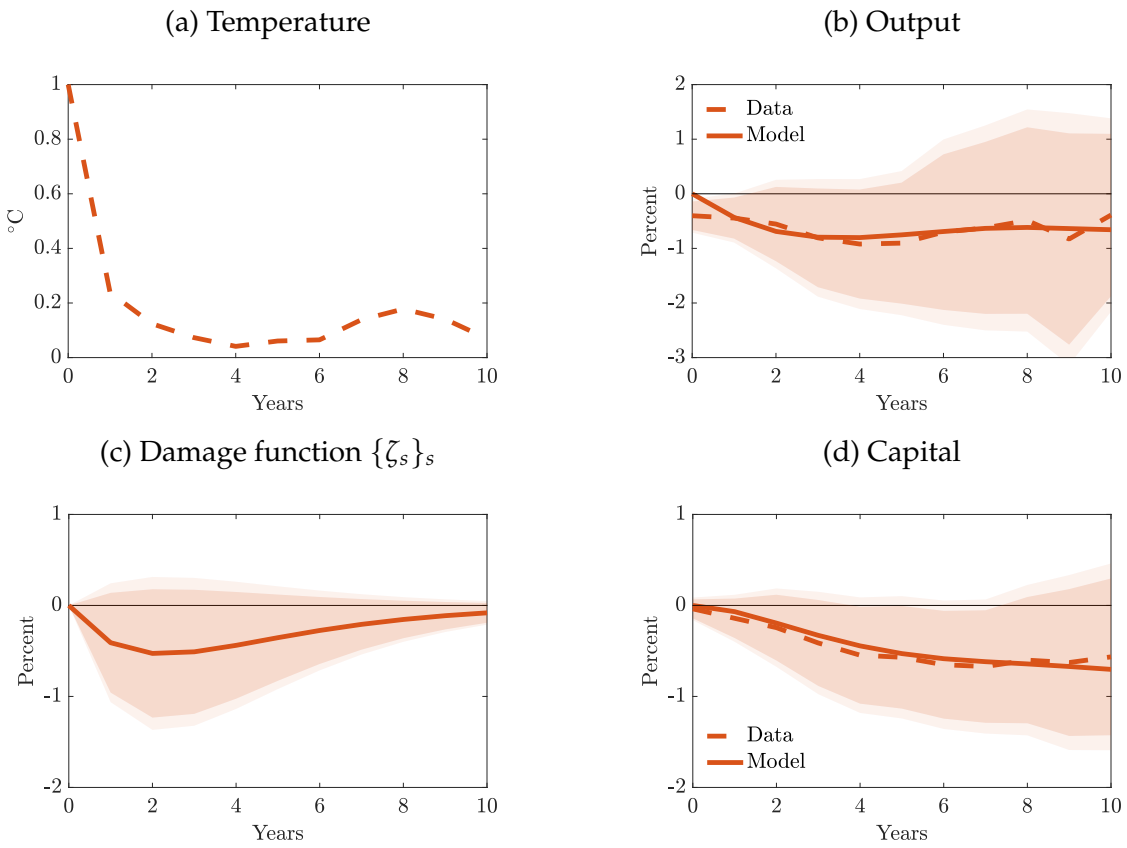

Estimation results from matching the model impulse response to the empirical response of output to local temperature shocks. Panel (a): underlying temperature path. Panel (b): output responses to this internally persistent temperature path. Panel (c): implied productivity shocks. Panel (d): non-targeted capital responses to internally persistent temperature path. Dashed lines: data. Solid lines: model fit. 90% (dark area) and 95% (light area) confidence intervals based on the Delta-method as detailed in Appendix D.4. PWT data.

D.5.3 Regional damage functions and counterfactuals

We estimate the model of Section 5 separately for each region, targeting the IRFs from Section 4.3. In this appendix, we report the resulting regional damage functions as well as counterfactual paths of GDP per capita for each region under our business-as-usual warming scenario in Figures D.2-D.3 .

Figure D.2: Regional Damage Functions

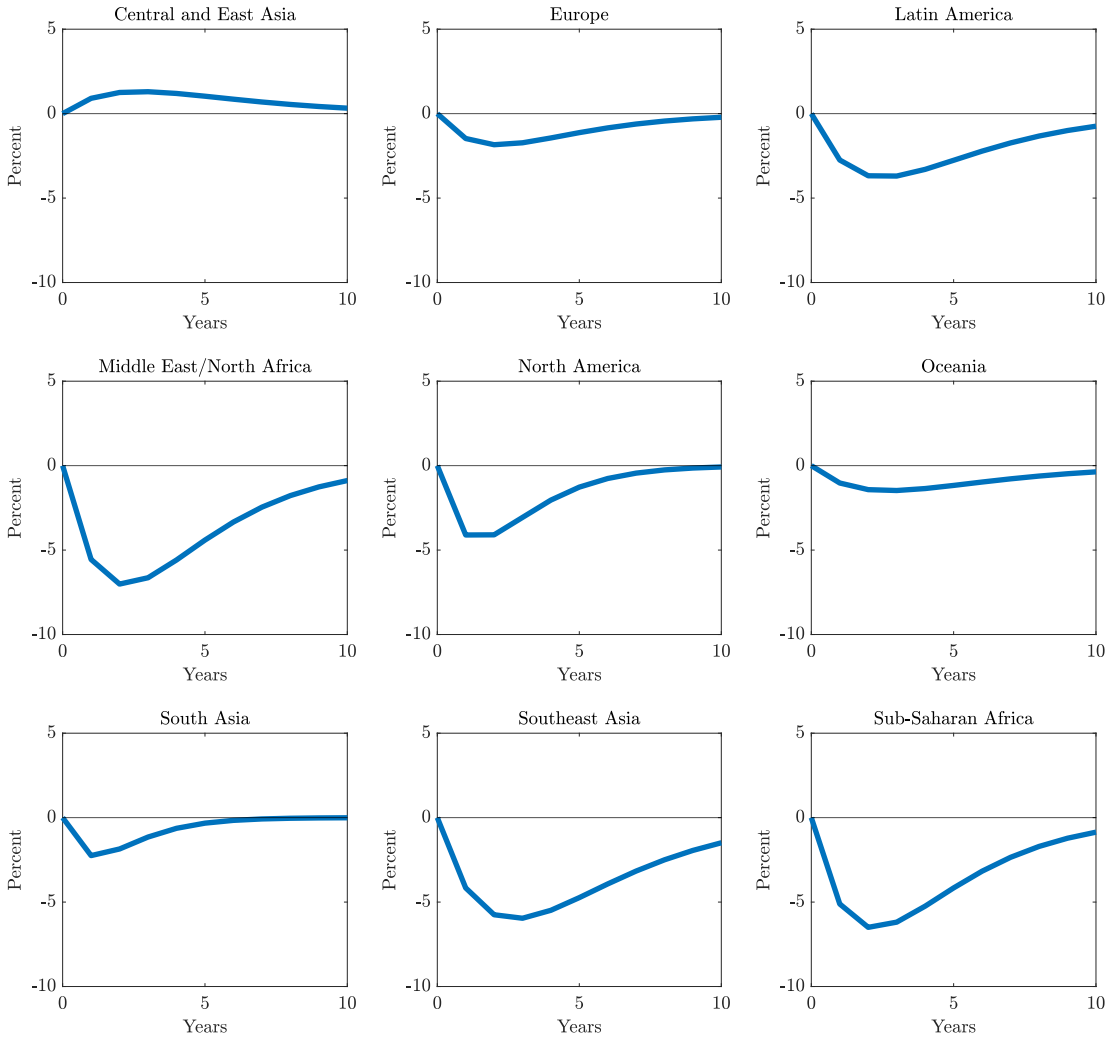

Estimation results from matching the model impulse response to the empirical response of output to local temperature shocks for each region. PWT data.

Figure D.3: GDP per Capita for Each Region Under Global Warming

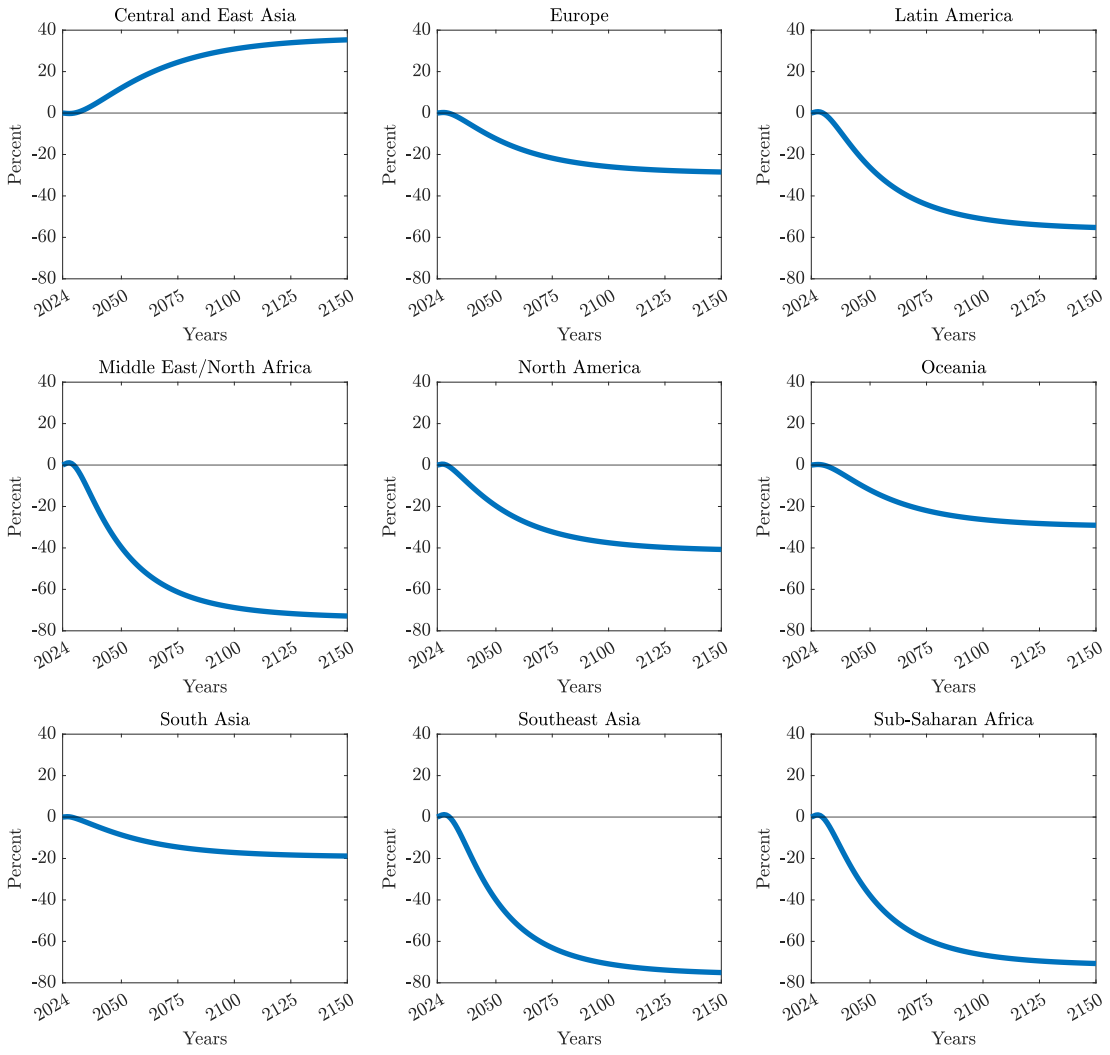

GDP per capita counterfactuals for each region. Global mean temperature path from Figure 13. Damage function estimated in PWT data.

References Appendix

Albright, Anna Lea, Cristian Proistosescu, and Peter Huybers (2021). "Origins of a Relatively Tight Lower Bound on Anthropogenic Aerosol Radiative Forcing from Bayesian Analysis of Historical Observations". *Journal of Climate* 34, 8777–8792.

Azar, Christian, Jorge García Martín, Daniel JA. Johansson, and Thomas Sterner (2023). "The Social Cost of Methane". *Climatic Change* 176.

Bansal, Ravi and Marcelo Ochoa (2011). "Temperature, Aggregate Risk, and Expected Returns". *National Bureau of Economic Research Working Paper Series 17575*.

Barro, Robert J. and José F. Ursúa (2008). "Macroeconomic Crises since 1870". *Brookings Papers on Economic Activity* 1, pp. 255–335.

Berkeley Earth (2023). *Data Overview*. https://berkeleyearth.org/data/.

Burke, Marshall, Solomon M. Hsiang, and Edward Miguel (2015). "Global non-linear effect of temperature on economic production". *Nature* 527.7577, pp. 235–239.

Center for International Earth Science Information Network (CIESIN), Columbia University (2018). *Gridded Population of the World, Version 4.11 (GPWv4): Population Count*. NASA Socioeconomic Data and Applications Center (SEDAC). Online Resource.

Dell, Melissa, Benjamin F. Jones, and Benjamin A. Olken (2012). "Temperature shocks and economic growth: Evidence from the last half century". *American Economic Journal: Macroeconomics* 4.3, pp. 66–95.

Dietz, Simon, Frederick van der Ploeg, Armon Rezai, and Frank Venmans (2021). "Are Economists Getting Climate Dynamics Right and Does It Matter?" *Journal of the Association of Environmental and Resource Economists* 8.5, pp. 895–921.

Dingel, Jonathan I., Kyle C. Meng, and Solomon M. Hsiang (2023). "Spatial correlation, trade, and inequality: Evidence from the global climate". *National Bureau of Economic Research Working Paper Series 25447*.

Feenstra, Robert C., Robert Inklaar, and Marcel P. Timmer (2015). "The Next Generation of the Penn World Table". *American Economic Review* 105.10, pp. 3150–3182.

Hamilton, James D. (2018). "Why you should never use the Hodrick-Prescott filter". *Review of Economics and Statistics* 100.5, pp. 831–843.

Lange, Stefan, Matthias Mengel, Simon Treu, and Matthias Büchner (2023). *ISIMIP3a atmospheric climate input data (v1.2)*. ISIMIP Repository. https://doi.org/10.48364/ISIMIP.982724.2.

Lenssen, Nathan J. L., Gavin A. Schmidt, James E. Hansen, Matthew J. Menne, Avraham Persin, Reto Ruedy, and Daniel Zyss (2019). "Improvements in the GISTEMP Uncertainty Model". *Journal of Geophysical Research: Atmospheres* 124.12, pp. 6307–6326.

Matsuura, Kenji and National Center for Atmospheric Research Staff (2023). *The Climate Data Guide: Global (land) precipitation and temperature: Willmott & Matsuura, University of Delaware*. Online Resource.

Müller, Karsten, Chenzi Xu, Mohamed Lehbib, and Ziliang Chen (2025). *The global macro database: A new international macroeconomic dataset*. Tech. rep. National Bureau of Economic Research.

NASA Earth Observatory (2020). *World of Change: Global Temperatures*. Online Resource.

NASA Goddard Institute for Space Studies (2023). *GISS Surface Temperature Analysis (GISTEMP v4)*. Online Resource.

Nath, Ishan B., Valerie A. Ramey, and Peter J. Klenow (2024). "How Much Will Global Warming Cool Global Growth?" *National Bureau of Economic Research Working Paper Series 32761*.

Neal, Timothy, Ben R. Newell, and Andy Pitman (2025). "Reconsidering the macroeconomic damage of severe warming". *Environmental Research Letters* 20.4, p. 044029.

NOAA National Centers for Environmental Information (2023a). *Climate at a Glance: Global Time Series*. Online Resource.

— (2023b). *Global Surface Temperature Anomalies: Mean Temperature Estimates*. Online Resource.

Ramey, Valerie A. (2016). "Macroeconomic shocks and their propagation". *Handbook of Macroeconomics* 2, pp. 71–162.

Rohde, Robert A. and Zeke Hausfather (2020). "The Berkeley Earth Land/Ocean Temperature Record". *Earth System Science Data* 12.4, pp. 3469–3479.

Sheffield, Justin, Gopi Goteti, and Eric F. Wood (2006). "Development of a 50-Year High-Resolution Global Dataset of Meteorological Forcings for Land Surface Modeling". *Journal of Climate* 19.13. Publisher: American Meteorological Society Section: Journal of Climate, pp. 3088–3111.

Sims, Christopher A. (1986). "Are forecasting models usable for policy analysis?" *Quarterly Review* 10, pp. 2–16.

Webb, Eric J. and Brian I. Magi (2022). "The ensemble oceanic Niño index". *International Journal of Climatology* 42.10, pp. 5321–5341.

Zappalà, Guglielmo (2023). "Estimating Sectoral Climate Impacts in a Global Production Network". *IMF Working Paper 2023/053*.